

Curriculum Vitae

Christian J. Kinney

Ph.D. Candidate Graduate Research Student, Department of Physiology
University of Maryland, Baltimore

Date April 22, 2021

Contact Information

Business

Address: Department of Physiology
685 West Baltimore Street
Health Sciences Facility 1 Room 556
Baltimore, MD 21201

Phone: 678-451-0716

Email: christian.kinney@gmail.com

Education

2014 - 2021 **Ph.D., Molecular Medicine: Genome Biology**, University of
Maryland, Baltimore

May 2021 Degree conferred (Ph.D.)

2010 - 2013 **B.S., Genetics**, University of Georgia, Athens, Georgia

Relevant Experience

2015 - present **Graduate Research Assistant**
Dr. Robert Bloch Laboratory, Department of Physiology, University
of Maryland, Baltimore

- Thesis Title: “ μ -Crystallin: A Novel Protein Regulator of Mammalian Metabolism”
- Analyzed bioinformatic transcriptomic RNA-seq and LC.MS/MS proteomic data to determine differentially regulated genes in a transgenic mouse strain
- Genome editing using multiplexed CRISPR-Cas12a sgRNAs to cut out a viral sequence in a mouse genome
- Performed transfection of *in vitro* mammalian cells via lipofection and *in vivo* mammalian cells via electroporation and sonoporation for the purpose of introducing episomal or transient plasmids I designed
- Transduced mammalian cells *in vitro* using adenovirus and quantified downstream genetic changes via qRT-PCR

- Measured metabolic variables *in vitro* using a Seahorse Metabolic Analyzer and *in situ* using whole animal metabolic chambers to determine altered metabolism in transgenic mice

Summer 2014 **Ph.D. Rotation Student**
Department of Psychiatry, University of Maryland, Baltimore

- Assembled a dual luciferase reporter plasmid system to determine regulatory sequences of a downstream gene
- Analyzed the *CACNA1C* gene using bioinformatics for putative regulatory regions

Spring 2013 **Research Intern**
Department of Entomology, University of Georgia, Athens, Georgia

- Labeled arthropod specimens for the Smithsonian and the Georgia Natural History Museum

2011 - 2012 **Lab Technician**
Department of Cellular Biology, University of Georgia, Athens, Georgia

- Maintained over 400 strains of *Drosophila melanogaster*
- Sexed flies and segregated virgins for the purpose of crossing fly strains
- Fixed and stained fly embryos to identify expression patterns of early embryonic genes

Laboratory Skills

Nucleic Acids

- | | | |
|--------------------------|--|---------------------------|
| • RNA-seq | • Primer/probe design | • cDNA generation |
| • qRT-PCR | • Transfection: sonoporation, lipofection, and electroporation | • Adenoviral transduction |
| • Bioinformatic analysis | • CRISPR-Cas12a gRNA design | • Plasmid design |
| | | • Sequence assembly |

Protein

- | | | |
|--|--|---------------------------------------|
| • Anisotropy based FRET | • IHC, ICC, IF | • Western blot/Capillary Western blot |
| • Mouse tissue dissection and sectioning | • Mammalian and bacterial tissue culture/selection | • LC.MS/MS sample prep |

- Machine learning image analysis
- Gel densitometry

Techniques

- IM, IP, and IV injections
- Drug compounding
- Perfusion
- Bleeds and exsanguination
- *In vivo* Xenogen imaging
- Auditory brainstem response testing/analysis

Publications

- Spring 2021 Kinney CJ, et al. μ -Crystallin: A Thyroid Hormone Binding Protein. *Endocrine Regulations*, 2021.
- Winter 2021 Kinney CJ, et al. μ -Crystallin in Mouse Skeletal Muscle Promotes a Shift from Glycolytic toward Oxidative Metabolism. *Current Research in Physiology* 4: 47-59, 2021.

Intellectual Property

- Spring 2019 Lead inventor of a patent pending protein therapeutic to treat certain metabolic disorders
- Summer 2017 Sole inventor of a gene therapy, disclosed to the University of Maryland, Baltimore

Awards

- Spring 2019 University System of Maryland Board of Regents guest
- Winter 2018 UMB Graduate School Centennial Celebration Invited Speaker
- Spring 2018 Graduate Research Innovation District (Grid) Pitch (\$1000 award)
- Entrepreneurial pitch competition held at UMB
- 2018 - present Graduate Research Innovation District Guild Member
- 2017 - present President's Entrepreneurial Fellow (\$5,000 award)
- Consultant moving a triple negative breast cancer drug forward to IND application
- 2017 - present President's Student Leadership Institute Candidate: Entrepreneurship and Innovation Track
- 2016 - present NIH R01 Underrepresented Minority Supplement grant
- 2014 - present Meyerhoff Graduate Fellow
- NIH funded competitive diversity fellowship with stipend

Organizations

- 2018 - present American Society of Human Genetics
- 2018 - present European Society of Human Genetics

Institutional Service

- 2018 - present Entrepreneurial Innovation Network executive board member
- Fall 2018 Managed a high school student working in the lab and taught him various scientific techniques
- Spring 2018 Taught a week-long course on genetics to high school students at Applications and Research Lab High School
- Fall 2017 Invited speaker for genetic research careers at Sollers Point Technical High School
- 2017 - 2018 Project Jump Start volunteer
- Prepared and distributed meals for the local homeless population
- Fall 2016 Contributing writer for the Grad Gazette
- 2015 - present Peer mentor
- Mentored incoming Ph.D. students

Abstract

Title of Dissertation: μ -Crystallin: A Novel Protein Regulator of Mammalian Metabolism

Christian Kinney, Doctor of Philosophy, 2021

Dissertation Directed by: Dr. Robert J. Bloch, Professor, Department of Physiology,
Department of Orthopedics

Thyroid hormones control many aspects of physiology such as metabolism and thermogenesis. Because thyroid hormones control such crucial bodily functions, their levels in the body are tightly regulated. Hypo- and hyperthyroidism can result when the level of thyroid hormone is too low or too high, respectively, with potentially serious pathophysiological consequences. μ -Crystallin is an NADPH-regulated thyroid hormone binding protein. The protein is minimally expressed in the skeletal muscle of most people; however, some individuals express relatively high baseline levels of μ -crystallin. We generated a transgenic mouse, the *Crym* tg mouse, that expresses high levels of μ -crystallin in its skeletal muscle, in order to explore the consequences of expressing high levels, comparable to those seen in some humans. The *Crym* tg mouse expresses mouse μ -crystallin at levels 2.6-147.5-fold higher than control mice in their skeletal muscle. Consequently, intramuscular triiodothyronine (T_3) levels are elevated \sim 190-fold in the tibialis anterior, while serum thyroxine levels are decreased by 1.2-fold. *Crym* tg mice have a decreased respiratory exchange ratio that corresponds to a 13.7% increase in fat

utilization as an energy source. Female *Crym* tg mice gained weight faster on high fat or high simple carbohydrate diets. Gene ontology enrichment analysis of transcriptomic and proteomic data revealed alterations to the expression of genes associated with metabolism and fiber type, while the fiber sizes of *Crym* tg soleus muscle are significantly smaller than those of controls. Taken together, these results suggest that μ -crystallin may play a role in regulating metabolism, perhaps through the control of thyroid hormone in muscle. Thus, humans who naturally express higher levels of μ -crystallin in their skeletal muscle may have an altered metabolism, comparable to the *Crym* tg mice.

μ -Crystallin: A Novel Protein Regulator of Mammalian Metabolism

by
Christian J. Kinney

Dissertation submitted to the Faculty of the Graduate School of the
University of Maryland, Baltimore in partial fulfillment
of the requirements for the degree of
Doctor of Philosophy
2021

©Copyright 2021 by Christian J. Kinney
All Rights Reserved

Dedication

To my mother, Mary Beth Kinney, who supported me throughout my Ph.D. and instilled in me a spirit of hard work and curiosity.

Acknowledgments

I am grateful to Dr. Robert J. Bloch, my mentor, as well as the other members of my thesis committee: Drs. Martin Schneider, Alexandros Pouloupoulos, Peter L. Jones, and Victor Frenkel. I am also grateful to the Graduate School, University of Maryland, Baltimore, where I have made many friends and fond memories.

Table of Contents

Chapter 1: μ-Crystallin: A Thyroid Hormone Binding Protein	1
Abstract.....	1
Introduction	2
Discovery of μ -Crystallin.....	3
Temporospatial Expression of CRYM.....	4
THs and Their Receptors	5
Regulation and Synthesis of TH.....	6
Thyroid Hormone Transport	7
Thyroid Receptors	8
μ-Crystallin (<i>CRYM</i>).....	9
μ -Crystallin in Animals	10
μ -Crystallin as a Ketimine Reductase.....	11
CRYM and Disease.....	12
CRYM Expression in the Brain.....	12
Huntington's Disease.....	13
Amyotrophic Lateral Sclerosis	14
Schizophrenia.....	14
CRYM as a Potential Therapeutic for Psychiatric Disorders	15
<i>CRYM</i> and Non-Syndromic Deafness.....	15
Genetics of <i>CRYM</i>.....	17
Effects of High Crym Expression	19
Conclusion.....	21
Bibliography.....	22

Chapter 2: μ -Crystallin in Mouse Skeletal Muscle Promotes a Shift from Glycolytic toward Oxidative Metabolism..... 48

Abstract..... 49

1. Introduction 50

2. Materials and methods..... 52

2.1. Creation of the *Crym* tg Mouse..... 52

2.1.1. Back-Crossing and Genotyping 53

2.1.2. Sequencing the Transgene Insertion Site..... 54

2.2. Staining of Longitudinal and Cross Sections for μ -Crystallin 54

2.2.1. Fiber Type Staining..... 55

2.2.2. Fat Staining..... 57

2.3.1. CNFs and Minimal Feret’s Diameter of TA Cross Sections..... 58

2.4. Measurements of Contractile Force 58

2.5. Treadmill and *ad libidum* Running 59

2.6. Protein Extraction 59

2.6.1. Immunoblotting Protocols 60

2.6.2. RNA and cDNA Preparation 62

2.7. Proteomic and Transcriptomic Comparison of Skeletal Muscle of *Crym* tg and Control Mice.. 64

2.9. Ca²⁺ Transients 65

2.9.1. Metabolic Chambers 65

2.9.2. Diet Studies 66

2.9.3. T₃, T₄, TSH Levels..... 67

2.9.4. Statistics 67

2.9.5. Materials..... 68

3. Results 68

3.1. RT-qPCR, Western Blot, and Immunofluorescence..... 69

3.2. Hormone levels.....	72
3.2.1. Morphology and physiology.....	76
3.2.2. Fiber Types.....	78
3.3. Metabolism.....	79
3.3.1. Diet Study.....	80
3.3.2. Global gene expression (RNA-seq).....	83
3.3.3. Global protein expression (LC.MS/MS).....	85
4. Discussion	86
Credit authorship contribution statement	97
Declaration of interests	98
Appendix A. Supplementary data	99
Funding	99
<i>Bibliography</i>.....	99
Discussion and Conclusion	112
<i>Chapter 3: CRISPR-Cas12a in Dysferlin Null Mice</i>.....	114
Introduction	114
Methods.....	115
CRISPR-Cas12a Plasmid.....	115
Electroporation of Murine Soleus Muscle.....	119
Genomic DNA Extraction and PCR Amplification	120
Genome Editing of Retrotransposon in the <i>Dysf</i> Gene of A/J Mice	124
Results	127
Discussion.....	128

<i>Chapter 4: Sonoporation of Murine Muscle</i>	131
Introduction	131
Methods	133
Results	134
Discussion	136
<i>Chapter 5: Discussion</i>	137
Effects of Increased μ-Crystallin Expression in Murine Skeletal Muscle	137
Generation of a Multiplexed gRNA CRISPR-Cas12a Cassette	139
Sonoporation of Murine Skeletal Muscle	140
Conclusions	141
Bibliography	142
<i>Comprehensive Bibliography</i>	183

List of Tables

Table 1. Thyroid Hormone Levels.....	73
Table 2. Respiratory Exchange Ratio	80
Table 3. Metabolic and Contractile Changes	83
Table 4. Biologic Gene Ontological Terms	85
Table 5. Contractile Proteins Identified via LC.MS/MS	92

List of Figures

Figure 1. Crym mRNA and Protein Levels.....	69
Figure 2. μ -Crystallin Subcellular Localization	71
Figure 3. Contractile Properties of Muscle	77
Figure 4. Weight Gain on Various Diets.....	81
Figure 5. Multiplexed CRISPR-Cas12a Plasmid Maps.....	117
Figure 6. Various Polymerases Tested for Efficacy	123
Figure 7. Dysf Amplicons After CRISPR.....	124
Figure 8. Heat Map of Sonoporated Mouse Muscle Tissue.....	135

List of Abbreviations

ABCB1	ATP binding cassette subfamily B member 1
ACO2	aconitase-2
ACTA1	actin alpha 1, skeletal muscle
AgRP	agouti related peptide
ALDH	aldehyde dehydrogenase 2 family member
ALS	amyotrophic lateral sclerosis
AUC	area under the curve
BA	Brodmann area
BGH	bovine growth hormone
cDNA	complementary DNA
CLAMS	Comprehensive Lab Monitoring System
CNF	centrally nucleated fiber
CNTN6	contactin 6
CRISPR	clustered regularly interspaced short palindromic repeats
crRNA	CRISPR RNA
CRYM	μ -crystallin
CSA	cross-sectional area
CTBP	cytosolic 3,5,3'-triiodo-L-thyronine binding protein
C _q	quantitation cycle
DEG	differentially expressed gene
DFNA40	autosomal dominant deafness-40

DIO	iodothyronine deiodinase
DLST	dihydrolipoamide s-succinyltransferase
DR4	direct repeat 4
DUX4	double homeobox 4
EDL	extensor digitorum longus
FDA	Food and Drug Administration
FDB	flexor digitorum brevis
FDR	false discovery rate
F_{\max}	maximal fluorescence intensity
F_0	background fluorescence
FSHD	facioscapulohumeral muscular dystrophy
Gastroc	gastrocnemius
gDNA	genomic DNA
GTE _x	Genotype-Tissue Expression
GO	gene ontology
gRNA	guide RNA
HDR	high dynamic range
HFD	high fat diet
HRP	horseradish peroxidase
IP6	inverted palindrome with a 6 base pair gap
IR	infrared
KARS	lysyl-tRNA synthetase
K_D	dissociation constant

K _i	inhibition constant
KO	knockout
LC.MS/MS	liquid chromatography-tandem mass spectrometry
MAF	minor allele frequency
MB	microbubbles
MCT8	solute carrier family 16 member 2
MCT10	solute carrier family 16 member 10
mRNA	messenger RNA
MYH2	myosin heavy chain 2
MYH4	myosin heavy chain 4
MYH7	myosin heavy chain 7
NADH	nicotinamide adenine dinucleotide
NADPH	nicotinamide adenine dinucleotide phosphate
NOM1	nucleolar protein with MIF4G domain 1
NPY	neuropeptide Y
OATP	organic anion transporting polypeptide
OGDH	oxoglutarate dehydrogenase
ORF	open reading frame
P2C	piperidine-2-carboxylate
padj	adjusted p value
PAM	protospacer-adjacent motif
PBS	phosphate buffered saline
PFC	prefrontal cortex

polyA	polyadenylation
Pyr2C	Δ^1 -pyrroline-2-carboxylate
REML	restricted maximum likelihood
RER	respiratory exchange ratio
RNA-seq	RNA sequencing
RM	repeated measures
rT ₃	reverse T ₃
RT-qPCR	real time quantitative PCR
RXR	retinoid X receptors
SCCPDH	saccharopine dehydrogenase
SETD7	SET Domain Containing 7
SD	standard deviation
SE	standard error
sgRNA	single guide RNA
SIMB	size isolated microbubbles
SLC01C1	solute carrier organic anion transporter family member 1C1
SLC10A1	solute carrier family 10 member 1
SLC3A2	solute carrier family 3 member 2
SLC7A5	solute carrier family 7 member 5
SLC7A8	solute carrier family 7 member 8
SNP	single nucleotide polymorphism
ssDNA	single stranded DNA
T ₂	3,5-diiodothyronine

T ₃	triiodothyronine
T ₄	thyroxine
TA	tibialis anterior
TERT	telomerase reverse transcriptase
tg	transgenic
TH	thyroid hormone
THRA	thyroid hormone receptor alpha
THRB	thyroid hormone receptor beta
TNNI1	troponin 1, slow skeletal type
TPM	transcripts per million
TR	thyroid hormone receptor
TRE	thyroid responsive elements
TRH	thyrotropin releasing hormone
TSH	thyroid stimulating hormone
UTR	untranslated region
WGA	wheat germ agglutinin
qPCR	quantitative PCR
qRT-PCR	quantitative real-time PCR

Chapter 1: μ -Crystallin: A Thyroid Hormone Binding Protein¹

Introduction

μ -Crystallin: A Thyroid Hormone Binding Protein

Christian J. Kinney^{1,*}, Robert J. Bloch¹

¹ Department of Physiology School of Medicine, University of Maryland,
Baltimore, Baltimore, MD 21201

Abstract

μ -Crystallin is a NADPH-regulated thyroid hormone binding protein encoded by the *CRYM* gene in humans. It is primarily expressed in the brain, muscle, prostate, and kidney, where it binds thyroid hormones, which regulate metabolism and thermogenesis. It also acts as a ketimine reductase in the lysine degradation pathway when it is not bound to thyroid hormone. Mutations in *CRYM* can result in non-syndromic deafness, while its aberrant expression, predominantly in the brain but also in other tissues, has been associated with psychiatric, neuromuscular, and inflammatory diseases. *CRYM* expression is highly variable in human skeletal muscle, with 15% of individuals expressing ≥ 13 fold more *CRYM* mRNA than the median level. Ablation of the *Crym* gene in murine models results in the hypertrophy of fast twitch muscle fibers and an increase in fat mass of mice fed a high fat diet. Overexpression of *Crym* in mice causes a shift in energy utilization away from glycolysis towards an increase in the catabolism of fat via β -oxidation, with

¹ Kinney CJ, and Bloch RJ. μ -Crystallin: A Thyroid Hormone Binding Protein. *Endocrine Regulations* 2021.

commensurate changes of metabolically involved transcripts and proteins. The history, attributes, functions, and diseases associated with *CRYM*, an important modulator of metabolism, are reviewed.

Introduction

Thyroid hormones (THs) are essential regulators of gene expression and metabolism and their precise control is therefore crucial to maintaining homeostasis and adapting to different environmental conditions. TH regulation is achieved at many levels and through multiple means, including synthesis, secretion, uptake into tissues, intracellular processing by deiodinases, and potentially, binding to proteins involved in intracellular storage. Here, we review the TH binding protein, μ -crystallin (*CRYM*), that may play a key role in the latter process, intracellular sequestration and storage.

T₃ and T₄ thyroid hormone (TH) are produced in the thyroid, though the thyroid primarily produces T₄ and less than 20% of the TH it releases is T₃ (Abdalla and Bianco 2014). Triiodothyronine (T₃) is primarily produced peripherally in the body via the monodeiodination of thyroxine (T₄) (Chopra 1977). THs typically act as transcription factors by binding to thyroid hormone receptors (TRs). T₃ has a 10-fold higher affinity for TRs than T₄ and therefore, it is a more potent transcription factor (Abdalla and Bianco 2014). Liganded and unliganded TRs act as strong regulators of metabolism and thermogenic homeostasis (Larsen, Silva, and Kaplan 1981) primarily by affecting transcription of genes containing thyroid response elements (Brent 2012).

The ability to bind TH with high affinity suggests that μ -crystallin may play a role in regulating TH levels by controlling the availability of TH to interact with receptors, with

possible downstream consequences to physiology and metabolism. Reed et al. (2007) have observed on a 2D proteomic gel of skeletal muscle biopsies taken from 3 individuals with FSHD and 2 healthy individuals that μ -crystallin showed increased expression and was the only differentially expressed protein in comparing individuals with facioscapulohumeral muscular dystrophy (FSHD) to healthy individuals (Reed 2007). In order to study increased levels of skeletal muscle μ -crystallin, which was at that time a candidate for the then, unknown pathological protein in FSHD, they constructed a transgenic mouse specifically overexpressing μ -crystallin in skeletal muscle, the *Crym* tg mouse. At the time, little was known about the pathological agent in FSHD, although Double Homeobox 4 (DUX4) is now widely believed to determine disease pathology (Tawil, Van Der Maarel, and Tapscott 2014).

Crym tg mice were created to specifically overexpress μ -crystallin in skeletal muscle by placing the mouse *Crym* open reading frame under the control of the human skeletal actin promoter (*ACTA1*) and the human slow troponin I enhancer (*TNNI1*). The transgenic plasmid incorporated randomly into intron 12 of the *Cntn6* gene after oocyte injection. The resultant transgenic mice were bred to homozygosity to be used to measure the effects of high μ -crystallin expression in skeletal muscle (Kinney et al. 2021).

Discovery of μ -Crystallin

μ -Crystallin was first identified in 1957 by Tata who called the protein a thyroxine-binding protein (Tata 1958). Hashizume et al. subsequently showed the same protein that they called Factor b, could bind T_3 and T_4 in the presence of NADH or preferably NADPH (Hashizume, Kobayashi, and Miyamoto 1986), the latter dinucleotide causing the increased

binding capacity of cytosolic 3,5,3'-triiodo-L-thyronine (T₃)-binding protein (CTBP), the next name for μ -crystallin (Hashizume, Miyamoto, Ichikawa, Yamauchi, Kobayashi, et al. 1989). NADP bound to CTBP (μ -crystallin) enhanced the presence of T₃ to the nucleus of rat kidney cells at sites that differed from other nuclear T₃ sites (Hashizume, Miyamoto, Kobayashi, et al. 1989), whereas NADPH diminished the amount of T₃ nuclear (Hashizume, Miyamoto, Yamauchi, et al. 1989). Maximal activation by NADP or NADPH was at concentrations of 0.1 μ M and 25 μ M respectively, 20 and 4 times less, respectively, than physiological levels (Hashizume, Miyamoto, Ichikawa, Yamauchi, Sakurai, et al. 1989), suggesting that μ -crystallin in cells was likely to be bound to both NADP and NADPH. CTBP was shown to increase cellular and nuclear uptake of T₃ as well as decrease cellular and nuclear efflux of T₃ in addition to suppressing expression of thyroid hormone responsive genes (Mori et al. 2002). Kobayashi et al. (1991) further characterized μ -crystallin as a dimer or two identical 38,000 Da subunits. At the time, it was referred to as p38CTBP, to distinguish it from a 58 kDa thyroxine-binding protein, p58CTBP (Hashizume, Miyamoto, Ichikawa, Yamauchi, Kobayashi, et al. 1989). Wistow and Kim (1991) gave μ -crystallin its current name after they found the protein highly expressed in the lens of some marsupials. More recently, μ -crystallin has been shown to function as a ketimine reductase in addition to its activity as a NADPH-regulated thyroid hormone binding protein (Hallen and Cooper 2017; Hallen et al. 2011; Hallen, Cooper, Jamie, et al. 2015; Hallen, Cooper, Smith, et al. 2015).

Temporospatial Expression of CRYM

μ -Crystallin is predominantly expressed in the cerebral cortex, heart, skeletal muscle, prostate, and kidney (Thul et al. 2017). Temporally, *Crym* expression in mice gradually increases from embryonic day 10.5 until its zenith at embryonic day 14.5, when the brain and inner ear have the highest expression. Expression subsequently decreases gradually and falls sharply postnatally in most tissues. Some *Crym* expressing organs such as the renal medulla of the kidney increase in expression of *Crym* postnatally while other organs continue to express *Crym*, albeit at lower levels than *in utero* (Smith et al. 2019). *CRYM* mRNA in humans is expressed at its highest levels in the basal ganglia of the brain followed by the heart; at the protein level, μ -crystallin is most highly expressed in the basal ganglia, cerebral cortex, kidney and prostate (data obtained from the normalized Consensus Dataset of the Human Protein Atlas) (Uhlén et al. 2015). Subcellularly, μ -crystallin localizes to the cytosol (Kobayashi et al. 1991). In humans, μ -crystallin is also expressed in the inner ear where two, rare mutations, X315Y and K314T, cause Deafness, Autosomal Dominant 40 (Abe et al. 2003). There are no other illnesses in which *CRYM* has been implicated, although it's aberrant expression has been associated with amyotrophic lateral sclerosis (Daoud et al. 2011; Fukada et al. 2007; Hommyo et al. 2018), facioscapulohumeral muscular dystrophy (FSHD) (Reed et al. 2007; Vanderplanck et al. 2011), endotoxin-induced uveitis (Imai et al. 2010), schizophrenia (Middleton et al. 2002; Miklos and Maleszka 2004), and Huntington's Disease (Francelle et al. 2015).

THs and Their Receptors

THs are crucial affecters of metabolism and thermogenesis, with 30% of resting energy expenditure under their control (Silva 2005). Significant changes in the levels of THs lead to illness. Hypothyroidism can cause depression, cardiovascular disease, fatigue and lethargy, and weight gain, among other consequences (Bello and Bakari 2012). Conversely, hyperthyroidism results in a wide range of largely distinct maladies, such as heart palpitations, fatigue, weight loss, and muscle weakness, among others (Mansourian 2010). Given their centrality to biological systems, the production of THs is under tight regulation.

Regulation and Synthesis of TH

TH production is governed by the Hypothalamic-Pituitary-Thyroid axis (Mendoza and Hollenberg 2017). Thyrotropin-releasing hormone neurons located in the paraventricular nucleus of the hypothalamus control secretion of thyrotropin releasing hormone (TRH) in response to THs (Morley 1979; Yarbrough 1979), Agouti Related Peptide (AgRP) (Fekete et al. 2002), Neuropeptide Y (NPY) (Fekete et al. 2001), cocaine and amphetamine-regulated transcript (Serrano et al.) Serrano et al. 2014; (Fekete et al. 2000), norepinephrine (Zimmermann et al. 2001), and leptin (Harris et al. 2001). These factors are directly and indirectly regulated by environmental stimuli such as cold exposure (Sotelo-Rivera et al. 2017), teat suckling (Sánchez et al. 2001), and shortage of food (Légrádi et al. 1997; Mihály et al. 2000) and the TH feedback loop, among other factors (Rodríguez-Rodríguez et al. 2019).

Upon secretion of TRH by the hypothalamus, the hormone enters fenestrated primary portal capillaries connected to the anterior pituitary pars distalis (Rodríguez-Rodríguez et al. 2019). TRH binding to its receptor (TRH receptor 1) in the anterior

pituitary induces the synthesis and release of thyroid stimulating hormone (TSH) (Heuer et al. 2000; Snyder and Utiger 1972). TSH then travels via the bloodstream to the thyroid gland where it binds TSH receptors (Schaefer and Klein 2011). This binding promotes the synthesis and release of the THs, T₃ and T₄. Approximately 80% of THs produced by the thyroid gland are T₄ (Pirahanchi, Tariq, and Jialal 2020) while 80% of T₃ comes from the peripheral deiodination of T₄ (Schimmel and Utiger 1977), with the remaining T₃ fraction generated by the intrathyroidal deiodination of T₄ and by the direct synthesis of T₃ within the thyroid gland itself (Dème et al. 1975; Kubota et al. 1984). T₃ and T₄ then travel via the bloodstream to peripheral organs, where they are taken up.

Thyroid Hormone Transport

THs are transported into cells primarily by *SLC16A2* (MCT8), *SLC16A10* (MCT10), and *SLCO1C1* (OATP1C1), which are largely specific transporters for T₃ and T₄ (Visser, Friesema, and Visser 2011). THs are also transported through more broadly acting transporters as well, such as *SLC10A1* (Friesema et al. 1999; Visser et al. 2010), *ABCB1* (efflux) (Mitchell, Tom, and Mortimer 2005), *SLC7A5* and *SLC3A2* (LAT1 and 4F2hc respectively, acting as a heterodimer), *SLC7A8* and *SLC3A2* (LAT2 and 4F2hc respectively, acting as a heterodimer) (Jansen et al. 2005), and thirteen organic anion transporting polypeptides (OATP) (Jansen et al. 2005). Once in the cell, deiodinases remove one or more iodine atoms from T₄ or T₃ to convert T₄ into T₃ or reverse T₃ (rT₃). T₃ and rT₃ can be converted into T₂. Deiodinase 1 (*DIO1*) is responsible for the production of T₃, rT₃, and T₂. Deiodinase 2 (*DIO2*) produces T₃ from T₄, and T₂ from rT₃. Finally, deiodinase 3 (*DIO3*) is capable of producing rT₃ and T₂ from T₄ and T₃ respectively

(Pihlajamäki et al. 2009; Williams and Bassett 2011). rT_3 and T_2 are largely inactive biologically (Beckett and Arthur 1994; Senese et al. 2014).

Thyroid Receptors

In mammals, THs, primarily in the form of T_3 , bind to nuclear TRs $\alpha 1$ (Sap et al. 1986; Weinberger et al. 1986), $\beta 1$ (Jhanwar, Chaganti, and Croce 1985), $\beta 2$ (Hodin et al. 1989), $\beta 3$ [rodent only] (Williams 2000), and $\beta 4$ (Tagami et al. 2010). T_3 can also bind to mitochondrial TRs p43 (Casas et al. 1999) and p28 (Sterling, Campbell, and Brenner 1984), and to the plasma membrane TR p30 TR $\alpha 1$ (Kalyanaraman et al. 2014). A number of additional isoforms of the TR subunits can be generated through alternative splicing of the *THRA* and *THRB* genes, including $\Delta\alpha 1$, $\Delta\alpha 2$ (Chassande et al. 1997), $\alpha 2$, $\alpha 3$, $\alpha\Delta E6$ (Pantos and Mourouzis 2018), and $\Delta\beta 3$ [rodent only] (Williams 2000). These do not bind TH and most instead act in a dominant negative fashion, competing against TH bound TRs for TRE sites in the genome (Casas et al. 2006; O'shea and Williams 2002; Raparti et al. 2013; Watanabe and Weiss 2018).

T_3 binds to TRs with a $K_D = 0.06$ nM. T_4 can also bind to thyroid hormone receptors, though with a much lower affinity, $K_D = 2$ nM (Sandler et al. 2004). TH binding to TRs alters the conformation of the protein affecting its ability to bind DNA (Apriletti et al. 1998). TRs act as transcriptional regulators as ligand-bound or unbound monomers, homodimers, heterotrimers, homotrimers (Mengeling, Pan, and Privalsky 2005), or most commonly as heterodimers with retinoid X receptors (RXR) (Velasco et al. 2007). TRs bind to thyroid hormone response elements (TREs), sequences in the genome that regulate transcription of associated genes. There are three consensus TRE sequences: direct repeat

4 (DR4) AGGTCAnnnnAGGTCA, a palindrome AGGTCATGACCT, and an inverted palindrome with a 6 base pair gap (IP6) TGACCTnnnnnnAGGTCA (Liu, Milanesi, and Brent 2020). Both unliganded and ligand-bound TRs can bind TREs to repress or promote transcription (Graupner et al. 1989). Some TRE sites are bound by unliganded TR and prevent transcription until TH binds to the receptor, while some TRE sites are repressed by TH-bound TR. The same is true with TRs acting as transcriptional activators (Eckey, Moehren, and Baniahmad 2003). There are many different ways activation or repression of gene expression can occur through the multitude of THs, TRs, RXRs, TREs, and various combinations thereof. The diversity of mechanisms by which THs can act through TRs, RXRs and TREs may help explain its ability to regulate so many different cellular and bodily functions and physiology, and why regulation of the unifying factor, TH, is so important.

μ -Crystallin (*CRYM*)

CRYM, the gene encoding CRYM mRNA and the μ -crystallin protein, is located at 16p12.2 in the human genome. The gene is 64.2 kb long, encoding a protein of 314 amino acids with a calculated molecular mass of 33.8 kD. Similarly, in mice, the *Crym* gene is located at 7qF2, is 15.7 kb long, and encodes a 313 amino acid protein, with a calculated molecular mass of 33.5 kD. μ -Crystallin binds strongly to T₃ with a K_D = 0.3 nM (Beslin et al. 1995) [see also Hallen et al. 2015a]. The crystal structure of mouse μ -crystallin has been solved to 1.75 Å. Five residues in the protein form a potassium ion binding pocket: Leu130, Gly219, Cys283, Lys285, and Thr287 (Borel et al. 2014). T₃ binds to murine μ -crystallin through the hydrophobic interactions of Phe58, Phe79, and Val49 as well as Arg229.

Ser228 and Arg47 form hydrogen bonds with T₃. Finally, Lys75, Arg118, Ser228, and Leu292 interact with T₃ through water molecules (Borel et al. 2014).

μ-Crystallin in Animals

μ-Crystallin may play a role in adapting metabolism to meet the specific energetic requirements determined by genetic and environmental factors. Joshi et al. showed in 2017 that the sleeping breath rate of female *Crym* knockout (KO) mice was higher than controls (Joshi et al. 2019). Serum T₃ and T₄ concentrations are decreased while influx and efflux of T₃ is increased in *Crym* KO mice (Suzuki et al. 2007). It's possible that *Crym* KO mice have higher levels of anaerobic glycolysis due to lower levels of free cytoplasmic TH, causing an increased buildup of lactate, which may be indirectly cleared by a higher breath rate (Ducros and Trippenbach 1991). Indeed, *Crym* KO mice had hypertrophy of glycolytic fast twitch Type IIb muscle fibers (Seko et al. 2016) and when *Crym* KO mice were placed on a high fat diet they had increased fat mass as assayed by computer tomography compared to control mice on the same diet (Ohkubo et al. 2019).

μ-Crystallin appears to play an important role in environmental and metabolic adaptation in other mammals as well. *CRYM* levels in the hypothalamus of dogs are significantly lower than in the hypothalami of wolves and coyotes (Saetre et al. 2004). This may be a difference in regulation of TRH production since TRH is produced in the hypothalamus which ultimately causes the production of TH. TH in the hypothalamus acts in a negative feedback loop to inhibit the production of TRH (Fekete and Lechan 2007). Lower levels of *CRYM* in the hypothalami of dogs may allow for greater inhibitory effects of TH on TRH production, reflecting adaptation to differences in food availability and

shelter of domesticated dogs versus wolves and coyotes. Mukai et al. (2009) used microarrays and qPCR to measure decreased levels of *CRYM* in the hypothalamus of song sparrows in autumn compared to spring, (Mukai et al. 2009) possibly implicating μ -crystallin again in controlling metabolic rate in relation to seasonal changes and the availability of food. Hinaux noted polymorphisms present in *crym* in *Astyanax mexicanus* surface fish compared to the same species of fish that dwell in caves devoid of any light and plentiful food sources (Hinaux et al. 2015). Curiously, the skeletal muscles of the cavefish are resistant to insulin, and the fish have a lower metabolic rate and higher percent of body fat than their surface-dwelling cousins (Ojha and Watve 2018). Chinese Erhualian pigs express 16-26 times more *CRYM* in their subcutaneous fat than in their visceral fat (intramuscular, retroperitoneal, and mesenteric adipose tissue) and *CRYM* is one of only seven genes specifically enriched in subcutaneous fat compared to visceral fat pads (Liu et al. 2019). Similarly, humans express 2.6-3.0 times more *CRYM* in their subcutaneous fat compared to their visceral fat (Serrano et al. 2014). Taken together, μ -crystallin may play a role in the metabolic adaptation of organisms to the energy requirements and food availability in their environments.

μ -Crystallin as a Ketimine Reductase

Although μ -Crystallin accounts for approximately a quarter of total lens protein in some Australian marsupials, the protein does not share sequence homology with other crystallins (Wistow and Kim 1991). Rather, mammalian μ -crystallin shares 31–33% amino acid sequence identity with bacterial ornithine cyclodeaminases (Kim, Gasser, and Wistow 1992) and 30% sequence identity with archaeal AF1665 AlaDH (Gallagher et al. 2004),

suggesting a potential role for μ -crystallin in amino acid metabolism. Consistent with this, μ -crystallin is a ketimine reductase and uses both NADH and NADPH as a cofactor (Hallen et al. 2011). μ -Crystallin acts on naturally occurring ketimines present in lysine degradation, Δ^1 -piperidine-2-carboxylate (P2C) and an analog of P2C, Δ^1 -pyrroline-2-carboxylate (Pyr2C), at neutral pH (7.2) and more efficiently at an acidic pH (5.0) (Hallen and Cooper 2017; Hallen et al. 2011; Hallen, Cooper, Jamie, et al. 2015; Hallen, Cooper, Smith, et al. 2015). Interestingly, μ -crystallin's activity as a ketimine reductase is competitively inhibited by sub-nanomolar concentrations of T_3 and T_4 , with $K_I = 0.60$ nM and $K_I = 0.75$ nM, respectively (compared to T_3 , which binds with a $K_D = 0.3$ nM) (Beslin et al. 1995). T_2 and rT_3 only minimally inhibit μ -crystallin (Hallen, Cooper, Jamie, et al. 2015). μ -Crystallin has been proposed to play a role in the pipecolate pathway, the dominant lysine degradation pathway in the brain, as opposed to the saccharopine pathway, which breaks down lysine in the rest of the body (Hallen and Cooper 2017).

CRYM and Disease

CRYM Expression in the Brain

Crym is highly specific to certain regions and cell types in the brain. Kim et al. (1992) were the first to measure μ -crystallin in the brain of kangaroo and humans in 1992. Arlotta et al. (2005) identified μ -crystallin expression in some corticospinal motor neurons and subcerebral neurons of layer V of the cerebral cortex. There is increased staining of μ -crystallin in the hippocampus with higher expression distal to the dentate gyrus of mice, and gradually diminishing proximally (Lein et al. 2007). Fink et al. (2015) showed μ -crystallin expression in the cortex to be limited to spinally projecting corticospinal motor

neurons, and not in layer V neurons sending projections either intracortically or corticofugally. They also documented μ -crystallin in the dorsal, lateral, and ventral funiculi of the cervical and lumbar spinal cord and spinal gray matter of mice.

CRYM mRNA in man is expressed in most areas of the brain assessed by GTEx (amygdala, anterior cingulate cortex, caudate, cerebellar hemisphere, cerebellum, cortex, frontal cortex, hippocampus, nucleus acumbens, putamen) but not in the substantia nigra or the spinal cord (Lonsdale et al. 2013). The absence of *CRYM* mRNA in human spinal cord does not agree with the findings of Fink et al. (Fink, Strittmatter, and Cafferty 2015) in mice. This incongruency may be due to a difference in species, condition, or due to temporal expression of mRNA versus protein. At the mRNA level the nucleus acumbens expresses the most *CRYM* (Lonsdale et al. 2013). Because labeling for μ -crystallin can clearly delineate the neuronal structures in the brain many researchers use its expression as a regional marker.

Huntington's Disease

μ -Crystallin's increased presence and function in the brain may have implications for disease. *CRYM* expression is significantly decreased in human caudate nucleus and cerebellum in individuals with Huntington's disease (Hodges et al. 2006). *Crym* also shows decreased expression in the brains of R6/2, BACHD, and Knock-In 140 CAG mice (Brochier et al. 2008; Francelle et al. 2015), murine models of Huntington's disease, and may play a neuroprotective role in striatal medium-size spiny neurons in Huntington's disease (Francelle et al. 2015).

Amyotrophic Lateral Sclerosis

μ -Crystallin has also been associated with amyotrophic lateral sclerosis (ALS). In a mouse model of familial ALS, $SOD1^{L126delTT}$, *Crym* shows an approximately 26-fold increase in expression in the spinal cord from pre-symptomatic to post-symptomatic mice (Fukada et al. 2007). Two mutations, R169C and H16P, in *CRYM* have been associated with sporadic ALS (Daoud et al. 2011); a recurrent mutation has also been identified in a mixed pool of familial and sporadic ALS patients (Pensato et al. 2020). The human *CRYM* gene is approximately 2.7 Mb away from a 37.8 Mb locus with genetic linkage to familial ALS (Sapp et al. 2003). μ -Crystallin progressively decreases in expression in the pyramidal tracts in ALS patients, in a mosaic expression pattern and leading to its total absence in the distal regions of the pyramidal tract (e.g., lateral and anterior corticospinal tracts of the spinal cord). Hommyo et al. (2018) suggest that this expression pattern may reflect the “dying back” phenomenon, in which progressive neurodegeneration begins with more distal tissues and axons. In addition, miR-155 and miR-142, predicted to be regulators of *CRYM*, are increased in the spinal cord of individuals with sporadic ALS (Figueroa-Romero et al. 2016).

Schizophrenia

Individuals with schizophrenia show decreased *CRYM* in Brodmann area (BA) 9 of the dorsal prefrontal cortex (PFC) (Arion et al. 2007; Middleton et al. 2002), as well as BA 46 of the PFC at the mRNA (Martins-de-Souza, Gattaz, Schmitt, Rewerts, et al. 2009) and protein level (Martins-de-Souza, Gattaz, Schmitt, Maccarrone, et al. 2009). Martins-de-Souza et al. (2010) reported the decreased expression of μ -crystallin in the mediodorsal

thalamus of the brain in individuals with schizophrenia as well as a negative correlation between μ -crystallin levels and duration of the disease. By contrast, Hakak et al. (2001) reported increased levels of *CRYM* in BA 46 of the PFC in individuals with schizophrenia. μ -Crystallin also increases in the corpus callosum of individuals with schizophrenia (Sivagnanasundaram et al. 2007).

CRYM is not implicated broadly in many neurologic disorders, however. For example, no associations between major depressive disorder or bipolar disorder have been observed (Beasley et al. 2006; Johnston-Wilson et al. 2000).

CRYM as a Potential Therapeutic for Psychiatric Disorders

CRYM appears to play an important, though yet unknown, role in the brain. Walker et al. (2020) show that *Crym* overexpression in the medial amygdala of adult mice can recapitulate the transcriptional and behavioral effects of adolescent social isolation. Amazingly, social isolation of adult mice does not result in these same changes, suggesting that *Crym* overexpression in the medial amygdala of adult mice can revert the brain to a more plastic state associated with adolescence (Walker et al. 2020). This raises the eventual possibility, though technically still unachievable, that overexpressing *CRYM* in human medial amygdala could be used to reprogram individuals to become more resilient to some psychiatric disorders (Walker et al. 2020).

CRYM and Non-Syndromic Deafness

Autosomal dominant deafness-40 (DFNA40), a non-syndromic deafness in man, is the only disease that is currently known to be caused by mutations in *CRYM*. It is not associated

with any intellectual, structural or other dysfunctions. Two heterozygous mutations were identified at the C-terminus of μ -crystallin, X315Y and K314T. The K314T mutation segregated in an autosomal dominant fashion, while the X315Y mutation was a *de novo* change (Abe et al. 2003). A third heterozygous mutation, P51L was later found to associate with DFNA40. This mutation also segregates in an autosomal dominant fashion, further confirming the inheritance pattern of DFNA40 (!!! INVALID CITATION !!!). The severity of hearing loss varies with the mutations noted above. Moderate bilateral hearing impairment (50–60 dB) has been observed in the individual with the X315Y mutation, starting at 19 months of age and progressing to a hearing loss of 70 dB by age 13. Individuals with the K314T show severe bilateral hearing loss (80–90 dB) starting at 1 year old, with no further progression (Abe et al. 2003). Individuals with the P51L mutation have moderate to severe hearing loss (50–110 dB) without progression, though only one individual was followed for 4 years (!!! INVALID CITATION !!!).

Correlating these auditory changes with changes in the activities of μ -crystallin is challenging. The X315Y mutation in μ -crystallin showed a similar binding affinity to T_3 as wild type μ -crystallin, but the K314T mutation in μ -crystallin was unable to bind to T_3 at all (Oshima et al. 2006). When expressed in COS-7 cells, the X315Y mutation in μ -crystallin localizes to vacuoles and the K314T mutation in μ -crystallin localizes perinuclearly, in contrast to the wild type protein, which is cytoplasmically distributed (Abe et al. 2003). Although Crym-X315Y can bind T_3 , its sequestration in vacuoles may reduce its access to cytoplasmic THs. Alternatively, these μ -crystallin mutants may affect potassium ion recycling of the endolymph, a function of lateral fibrocytes of the spiral

ligaments and the spiral limbus fibrocytes, where *Crym* is highly expressed (Abe et al. 2003).

Genetics of *CRYM*

CRYM has a mutation rate of $10^{-4.9127}$ mutations per chromosome (Samocha et al. 2014), which is outside the definition of a constrained gene (Samocha et al. 2014), i.e. a gene in which mutations are likely deleterious and result in their negative selection and removal from the gene pool. Congruent with the mutation rate, there are 209 “common” mutations (variants with a minor allele frequency [MAF] of at least 1%) in the 1000 Genomes Phase 3 dataset (www.internationalgenome.org/data). However, there is only one common exonic variant, rs34045013, a synonymous mutation in exon 8. Rs34045013 is only a common variant in African populations; its MAF does not rise to a frequency of 1% in European, East Asian, South Asian, or American populations in the 1000 Genomes Phase 3 dataset, though it is a common variant in the African American population examined in the GO Exome Sequencing Project (Tennessen et al. 2012). To the best of our knowledge, there are no *CRYM* null individuals. One individual has been identified with copy number loss of one chromosome [GRCh37/hg19 16p12.2(chr16:21313377-21947230)x1] where exon 1 of *CRYM* transcript variant 1 (RefSeq ID: NM_001888.5), the longer of the two *CRYM* variants observed in humans, is lost. A second individual shows a homozygous deletion [GRCh37/hg19 16p12.2(chr16:21300997-21308651)x0] of either intron 1 of *CRYM* transcript variant 1, or the putative promoter/upstream region of *CRYM* transcript variant 2 (RefSeq ID: NM_001376256.1). In contrast to the absence of *CRYM* null individuals, there are 22 individuals with a *CRYM* copy number gain (3 copies as opposed

to the normal 2 [diploid] copies) and one individual with maternal uniparental disomy without copy number change in NCBI ClinVar.

Rs3848259 is a “common” variant that occurs in the 5’ untranslated region (UTR) of *CRYM* transcript variant 1 and is upstream of *CRYM* transcript variant 2. Rs3848259 is present in approximately 24.8% of the European population while being present in only 5.0% of the African population according to data from the ALFA Project (Phan et al. 2020). Furthermore, rs3848259 is located in a DNase hypersensitive region (Miga, Eisenhart, and Kent 2015), a *ZIC3* and *ZNF341* transcription factor binding site (Fornes et al. 2020), and a CpG island (Gardiner-Garden and Frommer 1987). Rs3848259 alters one of the two most conserved base pairs in the DNA binding sequence motif of *ZIC3*, CC(C/T)GCTGGG (Ahmed et al. 2020) (underlined), from a cytosine to a guanine. This may inhibit the transcription factor *ZIC3* from binding to the 5’UTR/genic upstream region potentially affecting transcription of *CRYM*. In one of the two consensus DNA binding motifs in *ZNF341*, rs3848259 affects a non-conserved base pair in the sequence, TGGAACAGCCNC (underlined) (Béziat et al. 2018; Frey-Jakobs et al. 2018).

Because it is located in an epigenetically active region in the 5’UTR of *CRYM* transcript variant 1 and upstream of *CRYM* transcript variant 2, rs3848259 and its effects on *ZIC3* and *ZNF341* binding may alter transcription of *CRYM* in the approximately 25% of individuals of European descent and 5% of individuals of African descent in whom this common variant is found. Humans display a wide range of expression of *CRYM* in skeletal muscle. In 803 transcriptomes in GTEx Analysis V8, *CRYM* levels vary from 0 transcripts per million (TPM) to 39.1 TPM with a median of 0.1584 TPM. Most people express little to no *CRYM* in their skeletal muscle, yet 15.44% express 2 TPM of *CRYM* or more, and

5.85% of people express *CRYM* at levels of 10 TPM or greater (Lonsdale et al. 2013). SNPs like rs3848259 as well as other factors may play a role in the large degree of heterogeneity of *CRYM* expression seen skeletal muscle.

Effects of High Crym Expression

μ -Crystallin has been shown to modulate TH levels. Precise control of TH levels is crucial to physiology and metabolism. Serious diseases can arise from inadequate or overabundant levels of TH. Nevertheless, the most abundant tissue in humans, skeletal muscle, displays a wide range of *CRYM* levels (Lonsdale et al. 2013). What effects does μ -crystallin have in individuals who express high levels of μ -crystallin? Kinney et al. explored this question with a transgenic murine model that specifically overexpresses *Crym* in skeletal muscle (Kinney et al. 2021).

Along with a 27.5- to 154-fold increase of *Crym* mRNA and a 2.6- to 147.5-fold increase of μ -crystallin protein, depending on skeletal muscle, Kinney et al. (2021) observed a 192-fold increase in T_3 in extracts of tibialis anterior (TA) muscle and a 1.2-fold decrease of serum T_4 in *Crym* tg mice compared to control mice. Both changes were significant. The large increase in intramuscular T_3 due to the increased expression of *Crym* may be the cause for some of the phenotypes they observed in *Crym* tg mice.

Crym tg mice have a decreased respiratory exchange ratio (RER), a metric that can be used to discriminate between carbohydrates and fat as energy sources (Lusk 1924). This decreased RER in *Crym* tg mice corresponds to a 13.7% shift towards increased utilization of fat as an energy source compared to controls. Consistent with this, gene ontology (GO) enrichment analysis of RNA-seq transcriptomic and LC.MS/MS proteomic data revealed

significantly enriched ontological terms involving metabolism and muscle contraction. Kinney et al. (2021) found that almost all fiber types in *Crym* tg mouse soleus (but not TA) muscle had a smaller minimum Feret's diameter. Other groups have shown that slow twitch muscles like the soleus (Close 1965) mostly utilize β -oxidation of fat as opposed to fast twitch muscles that primarily utilize glycolysis of carbohydrates (Kalmar, Blanco, and Greensmith 2012) and have smaller fiber sizes (Schiaffino and Reggiani 2011). Thyrotoxic doses of TH cause shifts in slow twitch mouse soleus, but not in fast twitch extensor digitorum longus (Freake and Oppenheimer) muscle towards faster twitch characteristics such as shortened isometric twitch duration and increased rate of tension development (Fitts et al. 1984). By these metrics, TH has a greater impact on slow twitch muscle than fast twitch muscle. Taken together, the shift in metabolism from glycolytic towards β -oxidative in *Crym* tg mice, the concomitant GO terms at the transcriptomic and proteomic level, and the smaller soleus muscle fibers and the unchanged fiber sizes in fast twitch TA in the TH rich muscle of *Crym* tg mice all point towards μ -crystallin shifting the metabolic and morphologic state of the muscle through the regulation of TH. Although this is difficult to reconcile with the fact that most muscle fibers in mice are fast twitch, a large proportion of them are also oxidative (i.e., Type IIA) and thus may be subject to the same shifts in gene regulation and morphology induced by *Crym* and T_3 as soleus.

Although *Crym* tg mice show significant alterations in metabolism, transcripts and proteins expressed, and fiber size of slow twitch muscle, *Crym* tg mice do not show significant differences compared to controls in a number of physiologic tests including: specific isometric force of contraction, maximal rate of twitch force contraction/relaxation, grip strength, maximum treadmill running speed, and voluntary distance run. Fiber type as

assayed by immunohistochemistry of myosin heavy chains, weight of most muscles and fat pads, diameter of TA muscle, percent of centrally nucleated fibers, voltage-induced Ca^{2+} transients, maximal amplitudes of transients and transient decay rates, total number of muscle fibers, and intramuscular fat were also unchanged compared to control mice (Kinney et al. 2021). *Crym* therefore appears to play an important but subtle role in skeletal muscle, through a mechanism that remains unknown.

Conclusion

μ -Crystallin binds thyroid hormones and can act as a ketimine reductase in the brain when unbound by TH. As demonstrated by a number of studies, μ -crystallin plays a crucial role in regulating the availability and level of thyroid hormone. Consequently, it's of no surprise that μ -crystallin expression is tightly regulated both temporally and spatially. When mutated at particular moieties, μ -crystallin becomes less active or mislocalized, leading to nonsyndromic deafness, DFNA40. Inappropriate expression of *CRYM* may be involved in several neurologic disorders as well. Despite this tight regulation in many tissues, men and women can express a wide range of *CRYM* in their skeletal muscle. The regulatory elements that lead to this difference are still unknown, and the physiological consequences to humans with high vs. low levels of muscle *CRYM* are still unclear. Our studies of transgenic mice that express high levels of muscle μ -crystallin suggest that the physiological consequences are significant but subtle, with perhaps the most intriguing result indicating a change in the use of fat vs. carbohydrate as an energy source. For now, however, *CRYM*'s physiological role remains to be determined. Future studies will help define its function at the cellular, tissue and system levels.

Bibliography

Abdalla SM, Bianco AC. Defending plasma T3 is a biological priority. *Clin Endocrinol (Oxf)* 81, 633–641, 2014.

Abe S, Katagiri T, Saito-Hisaminato A, Usami S, Inoue Y, Tsunoda T, Nakamura Y. Identification of CRYM as a candidate responsible for nonsyndromic deafness, through cDNA microarray analysis of human cochlear and vestibular tissues. *Am J Hum Genet* 72, 73–82, 2003.

Ahmed JN, Diamand KEM, Bellchambers HM, Arkell RM. Systematized reporter assays reveal ZIC protein regulatory abilities are Subclass-specific and dependent upon transcription factor binding site context. *Sci Rep* 10, 13130, 2020.

Apriletti JW, Ribeiro RC, Wagner RL, Feng W, Webb P, Kushner PJ, West BL, Nilsson S, Scanlan TS, Fletterick RJ, Baxter JD. Molecular and structural biology of thyroid hormone receptors. *Clin Exp Pharmacol Physiol Suppl* 25, S2–S11, 1998.

Arion D, Unger T, Lewis DA, Levitt P, Mirnics K. Molecular evidence for increased expression of genes related to immune and chaperone function in the prefrontal cortex in schizophrenia. *Biol Psychiatry* 62, 711–721, 2007.

Arlotta P, Molyneaux BJ, Chen J, Inoue J, Kominami R, Macklis JD. Neuronal subtype-specific genes that control corticospinal motor neuron development in vivo. *Neuron* 45, 207–221, 2005.

Beasley CL, Pennington K, Behan A, Wait R, Dunn MJ, Cotter D. Proteomic analysis of the anterior cingulate cortex in the major psychiatric disorders: evidence for disease-associated changes. *Proteomics* 6, 3414–3425, 2006.

Beckett GJ, Arthur JR. 3 The iodothyronine deiodinases and 5'-deiodination. *Baillière's clinical endocrinology and metabolism* 8, 285–304, 1994.

Bello F, and Bakari A. Hypothyroidism in adults: A review and recent advances in management. *J Diabetes Endocrinol* 3, 57–69, 2012.

Beslin A, Vie MP, Blondeau JP, Francon J. Identification by photoaffinity labelling of a pyridine nucleotide-dependent tri-iodothyronine-binding protein in the cytosol of cultured astroglial cells. *Biochem J* 305, 729–737, 1995.

Beziat V, Li J, Lin JX, Ma CS, Li P, Bousfiha A, Pellier I, Zoghi S, Baris S, Keles S, Gray P, Du N, Wang Y, Zerbib Y, Levy R, Leclercq T, About F, Lim AI, Rao G, Payne K, Pelham SJ, Avery DT, Deenick EK, Pillay B, Chou J, Guery R, Belkadi A, Guerin A, Migaud M, Rattina V, Ailal F, Benhsaien I, Bouaziz M, Habib T, Chaussabel D, Marr N, El-Benna J, Grimbacher B, Wargon O, Bustamante J, Boisson B, Müller-Fleckenstein I,

Fleckenstein B, Chandesris MO, Titeux M, Fraitag S, Alyanakian MA, Leruez-Ville M, Picard C, Meyts I, Di Santo JP, Hovnanian A, Somer A, Ozen A, Rezaei N, Chatila TA, Abel L, Leonard WJ, Tangye SG, Puel A, Casanova JL. A recessive form of hyper-IgE syndrome by disruption of ZNF341-dependent STAT3 transcription and activity. *Sci Immunol* 3, eaat4956, 2018.

Borel F, Hachi I, Palencia A, Gaillard MC, Ferrer JL. Crystal structure of mouse mu-crystallin complexed with NADPH and the T3 thyroid hormone. *FEBS J* 281, 1598–1612, 2014.

Brent GA. Mechanisms of thyroid hormone action. *J Clin Invest* 122, 3035–3043, 2012.

Brochier C, Gaillard MC, Diguët E, Caudy N, Dossat C, Segurens B, Wincker P, Roze E, Caboche J, Hantraye P, Brouillet E, Elalouf JM, de Chaldee M. Quantitative gene expression profiling of mouse brain regions reveals differential transcripts conserved in human and affected in disease models. *Physiol Genomics* 33, 170–179, 2008.

Casas F, Rochard P, Rodier A, Cassar-Malek I, Marchal-Victorion S, Wiesner RJ, Cabello G, Wrutniak C. A variant form of the nuclear triiodothyronine receptor $\alpha 1$ plays a direct role in regulation of mitochondrial RNA synthesis. *Mol Cell Biol* 19, 7913–7924, 1999.

Casas F, Busson M, Grandemange S, Seyer P, Carazo A, Pessemesse L, Wrutniak-Cabello C, Cabello G. Characterization of a novel thyroid hormone receptor α variant involved in the regulation of myoblast differentiation. *Mol Endocrinol* 20, 749–763, 2006.

Chassande O, Fraichard A, Gauthier K, Flamant F, Legrand C, Savatier P, Laudet V, Samarut J. Identification of transcripts initiated from an internal promoter in the c-erbA alpha locus that encode inhibitors of retinoic acid receptor-alpha and triiodothyronine receptor activities. *Mol Endocrinol* 11, 1278–1290, 1997.

Chopra IJ. A study of extrathyroidal conversion of thyroxine (T₄) to 3, 3', 5-triiodothyronine (T₃) in vitro. *Endocrinology* 101, 453–463, 1977.

Close R. Force: velocity properties of mouse muscles. *Nature* 206, 718–719, 1965.

Daoud H, Valdmanis PN, Gros-Louis F, Belzil V, Spiegelman D, Henrion E, Diallo O, Desjarlais A, Gauthier J, Camu W, Dion PA, Rouleau GA. Resequencing of 29 candidate genes in patients with familial and sporadic amyotrophic lateral sclerosis. *Arch Neuro* 68, 587–593, 2011.

Deme D, Fimiani E, Pommier J, Nunez J. Free diiodotyrosine effects on protein iodination and thyroid hormone synthesis catalyzed by thyroid peroxidase. *Eur J Biochem* 51, 329–336, 1975.

Ducros G, Trippenbach T. Respiratory effects of lactic acid injected into the jugular vein of newborn rabbits. *Pediatr Res* 29, 548–552, 1991.

Eckey M, Moehren U, Baniahmad A. Gene silencing by the thyroid hormone receptor. *Mol Cell Endocrinol* 213, 13–22, 2003.

Fekete C, Mihaly E, Luo LG, Kelly J, Clausen JT, Mao Q, Rand WM, Moss LG, Kuhar M, Emerson CH, Jackson IM, Lechan RM. Association of cocaine- and amphetamine-regulated transcript-immunoreactive elements with thyrotropin-releasing hormone-synthesizing neurons in the hypothalamic paraventricular nucleus and its role in the regulation of the hypothalamic-pituitary-thyroid axis during fasting. *J Neurosci* 20, 9224–9234, 2000.

Fekete C, Kelly J, Mihaly E, Sarkar S, Rand WM, Legradi G, Emerson CH, Lechan RM. Neuropeptide Y has a central inhibitory action on the hypothalamic-pituitary-thyroid axis. *Endocrinology* 142, 2606–2613, 2001.

Fekete C, Sarkar S, Rand WM, Harney JW, Emerson CH, Bianco AC, Lechan RM. Agouti-related protein (AGRP) has a central inhibitory action on the hypothalamic-pituitary-thyroid (HPT) axis; comparisons between the effect of AGRP and neuropeptide Y on energy homeostasis and the HPT axis. *Endocrinology* 143, 3846–3853, 2002.

Fekete C, Lechan RM. Negative feedback regulation of hypophysiotropic thyrotropin-releasing hormone (TRH) synthesizing neurons: role of neuronal afferents and type 2 deiodinase. *Front Neuroendocrinol* 28, 97–114, 2007.

Figuroa-Romero C, Hur J, Lunn JS, Paez-Colasante X, Bender DE, Yung R, Sakowski SA, Feldman EL. Expression of microRNAs in human post-mortem amyotrophic lateral sclerosis spinal cords provides insight into disease mechanisms. *Mol Cell Neurosci* 71, 34–45, 2016.

Fink KL, Strittmatter SM, Cafferty WB. Comprehensive Corticospinal Labeling with mu-crystallin Transgene Reveals Axon Regeneration after Spinal Cord Trauma in *ngr1*^{-/-} Mice. *J Neurosci* 35, 15403–15418, 2015.

Fitts RH, Brimmer CJ, Troup JP, Unsworth BR. Contractile and fatigue properties of thyrotoxic rat skeletal muscle. *Muscle Nerve* 7, 470–477, 1984.

Fornes O, Castro-Mondragon JA, Khan A, van der Lee R, Zhang X, Richmond PA, Modi BP, Correard S, Gheorghe M, Baranasic D, Santana-Garcia W, Tan G, Cheneby J, Ballester B, Parcy F, Sandelin A, Lenhard B, Wasserman WW, Mathelier A. JASPAR 2020: update of the open-access database of transcription factor binding profiles. *Nucleic Acids Res* 48, D87–D92, 2020.

Francelle L, Galvan L, Gaillard MC, Guillermier M, Houitte D, Bonvento G, Petit F, Jan C, Dufour N, Hantraye P, Elalouf JM, De Chaldee M, Deglon N, Brouillet E. Loss of the

thyroid hormone-binding protein Crym renders striatal neurons more vulnerable to mutant huntingtin in Huntington's disease. *Hum Mol Genet* 24, 1563–1573, 2015.

Freake HC, Oppenheimer JH. Thermogenesis and thyroid function. *Annu Rev Nutr* 15, 263–291, 1995.

Frey-Jakobs S, Hartberger JM, Fliegau M, Bossen C, Wehmeyer ML, Neubauer JC, Bulashevskaya A, Proietti M, Frobel P, Noltner C, Yang L, Rojas-Restrepo J, Langer N, Winzer S, Engelhardt KR, Glocker C, Pfeifer D, Klein A, Schaffer AA, Lagovsky I, Lachover-Roth I, Beziat V, Puel A, Casanova JL, Fleckenstein B, Weidinger S, Kilic SS, Garty BZ, Etzioni A, Grimbacher B. ZNF341 controls STAT3 expression and thereby immunocompetence. *Sci Immunol* 3, eaat4941, 2018.

Friesema EC, Docter R, Moerings EP, Stieger B, Hagenbuch B, Meier PJ, Krenning EP, Hennemann G, Visser TJ. Identification of thyroid hormone transporters. *Biochem Biophys Res Commun* 254, 497–501, 1999.

Fukada Y, Yasui K, Kitayama M, Doi K, Nakano T, Watanabe Y, Nakashima K. Gene expression analysis of the murine model of amyotrophic lateral sclerosis: studies of the Leu126delTT mutation in SOD1. *Brain Res* 1160, 1–10, 2007.

Gallagher DT, Monbouquette HG, Schroder I, Robinson H, Holden MJ, Smith NN. Structure of alanine dehydrogenase from *Archaeoglobus*: active site analysis and relation

to bacterial cyclodeaminases and mammalian mu crystallin. *J Mol Biol* 342, 119–130, 2004.

Gardiner-Garden M, Frommer M. CpG islands in vertebrate genomes. *J Mol Biol* 196, 261–282, 1987.

Graupner G, Wills KN, Tzukerman M, Zhang XK, Pfahl M. Dual regulatory role for thyroid-hormone receptors allows control of retinoic-acid receptor activity. *Nature* 340, 653–656, 1989.

GTEX Consortium. The Genotype-Tissue Expression (GTEx) project. *Nat Genet* 45, 580–585, 2013.

Hakak Y, Walker JR, Li C, Wong WH, Davis KL, Buxbaum JD, Haroutunian V, Fienberg AA. Genome-wide expression analysis reveals dysregulation of myelination-related genes in chronic schizophrenia. *Proc Natl Acad Sci U S A* 98, 4746–4751, 2001.

Hallen A, Cooper AJ, Jamie JF, Haynes PA, Willows RD. Mammalian forebrain ketimine reductase identified as μ -crystallin; potential regulation by thyroid hormones. *J Neurochem* 118, 379–387, 2011.

Hallen A, Cooper AJ, Jamie JF, Karuso P. Insights into Enzyme Catalysis and Thyroid Hormone Regulation of Cerebral Ketimine Reductase/ μ -Crystallin Under Physiological Conditions. *Neurochem Res* 40, 1252–1266, 2015a.

Hallen A, Cooper AJ, Smith JR, Jamie JF, Karuso P. Ketimine reductase/CRYM catalyzes reductive alkylamination of α -keto acids, confirming its function as an imine reductase. *Amino Acids* 47, 2457–2461, 2015b.

Hallen A, Cooper AJ. Reciprocal Control of Thyroid Binding and the Pipecolate Pathway in the Brain. *Neurochem Res* 42, 217–243, 2017.

Harris M, Aschkenasi C, Elias CF, Chandrankunnel A, Nillni EA, Bjørbaek C, Elmquist JK, Flier JS, Hollenberg AN. Transcriptional regulation of the thyrotropin-releasing hormone gene by leptin and melanocortin signaling. *J Clin Invest* 107, 111–120, 2001.

Hashizume K, Kobayashi M, Miyamoto T. Active and inactive forms of 3,5,3'-triiodo-L-thyronine (T3)-binding protein in rat kidney cytosol: possible role of nicotinamide adenine dinucleotide phosphate in activation of T3 binding. *Endocrinology* 19, 710–719, 1986.

Hashizume K, Miyamoto T, Ichikawa K, Yamauchi K, Kobayashi M, Sakurai A, Ohtsuka H, Nishii Y, Yamada T. Purification and characterization of NADPH-dependent cytosolic 3,5,3'-triiodo-L-thyronine binding protein in rat kidney. *J Biol Chem* 264, 4857–4863, 1989a.

Hashizume K, Miyamoto T, Kobayashi M, Suzuki S, Ichikawa K, Yamauchi K, Ohtsuka H, Takeda T. Cytosolic 3,5,3'-triiodo-L-thyronine (T3)-binding protein (CTBP) regulation of nuclear T3 binding: evidence for the presence of T3-CTBP complex-binding sites in nuclei. *Endocrinology* 124, 2851–2856, 1989b.

Hashizume K, Miyamoto T, Yamauchi K, Ichikawa K, Kobayashi M, Ohtsuka H, Sakurai A, Suzuki S, Yamada T. Counterregulation of nuclear 3,5,3'-triiodo-L-thyronine (T3) binding by oxidized and reduced-nicotinamide adenine dinucleotide phosphates in the presence of cytosolic T3-binding protein in vitro. *Endocrinology* 124, 1678–1683, 1989c.

Hashizume K, Miyamoto T, Ichikawa K, Yamauchi K, Sakurai A, Ohtsuka H, Kobayashi M, Nishii Y, Yamada T. Evidence for the presence of two active forms of cytosolic 3,5,3'-triiodo-L-thyronine (T3)-binding protein (CTBP) in rat kidney. Specialized functions of two CTBPs in intracellular T3 translocation. *J Biol Chem* 264, 4864–4871, 1989d.

Heuer H, Schafer MK, O'Donnell D, Walker P, Bauer K. Expression of thyrotropin-releasing hormone receptor 2 (TRH-R2) in the central nervous system of rats. *J Comp Neurol* 428, 319–336, 2000.

Hinaux H, Blin M, Fumey J, Legendre L, Heuzé A, Casane D, Rétaux S. Lens defects in *Astyanax mexicanus* Cavefish: evolution of crystallins and a role for alphaA-crystallin. *Dev Neurobiol* 75, 505–521, 2015.

Hodges A, Strand AD, Aragaki AK, Kuhn A, Sengstag T, Hughes G, Elliston LA, Hartog C, Goldstein DR, Thu D, Hollingsworth ZR, Collin F, Synek B, Holmans PA, Young AB, Wexler NS, Delorenzi M, Kooperberg C, Augood SJ, Faull RL, Olson JM, Jones L, Luthi-Carter R. Regional and cellular gene expression changes in human Huntington's disease brain. *Hum Mol Genet* 15, 965–977, 2006.

Hodin RA, Lazar MA, Wintman BI, Darling DS, Koenig RJ, Larsen PR, Moore DD, Chin WW. Identification of a thyroid hormone receptor that is pituitary-specific. *Science* 244, 76–79, 1989.

Hommyo R, Suzuki SO, Abolhassani N, Hamasaki H, Shijo M, Maeda N, Honda H, Nakabeppu Y, Iwaki T. Expression of CRYM in different rat organs during development and its decreased expression in degenerating pyramidal tracts in amyotrophic lateral sclerosis. *Neuropathology* 38, 247–259, 2018.

Imai H, Ohta K, Yoshida A, Suzuki S, Hashizume K, Usami S, Kikuchi T. μ -Crystallin, new candidate protein in endotoxin-induced uveitis. *Invest Ophthalmol Vis Sci* 51, 3554–3559, 2010.

Jansen J, Friesema EC, Milici C, Visser TJ. Thyroid hormone transporters in health and disease. *Thyroid* 15, 757–768, 2005.

Jhanwar SC, Chaganti RS, Croce CM. Germ-line chromosomal localization of human C-Erb-A oncogene. *Somat Cell Mol Genet* 11, 99–102, 1985.

Johnston-Wilson NL, Sims CD, Hofmann JP, Anderson L, Shore AD, Torrey EF, Yolken RH. Disease-specific alterations in frontal cortex brain proteins in schizophrenia, bipolar disorder, and major depressive disorder. The Stanley Neuropathology Consortium. *Mol Psychiatry* 5, 142–149, 2000.

Joshi SS, Sethi M, Striz M, Cole N, Denegre JM, Ryan J, Lhamon ME, Agarwal A, Murray S, Braun RE, Fardo DW, Kumar V, Donohue KD, Sunderam S, Chesler EJ, Svenson KL, O'Hara BF. Noninvasive sleep monitoring in large-scale screening of knock-out mice reveals novel sleep-related genes. *bioRxiv*, 517680, 2019.

Kalmar B, Blanco G, Greensmith L. Determination of Muscle Fiber Type in Rodents. *Curr Protoc Mouse Biol* 2, 231–243, 2012.

Kalyanaraman H, Schwappacher R, Joshua J, Zhuang S, Scott BT, Klos M, Casteel DE, Frangos JA, Dillmann W, Boss GR, Pilz RB. Nongenomic thyroid hormone signaling occurs through a plasma membrane-localized receptor. *Sci Signal* 7, ra48, 2014.

Kim RY, Gasser R, Wistow GJ. μ -crystallin is a mammalian homologue of *Agrobacterium* ornithine cyclodeaminase and is expressed in human retina. *Proc Natl Acad Sci U S A* 89, 9292–9296, 1992.

Kinney CJ, O'Neill A, Noland K, Huang W, Muriel J, Lukyanenko V, Kane MA, Ward CW, Collier AF, Roche JA, McLenithan JC, Reed PW, Bloch RJ. μ -Crystallin in mouse skeletal muscle promotes a shift from glycolytic toward oxidative metabolism. *Current Research in Physiology* 4, 47–59, 2021.

Kobayashi M, Hashizume K, Suzuki S, Ichikawa K, Takeda T. A novel NADPH-dependent cytosolic 3,5,3'-triiodo-L-thyronine-binding protein (CTBP; 5.1S) in rat liver: a comparison with 4.7S NADPH-dependent CTBP. *Endocrinology* 129, 1701–1708, 1991.

Kubota K, Uchimura H, Mitsuhashi T, Chiu SC, Kuzuya N, Nagataki S. Effects of intrathyroidal metabolism of thyroxine on thyroid hormone secretion: increased degradation of thyroxine in mouse thyroids stimulated chronically with thyrotrophin. *Acta Endocrinol (Copenh)* 105, 57–65, 1984.

Larsen PR, Silva JE, Kaplan MM. Relationships between circulating and intracellular thyroid hormones: physiological and clinical implications. *Endocr Rev* 2, 87–102, 1981.

Legradi G, Emerson CH, Ahima RS, Flier JS, Lechan RM. Leptin prevents fasting-induced suppression of prothyrotropin-releasing hormone messenger ribonucleic acid in neurons of the hypothalamic paraventricular nucleus. *Endocrinology* 138, 2569–2576, 1997.

Lein ES, Hawrylycz MJ, Ao N, Ayres M, Bensinger A, Bernard A et al. Genome-wide atlas of gene expression in the adult mouse brain. *Nature* 445, 168–176, 2007.

Liu X, Wei S, Deng S, Li D, Liu K, Shan B, Shao Y, Wei W, Chen J, Zhang L. Genome-wide identification and comparison of mRNAs, lncRNAs and circRNAs in porcine intramuscular, subcutaneous, retroperitoneal and mesenteric adipose tissues. *Anim Genet* 50, 228–241, 2019.

Liu YY, Milanesi A, Brent GA. Thyroid Hormones. In: *Hormonal Signaling in Biology and Medicine* (Ed. G. Litwack), pp. 487–506, Elsevier, 2020.

Lusk G. Animal calorimetry: twenty-fourth paper. Analysis of the oxidation of mixtures of carbohydrate and fat *J Biol Chem* 59, 41–42, 1924.

Mansourian AR. A review on hyperthyroidism: thyrotoxicosis under surveillance. *Pak J Biol Sci* 13, 1066–1076, 2010.

Martins-de-Souza D, Gattaz WF, Schmitt A, Rewerts C, Maccarrone G, Dias-Neto E, Turck CW. Prefrontal cortex shotgun proteome analysis reveals altered calcium homeostasis and immune system imbalance in schizophrenia. *Eur Arch Psychiatry Clin Neurosci* 259, 151–163, 2009a.

Martins-de-Souza D, Gattaz WF, Schmitt A, Maccarrone G, Hunyadi-Gulyás E, Eberlin MN, Souza GH, Marangoni S, Novello JC, Turck CW, Dias-Neto E. Proteomic analysis of

dorsolateral prefrontal cortex indicates the involvement of cytoskeleton, oligodendrocyte, energy metabolism and new potential markers in schizophrenia. *J Psychiatr Res* 43, 978–986, 2009b.

Martins-de-Souza D, Maccarrone G, Wobrock T, Zerr I, Gormanns P, Reckow S, Falkai P, Schmitt A, Turck CW. Proteome analysis of the thalamus and cerebrospinal fluid reveals glycolysis dysfunction and potential biomarkers candidates for schizophrenia. *J Psychiatr Res* 44, 1176–1189, 2010.

Mendoza A, Hollenberg AN. New insights into thyroid hormone action. *Pharmacol Ther* 173, 135–145, 2017.

Mengeling BJ, Pan F, Privalsky ML. Novel mode of deoxyribonucleic acid recognition by thyroid hormone receptors: thyroid hormone receptor beta-isoforms can bind as trimers to natural response elements comprised of reiterated half-sites. *Mol Endocrinol* 19, 35–51, 2005.

Middleton FA, Mirnics K, Pierri JN, Lewis DA, Levitt P. Gene expression profiling reveals alterations of specific metabolic pathways in schizophrenia. *J Neurosci* 22, 2718–2729, 2002.

Miga KH, Eisenhart C, Kent WJ. Utilizing mapping targets of sequences underrepresented in the reference assembly to reduce false positive alignments. *Nucleic Acids Res* 43, e133, 2015.

Mihaly E, Fekete C, Tatro JB, Liposits Z, Stopa EG, Lechan RM. Hypophysiotropic thyrotropin-releasing hormone-synthesizing neurons in the human hypothalamus are innervated by neuropeptide Y, agouti-related protein, and alpha-melanocyte-stimulating hormone. *J Clin Endocrinol Metab* 85, 2596–2603, 2000.

Miklos GL, Maleszka R. Microarray reality checks in the context of a complex disease. *Nat Biotechnol* 22, 615–621, 2004.

Mitchell AM, Tom M, Mortimer RH. Thyroid hormone export from cells: contribution of P-glycoprotein. *J Endocrinol* 185, 93–98, 2005.

Mori J, Suzuki S, Kobayashi M, Inagaki T, Komatsu A, Takeda T, Miyamoto T, Ichikawa K, Hashizume K. Nicotinamide adenine dinucleotide phosphate-dependent cytosolic T(3) binding protein as a regulator for T(3)-mediated transactivation. *Endocrinology* 143, 1538–1544, 2002.

Morley JE. Extrahypothalamic thyrotropin releasing hormone (TRH) -- its distribution and its functions. *Life Sci* 25, 1539–1550, 1979.

Mukai M, Replogle K, Drnevich J, Wang G, Wacker D, Band M, Clayton DF, Wingfield JC. Seasonal differences of gene expression profiles in song sparrow (*Melospiza melodia*) hypothalamus in relation to territorial aggression. *PLoS One* 4, e8182, 2009.

O'Shea PJ, Williams GR. Insight into the physiological actions of thyroid hormone receptors from genetically modified mice. *J Endocrinol* 175, 553–570, 2002.

Ohkubo Y, Sekido T, Nishio SI, Sekido K, Kitahara J, Suzuki S, Komatsu M. Loss of μ -crystallin causes PPAR γ activation and obesity in high-fat diet-fed mice. *Biochem Biophys Res Commun* 508, 914–920, 2019.

Ojha A, Watve M. Blind fish: An eye opener. *Evol Med Public Health* 2018, 186–189, 2018.

Oshima A, Suzuki S, Takumi Y, Hashizume K, Abe S, Usami S. CRYM mutations cause deafness through thyroid hormone binding properties in the fibrocytes of the cochlea. *J Med Genet* 43, e25, 2006.

Pantos C, Mourouzis I. Thyroid hormone receptor α 1 as a novel therapeutic target for tissue repair. *Ann Transl Med* 6, 254, 2018.

Pensato V, Magri S, Bella ED, Tannorella P, Bersano E, Sorarù G, Gatti M, Ticozzi N, Taroni F, Lauria G, Mariotti C, Gellera C. Sorting Rare ALS Genetic Variants by Targeted

Re-Sequencing Panel in Italian Patients: OPTN, VCP, and SQSTM1 Variants Account for 3% of Rare Genetic Forms. *J Clin Med* 9, 412, 2020.

Phan L, Jin Y, Zhang H, Qiang W, Shekhtman E, Shao D, Revoe D, Villamarin R, Ivanchenko E, Kimura M, Wang ZY, Hao L, Sharopova N, Bihan M, Sturcke A, Lee M, Popova N, Wu W, Bastiani C, Ward M, Holmes JB, Lyoshin V, Kaur K, Moyer E, Feolo M, Kattman BL. "ALFA: Allele Frequency Aggregator." National Center for Biotechnology Information, U.S. National Library of Medicine, 10 Mar. 2020, www.ncbi.nlm.nih.gov/snp/docs/gsr/alfa/.

Pihlajamaki J, Boes T, Kim EY, Dearie F, Kim BW, Schroeder J, Mun E, Nasser I, Park PJ, Bianco AC, Goldfine AB, Patti ME. Thyroid hormone-related regulation of gene expression in human fatty liver. *J Clin Endocrinol Metab* 94, 3521–3529, 2009.

Pirahanchi Y, Tariq MA, Jialal I. Physiology, Thyroid. [Updated 2021 Feb 9]. In: StatPearls [Internet]. Treasure Island (FL): StatPearls Publishing; 2021. Available from: <https://www.ncbi.nlm.nih.gov/books/NBK519566/>.

Raparti G, Jain S, Ramteke K, Murthy M, Ghanghas R, Ramanand S, Ramanand J. Selective thyroid hormone receptor modulators. *Indian J Endocrinol Metab* 17, 211–218, 2013.

Reed PW, Corse AM, Porter NC, Flanigan KM, Bloch RJ. Abnormal expression of mu-crystallin in facioscapulohumeral muscular dystrophy. *Exp Neurol* 205, 583–586, 2007.

Rodriguez-Rodriguez A, Lazcano I, Sanchez-Jaramillo E, Uribe RM, Jaimes-Hoy L, Joseph-Bravo P, Charli JL. Tancytes and the control of thyrotropin-releasing hormone flux into portal capillaries. *Front Endocrinol (Lausanne)*10, 401, 2019.

Saetre P, Lindberg J, Leonard JA, Olsson K, Pettersson U, Ellegren H, Bergstrom TF, Vila C, Jazin E. From wild wolf to domestic dog: gene expression changes in the brain. *Brain Res Mol Brain Res* 126, 198–206, 2004.

Samocha KE, Robinson EB, Sanders SJ, Stevens C, Sabo A, McGrath LM, Kosmicki JA, Rehnstrom K, Mallick S, Kirby A, Wall DP, MacArthur DG, Gabriel SB, DePristo M, Purcell SM, Palotie A, Boerwinkle E, Buxbaum JD, Cook EH Jr, Gibbs RA, Schellenberg GD, Sutcliffe JS, Devlin B, Roeder K, Neale BM, Daly MJ. A framework for the interpretation of de novo mutation in human disease. *Nat Genet* 46, 944–950, 2014.

Sanchez E, Uribe RM, Corkidi G, Zoeller RT, Cisneros M, Zacarias M, Morales-Chapa C, Charli JL, Joseph-Bravo P. Differential responses of thyrotropin-releasing hormone (TRH) neurons to cold exposure or suckling indicate functional heterogeneity of the TRH system in the paraventricular nucleus of the rat hypothalamus. *Neuroendocrinology* 74, 407–422, 2001.

Sandler B, Webb P, Apriletti JW, Huber BR, Togashi M, Cunha Lima ST, Juric S, Nilsson S, Wagner R, Fletterick RJ, Baxter JD. Thyroxine-thyroid hormone receptor interactions. *J Biol Chem* 279, 55801–55808, 2004.

Sap J, Munoz A, Damm K, Goldberg Y, Ghysdael J, Leutz A, Beug H, Vennstrom B. The c-erb-A protein is a high-affinity receptor for thyroid hormone. *Nature* 324, 635–640, 1986.

Sapp PC, Hosler BA, McKenna-Yasek D, Chin W, Gann A, Genise H, Gorenstein J, Huang M, Sailer W, Scheffler M, Valesky M, Haines JL, Pericak-Vance M, Siddique T, Horvitz HR, Brown RH Jr. Identification of two novel loci for dominantly inherited familial amyotrophic lateral sclerosis. *Am J Hum Genet* 73, 397–403, 2003.

Schaefer JS, Klein JR. Immunological regulation of metabolism--a novel quintessential role for the immune system in health and disease. *FASEB J* 25, 29–34, 2011.

Schiaffino S, Reggiani C. Fiber types in mammalian skeletal muscles. *Physiol Rev* 91, 1447–1531, 2011.

Schimmel M, Utiger RD. Thyroidal and peripheral production of thyroid hormones. Review of recent findings and their clinical implications. *Ann Intern Med* 87, 760–768, 1977.

Seko D, Ogawa S, Li TS, Taimura A, Ono Y. μ -Crystallin controls muscle function through thyroid hormone action. *FASEB J* 30, 1733–1740, 2016.

Senese R, Cioffi F, de Lange P, Goglia F, Lanni A. Thyroid: biological actions of 'nonclassical' thyroid hormones. *J Endocrinol* 221, R1–R12, 2014.

Serrano M, Moreno M, Ortega FJ, Xifra G, Ricart W, Moreno-Navarrete JM, Fernandez-Real JM. Adipose tissue μ -crystallin is a thyroid hormone-binding protein associated with systemic insulin sensitivity. *J Clin Endocrinol Metab* 99, E2259–E2268, 2014.

Silva JE. Thyroid hormone and the energetic cost of keeping body temperature. *Biosci Rep* 25, 129–148, 2005.

Sivagnanasundaram S, Crossett B, Dedova I, Cordwell S, Matsumoto I. Abnormal pathways in the genu of the corpus callosum in schizophrenia pathogenesis: a proteome study. *Proteomics Clin Appl* 1, 1291–1305, 2007.

Smith CM, Hayamizu TF, Finger JH, Bello SM, McCright IJ, Xu J, Baldarelli RM, Beal JS, Campbell J, Corbani LE, Frost PJ, Lewis JR, Giannatto SC, Miers D, Shaw DR, Kadin JA, Richardson JE, Smith CL, Ringwald M. The mouse Gene Expression Database (GXD): 2019 update. *Nucleic Acids Res* 47, D774–D779, 2019.

Snyder PJ, Utiger RD. Response to thyrotropin releasing hormone (TRH) in normal man. *J Clin Endocrinol Metab* 34, 380–385, 1972.

Sotelo-Rivera I, Cote-Velez A, Uribe RM, Charli JL, Joseph-Bravo P. Glucocorticoids curtail stimuli-induced CREB phosphorylation in TRH neurons through interaction of the glucocorticoid receptor with the catalytic subunit of protein kinase A. *Endocrine* 55, 861–871, 2017.

Sterling K, Campbell GA, Brenner MA. Purification of the mitochondrial triiodothyronine (T₃) receptor from rat liver. *Acta Endocrinol (Copenh)* 105, 391–397, 1984.

Suzuki S, Suzuki N, Mori J, Oshima A, Usami S, Hashizume K. micro-Crystallin as an intracellular 3,5,3'-triiodothyronine holder in vivo. *Mol Endocrinol* 21, 885–894, 2007.

Tagami T, Yamamoto H, Moriyama K, Sawai K, Usui T, Shimatsu A, Naruse M. Identification of a novel human thyroid hormone receptor beta isoform as a transcriptional modulator. *Biochem Biophys Res Commun* 396, 983–988, 2010.

Tata JR. A cellular thyroxine-binding protein fraction. *Biochim Biophys Acta* 28, 91–94, 1958.

Tawil R, van der Maarel SM, Tapscott SJ. Facioscapulohumeral dystrophy: the path to consensus on pathophysiology. *Skelet Muscle* 4, 12, 2014.

Tennessen JA, Bigham AW, O'Connor TD, Fu W, Kenny EE, Gravel S, McGee S, Do R, Liu X, Jun G, Kang HM, Jordan D, Leal SM, Gabriel S, Rieder MJ, Abecasis G, Altshuler D, Nickerson DA, Boerwinkle E, Sunyaev S, Bustamante CD, Bamshad MJ, Akey JM; Broad GO; Seattle GO; NHLBI Exome Sequencing Project. Evolution and functional impact of rare coding variation from deep sequencing of human exomes. *Science* 337, 64–69, 2012.

Thul PJ, Akesson L, Wiking M, Mahdessian D, Geladaki A, Ait Blal H, Alm T, Asplund A, Bjork L, Breckels LM, Backstrom A, Danielsson F, Fagerberg L, Fall J, Gatto L, Gnann C, Hober S, Hjelmare M, Johansson F, Lee S, Lindskog C, Mulder J, Mulvey CM, Nilsson P, Oksvold P, Rockberg J, Schutten R, Schwenk JM, Sivertsson A, Sjostedt E, Skogs M, Stadler C, Sullivan DP, Tegel H, Winsnes C, Zhang C, Zwahlen M, Mardinoglu A, Ponten F, von Feilitzen K, Lilley KS, Uhlen M, Lundberg E. A subcellular map of the human proteome. *Science* 356, eaal3321, 2017.

Uhlen M, Fagerberg L, Hallstrom BM, Lindskog C, Oksvold P, Mardinoglu A, Sivertsson A, Kampf C, Sjostedt E, Asplund A, Olsson I, Edlund K, Lundberg E, Navani S, Szigartyo CA, Odeberg J, Djureinovic D, Takanen JO, Hober S, Alm T, Edqvist PH, Berling H, Tegel H, Mulder J, Rockberg J, Nilsson P, Schwenk JM, Hamsten M, von Feilitzen K, Forsberg M, Persson L, Johansson F, Zwahlen M, von Heijne G, Nielsen J, Ponten F. Proteomics. Tissue-based map of the human proteome. *Science* 347, 1260419, 2015.

Vanderplanck C, Anseau E, Charron S, Stricwant N, Tassin A, Laoudj-Chenivesse D, Wilton SD, Coppee F, Belayew A. The FSHD atrophic myotube phenotype is caused by DUX4 expression. *PLoS One* 6, e26820, 2011.

Velasco LF, Togashi M, Walfish PG, Pessanha RP, Moura FN, Barra GB, Nguyen P, Rebong R, Yuan C, Simeoni LA, Ribeiro RC, Baxter JD, Webb P, Neves FA. Thyroid hormone response element organization dictates the composition of active receptor. *J Biol Chem* 282, 12458–12466, 2007.

Visser WE, Wong WS, van Mullem AA, Friesema EC, Geyer J, Visser TJ. Study of the transport of thyroid hormone by transporters of the SLC10 family. *Mol Cell Endocrinol* 315, 138–145, 2010.

Visser WE, Friesema EC, Visser TJ. Minireview: thyroid hormone transporters: the knowns and the unknowns. *Mol Endocrinol* 25, 1–14, 2011.

Walker DM, Zhao X, Ramakrishnan A, Cates HM, Cunningham AM, Pena CJ, Bagot RC, Issler O, Van der Zee Y, Lipschultz AP, Godino A, Browne CJ, Hodes GE, Parise EM, Torres-Berrio A, Kennedy PJ, Shen L, Zhang B, Nestler EJ. Adolescent social isolation reprograms the medial amygdala: transcriptome and sex differences in reward. *bioRxiv*, 955187, 2020.

Wang M, Li Q, Deng A, Zhu X, Yang J. Identification of a novel mutation in CRYM in a Chinese family with hearing loss using whole-exome sequencing. *Exp Ther Med* 20, 1447–1454, 2020.

Watanabe Y, Weiss RE. Thyroid hormone action. In: *Encyclopedia of Endocrine Diseases*, pp. 452–462, Elsevier, 2018.

Weinberger C, Thompson CC, Ong ES, Lebo R, Gruol DJ, Evans RM. The c-erb-A gene encodes a thyroid hormone receptor. *Nature* 324, 641–646, 1986.

Williams GR. Cloning and characterization of two novel thyroid hormone receptor beta isoforms. *Mol Cell Biol* 20, 8329–8342, 2000.

Williams GR, Bassett JH. Deiodinases: the balance of thyroid hormone: local control of thyroid hormone action: role of type 2 deiodinase. *J Endocrinol* 209, 261–272, 2011.

Wistow G, Kim H. Lens protein expression in mammals: taxon-specificity and the recruitment of crystallins. *J Mol Evol* 32, 262–269, 1991.

Yarbrough GG. On the neuropharmacology of thyrotropin releasing hormone (TRH). *Prog Neurobiol* 12, 291–312, 1979.

Zimmermann RC, Krahn LE, Klee GG, Ditkoff EC, Ory SJ, Sauer MV. Prolonged inhibition of presynaptic catecholamine synthesis with alpha-methyl-para-tyrosine attenuates the circadian rhythm of human TSH secretion. *J Soc Gynecol Investig* 8, 174–178, 2001.

Chapter 2: μ -Crystallin in Mouse Skeletal Muscle Promotes a Shift from Glycolytic toward Oxidative Metabolism ²

**Christian J. Kinney^a, Andrea O'Neill^a, Kaila Noland^a, Weiliang Huang^b,
Joaquin Muriel^a, Valeriy Lukyanenko^a, Maureen A. Kane^b,
Christopher W. Ward^c, Alyssa F. Collier^{a,2}, Joseph A. Roche^{a,1},
John C. McLenithan^d, Patrick W. Reed^a, Robert J. Bloch^{a,*}**

^a Department of Physiology School of Medicine, University of Maryland
Baltimore, Baltimore, MD 21201

^b Department of Pharmaceutical Sciences School of Pharmacy, University of
Maryland Baltimore, Baltimore, MD 21201

^c Department of Orthopedics School of Medicine, University of Maryland
Baltimore, Baltimore, MD 21201

^d Department of Medicine School of Medicine, University of Maryland Baltimore,
Baltimore, MD 21201

¹ Present address: Physical Therapy Program, Department of Health Care Sciences,
Wayne State University, Detroit, MI 48201

² Present address: Department of Rehabilitation Services, Emory University
Hospital, Atlanta, GA 30322

² Kinney CJ, O'Neill A, Noland K, Huang W, Muriel JM, Lukyanenko V, Kane MA, Ward CW, Collier AF, Roche JA, McLenithan JC, Reed PW, and Bloch RJ. μ -Crystallin in Mouse Skeletal Muscle Promotes a Shift from Glycolytic toward Oxidative Metabolism. *Current Research in Physiology* 2020.

* Corresponding author: Dept. of Physiology, University of Maryland School of Medicine

655 W. Baltimore St., Baltimore, MD 21201. Phone: 410-706-3020; Fax: 410-706-834;
Cell: 443-938-1228; Email: rbloch@som.umaryland.edu

Keywords: Glycolysis, β -oxidation, RER, RNA-seq, proteomics, thyroid hormone

Abstract

μ -Crystallin, encoded by the *CRYM* gene, binds the thyroid hormones, T₃ and T₄. Because T₃ and T₄ are potent regulators of metabolism and gene expression, and *CRYM* levels in human skeletal muscle can vary widely, we investigated the effects of overexpression of *Crym*. We generated transgenic mice, *Crym* tg, that expressed *Crym* protein specifically in skeletal muscle at levels 2.6-147.5 fold higher than in controls. Muscular functions, Ca²⁺ transients, contractile force, fatigue, running on treadmills or wheels, were not significantly altered, although T₃ levels in tibialis anterior (TA) muscle were elevated ~190-fold and serum T₄ was decreased 1.2-fold. Serum T₃ and thyroid stimulating hormone (TSH) levels were unaffected. *Crym* transgenic mice studied in metabolic chambers showed a significant decrease in the respiratory exchange ratio (RER) corresponding to a 13.7% increase in fat utilization as an energy source compared to controls. Female but not male *Crym* tg mice gained weight more rapidly than controls when fed high fat or high simple carbohydrate diets. Although labeling for myosin heavy chains showed no fiber type differences in TA or soleus muscles, application of machine learning algorithms revealed small but significant morphological differences between

Crym tg and control soleus fibers. RNA-seq and gene ontology enrichment analysis showed a significant shift towards genes associated with slower muscle function and its metabolic correlate, β -oxidation. Protein expression showed a similar shift, though with little overlap. Our study shows that μ -crystallin plays an important role in determining substrate utilization in mammalian muscle and that high levels of μ -crystallin are associated with a shift toward greater fat metabolism.

1. Introduction

μ -Crystallin was first discovered in 1957 and called cellular thyroxine-binding protein (Tata 1958). It was subsequently shown to bind both T_3 and T_4 in an NADPH-dependent manner (Hashizume, Miyamoto, Ichikawa, Yamauchi, Sakurai, et al. 1989; Tata 1958), and to have ketimine reductase activity (Hallen et al. 2011). In 1991, μ -crystallin was characterized as a 38,000 Da polypeptide that readily forms dimers (Kobayashi et al. 1991) and shares structural homology with bacterial ornithine cyclodeaminase (Kim, Gasser, and Wistow 1992). Its structure has since been solved to 1.75 Å (Borel et al. 2014).

CRYM is highly expressed in the cerebral cortex, heart, skeletal muscle, and kidney (Kim, Gasser, and Wistow 1992), and has been linked to Deafness, Autosomal Dominant 40 (Abe et al. 2003). Importantly, μ -crystallin binds T_3 with a $K_D = 0.3$ nM (Beslin et al. 1995) while T_3 binds thyroid hormone receptors (TR) α and β with a $K_D = 0.06$ nM; T_4 binds TRs at a $K_D = 2$ nM (Sandler et al. 2004). μ -Crystallin's activity as a ketimine reductase is inhibited by T_3 and T_4 at subnanomolar levels, $K_I = 0.60$ nM and $K_I = 0.75$ nM, respectively (Hallen, Cooper, Jamie, et al. 2015). T_3 and T_4 are strong

regulators of metabolism and thermogenic homeostasis (Larsen, Silva, and Kaplan 1981). Because of this, proteins that interact with and regulate thyroid hormones may have a broad influence on integrative functions like gene expression and metabolism.

Consistent with its possible role in regulating metabolism associated with thyroid hormones, *Crym* knockout mice (*Crym* KO) fed a high fat diet (HFD) show increased fat mass by computer tomography and increased body weight compared to control mice (Ohkubo et al. 2019). Furthermore, *Crym* KO mice show significant hypertrophy of glycolytic fast twitch type IIb muscle fibers (Seko et al. 2015).

Here we address the effects of high levels of *Crym* expression in mammalian muscle. We initially observed high levels of μ -crystallin in several muscle biopsies of patients with facioscapulohumeral muscular dystrophy (FSHD) (Reed et al. 2007), a muscle wasting disease in which patients progressively lose muscle. At the time, the cause of FSHD was unknown and we speculated that *CRYM* might play a role in the disease. Later studies showed that mRNA and protein both varied widely in expression in both healthy and diseased muscle (Klooster et al. 2009). It is now widely accepted that the primary pathogen in FSHD is DUX4 (Tawil, Van Der Maarel, and Tapscott 2014), a transcription factor (Dixit et al. 2007) that promotes *CRYM* expression (Vanderplanck et al. 2011). Thus, increases in *CRYM* may perturb muscle metabolism and contribute to pathology.

To examine the differences that result from the high level of expression of *Crym* in skeletal muscle, we developed a transgenic mouse (*Crym* tg) that overexpresses μ -crystallin under the control of the human skeletal actin promoter (*ACTA1*) and the human slow troponin I enhancer (*TNNI1*), to drive skeletal muscle-specific expression (Ebashi,

Endo, and Ohtsuki 1969; Gunning et al. 1983). Here we explore the effects of overexpression of μ -crystallin on the structure and function of muscle.

2. Materials and methods

2.1. Creation of the *Crym* tg Mouse

Mouse *Crym* was cloned downstream of the human skeletal actin promoter (*ACTA1*) and human slow troponin I enhancer element (*TNNI1*), (kindly provided by Dr. J. Molckentin, Cincinnati Children's Hospital Medical Center), to limit expression to differentiated skeletal muscle. The expression construct was linearized and injected into C57BL/6J mouse embryos at the Genome Modification Facility, Harvard University (Cambridge, MA). Mice received from the Harvard facility were genotyped by PCR and then rederived by artificial insemination of C57BL/6J mice, due to pinworm infestation. This was performed by Veterinary Resources, University of Maryland School of Medicine. The rederived offspring were bred; all mice were tail snipped at weaning. Genomic DNA was purified from mouse tail snips using the Nucleon Genomic DNA extraction kit (Tepnel Life Sciences, Scotland). PCR of genomic DNA was used to identify mice positive for the transgene, with the following primers: forward: TGGCCACGCGTCGACTAGTACG; reverse: AATTCGTACTAGTCGACGCGTGGCC.

As it was initially difficult to differentiate between heterozygotes and homozygotes with PCR methods, qPCR was done on several of the *Crym*-positive genomic DNA samples. Mice with higher levels of *Crym* were then bred to controls and the F1 and F2 offspring were crossed and screened to generate probable homozygotes.

Mice were identified as tg/tg homozygotes if after crossing with controls they gave at least 12 *Crym*-positive offspring and no *Crym*-negative offspring by PCR. Homozygotes were then bred together to establish the line of *Crym* tg/tg mice.

All histologic and physiologic experiments used approximately three-month-old, male control and *Crym* tg mice that were anesthetized under isoflurane (2.5%). Euthanasia was by cervical dislocation under anesthesia.

All procedures were approved by the Institutional Animal Care and Use Committee, University of Maryland School of Medicine.

2.1.1. Back-Crossing and Genotyping

Crym tg mice were backcrossed with control C57BL/6J mice. Non-littermate F1 heterozygotes were then bred together to generate F2 mice. Tail snips of *Crym* tg, C57BL/6J, F1 heterozygotes, and F2 mice were then taken at 6 weeks of age or older. Genomic DNA was extracted from the tail snips by following the manufacturers protocol from the PureLink Genomic DNA Mini Kit (K182001; Invitrogen) modified only by substituting DirectPCR Lysis Reagent (Tail) (102-T; Viagen Biotech, Los Angeles, CA) in place of PureLink Genomic Digestion Buffer. *Crym* tg, F1 heterozygotes, and C57BL/6J mice were genotyped using a multiplexed probe-based assay from IDT for *Crym* and *Tert*. The *Crym* assay was designed such that it would produce the same amplicon from the native *Crym* gene as well as the inserted transgene. A synthetic *Crym* amplicon was used as an interplate control and *Tert* was used as the control for copy number. RT-qPCR was used to determine copy number and average normalized C_q for each mouse. The amplification protocol followed the manufacturer's instructions (IDT).

Mice were genotyped to one of the three genotypes when the calculated copy number and average normalized C_q was closest to a known genotype (i.e. *Crym* tg, C57BL/6J, or F1 heterozygotes).

2.1.2. Sequencing the Transgene Insertion Site

Genomic DNA obtained from *Crym* tg mice was digested with EcoRI. We designed and had synthesized a double stranded short oligonucleotide with overhanging sequences corresponding to an EcoRI digestion that we called *Crym*-Adaptor. *Crym*-Adaptor was ligated to the digested genomic DNA. The resulting ligation fragments were amplified using a forward primer in the multiple cloning site of the transgene and a reverse primer in the *Crym*-Adaptor sequence. Nested primers were used to specifically amplify the sequence. The products of this last reaction were purified by gel purification and sequenced from both ends. The sequence was then evaluated with NCBI BLASTn.

2.2. Staining of Longitudinal and Cross Sections for μ -Crystallin

Mice were perfusion fixed with 2% paraformaldehyde in phosphate-buffered saline (PBS). TA and soleus muscles were collected, snap frozen in a liquid nitrogen slush, mounted in O.C.T. (Fisher Healthcare, Hampton, NH) and sectioned at 10-20 μ m with a Reichert Jung cryostat (Leica, Buffalo Grove, IL). Sections were stained using the Mouse-On-Mouse (M.O.M.) Basic Kit (BMK-2202; Vector labs, Burlingame, CA). Sections were incubated for at least 1 h at room temperature in M.O.M. blocking reagent followed by a 10 min incubation in M.O.M. diluent. Sections were incubated overnight at 4°C in mouse monoclonal anti- μ -crystallin antibody (GTX84654; GeneTex Inc., Irvine,

CA) diluted 1:100. Some sections were also incubated with rabbit anti-desmin (PA5-16705; Thermo Fisher, Waltham, MA), also diluted 1:100. Sections were washed in PBS and then stained for 1 h at room temperature with Alexa Fluor 568 goat anti-mouse secondary antibody (A11031) and Alexa Fluor 488 goat anti-rabbit (A32731), both from Alexa Molecular Probes (Invitrogen, Carlsbad, CA), diluted 1:200. All antibodies were made up in M.O.M. diluent. Samples were washed with PBS, mounted in Vectashield + DAPI (H-1500; Vector Laboratory), and imaged with a Nikon W-1 spinning disc confocal microscope (Nikon USA, Melville, NY). We used identical laser power and exposure settings to compare cross sections of TA muscle, of soleus muscle, and of longitudinal sections of TA muscle, but we adjusted them for each set of comparisons to optimize image clarity.

2.2.1. Fiber Type Staining

We used a slightly modified version of Kammoun et al.'s fiber typing protocol (Kammoun et al. 2014). Primary murine monoclonal antibodies specific for the myosin isoforms *Myh7* (type I; BA-D5, isotype IgG2b), *Myh2* (type IIa; SC-71, isotype IgG1), and *Myh4* (type IIb; BF-F3, isotype IgM) were from the Developmental Studies Hybridoma Bank, (Iowa City, IA). Alexa Fluor 647 conjugated wheat germ agglutinin (WGA) was used to stain the myofiber surface (W32466, Thermo Fisher). The 4 reagents were used on 10 µm thick cross sections of snap frozen soleus and TA muscles (n = 5). The following secondary antibodies were used: goat anti-mouse IgG2b Cross-Adsorbed Secondary Antibody Alexa Fluor 568 (A-21144, Thermo Fisher), goat anti-mouse IgG1 Cross-Adsorbed Secondary Antibody Alexa Fluor 488 (A-21121, Thermo Fisher), and

goat anti-mouse IgM mu chain Alexa Fluor 405 (ab175662, Abcam). Slides were imaged on a Nikon W-1 spinning disc microscope. Laser power and exposure were identical for comparisons of sections of control and tg TA muscles, and for soleus muscles, but were different between these tissues. We used 5 *Crym* tg and 4 control mice to study soleus fiber type. Four stacked images were taken at approximately 2 μm intervals and stacked to generate a single image, which were flattened using Aguet et al.'s Model-Based 2.5-D Deconvolution for Extended Depth of Field algorithm (Aguet, Van De Ville, and Unser 2008). We determined that a $\eta_0 = 0.2$ and a $\eta_1 = 1.3$ were optimal in our images to generate an in-focus image of the flattened z stacks. For soleus muscle sections we used Myosoft (Encarnacion-Rivera et al. 2020), a Fiji (Schindelin et al. 2012) macro, to categorize fibers by their myosin heavy chain composition and measure several traits (count, area, perimeter, circularity, minimal Feret's diameter, roundness, and solidity). Statistical analysis used Real Statistics Resource Pack software (Release 6.8) (Zaiontz 2020) as a plugin in Microsoft Excel with $\alpha = 0.05$. Normality of the 7 measured metrics for each fiber type (I, IIa, IIb, IIx, I/IIa, I/IIb, IIa/IIb, and I/IIa/IIb) were determined with the Shapiro-Wilks and d'Agostino-Pearson tests, while scedasticity was determined with the mean, median, and trimmed method in Levene's test. If a dataset failed any individual test for normality or homoscedasticity it was considered not normal and heteroscedastic. Measurements that were both normal and homoscedastic were tested for significance using Student's t test, while measurements that were normal but heteroscedastic were tested for significance using either Welch's t test or the Brown-Forsythe test. The Kruskal-Wallis test for significance was used on measurements that failed the tests for

normality but were homoscedastic. Either the Yuen-Welch or the Mann-Whitney U test were used on measurements that failed tests for both normality and homoscedasticity.

2.2.2. Fat Staining

Cryosections of 5 snap frozen soleus and TA muscles from control and *Crym tg* mice were stained with BODIPY (493/503) according to Spangenburg et al (Spangenburg et al. 2011) and imaged with a Nikon spinning disk microscope (see above). Laser power and exposure settings were maintained for each section regardless of mouse strain, but these were altered between TA and soleus tissues. Accordingly, look up table values were also different from TA to soleus samples but the same within a tissue regardless of mouse strain.

2.3. μ -Crystallin Staining of Isolated FDB Fibers

FDB muscles were harvested bilaterally and digested in Dulbecco's modified Eagle's medium with 4 mg/mL type II collagenase (Gibco, Thermo Fisher Scientific, Waltham, MA) for 3 h at 37 °C. Tissue was transferred to FDB medium (Dulbecco's modified Eagle's medium with 2% BSA, 1 μ l/mL gentamicin, and 1 μ l/ml fungizone). Single myofibers were mechanically separated by trituration and allowed to incubate overnight. Isolated fibers were plated down on coverslips coated with Geltrex (A1413201; Thermo Fisher Scientific) for 2 h. Coverslips were fixed in 2% paraformaldehyde at room temperature for 15 min. They were then permeabilized with 0.25% TritonX-100 in PBS for 10 min and stained with antibody to μ -crystallin (H00001428-M03; Abnova, Taiwan), diluted 1:100, followed by Alexa Fluor 488, goat

anti-mouse secondary antibody (A11029; Alexa Molecular Probes, Invitrogen), diluted 1:200, with the M.O.M. kit, as described above. Each incubation was for 1 h at room temperature. Samples were imaged on a Zeiss 510 Duo microscope (Carl Zeiss, Thornwood, NY).

2.3.1. CNFs and Minimal Feret's Diameter of TA Cross Sections

Cross sections of TA muscles were used to measure centrally nucleated fibers (CNFs) and minimal Feret's diameter (Briguet et al. 2004). Sections were stained as above but with rabbit anti-dystrophin (PAS-16734; Thermo Fisher Scientific), mounted in Vectashield + DAPI as above and imaged by confocal microscopy with a Zeiss 510 Duo microscope (Carl Zeiss). DAPI labeling was evaluated with ImageJ (NIH, Bethesda, MD), for determination of centrally nucleated fibers. Measurements of minimal Feret's diameter were obtained with Zeiss LSM Image Browser (Carl Zeiss). A total of 312 myofibers from 5 *Crym tg* mice and 722 fibers from 5 control mice were analyzed.

2.4. Measurements of Contractile Force

Nerve-evoked contractile function of gastrocnemius, extensor digitorum longus, or soleus muscles *in vivo* was evaluated as described (Burks et al. 2011; Olojo et al. 2011). In brief, isoflurane-anesthetized mice were placed supine on a warming pad (37°C) of an Aurora 1300A system with knee position fixed and paw secured to the foot-plate of the 300C-FP. Percutaneous nerve stimulation was with brief (100 µsec) pulses with current adjusted to achieve maximal isometric force. The force vs frequency relationship was determined with 250 msec trains of pulses between 1 and 150 Hz and normalized to muscle mass or

cross-sectional area (CSA). Fatigability was determined by delivering tetanic trains (250 msec at 80 Hz) every 2 sec for 10 min for soleus or for 5 min for gastrocnemius. Data were analyzed with DMA-HT analysis software (Aurora Scientific, Ontario, Canada) and evaluated for statistical difference via the Holm-Šídák test with GraphPad Prism version 8.2.0 for Mac (GraphPad Software, La Jolla, CA).

2.5. Treadmill and *ad libidum* Running

Mice were conditioned to the treadmill over 3 days, as follows. Mice were placed in the treadmill with no belt movement for 10 min. The next day they were made to walk at 5 m/min for 10 min; this was increased to 10 m/min the following day. For testing, mice were placed in the treadmill at a 7° incline. The speed was set at 10 m/min and was increased by 1.5 m/min every 2 min. Mice were considered exhausted when they were unable to run for 30 sec consecutively. Each mouse was run 3 times with a minimum of 2 d rest between each run.

Additional *Crym tg* and control mice were housed in cages equipped with running wheels for 7 d. The number of times the wheel spun per minute was recorded every 6 min and analyzed to determine total distance run in different time periods, day and night.

2.6. Protein Extraction

Tissues of interest (gastrocnemius, TA, soleus, diaphragm, heart, kidney, cerebral cortex and liver) were collected from 3-month old *Crym tg* and control mice, snap frozen in liquid nitrogen and stored at -80 °C. Protein was extracted in RIPA Buffer (R0278-

50ML, Sigma-Aldrich), prepared with cOmplete Mini, EDTA-free protease inhibitor tablets (11836170001, Sigma-Aldrich; 10 mL of RIPA buffer to every protease inhibitor tablet). Tissue was weighed and 100 μ L per 10 mg of tissue of RIPA/protease inhibitor solution was added along with two 5 mm steel beads (69989; Qiagen, Hilden, Germany). Samples were placed in a TissueLyser LT (Qiagen) at 50 oscillations/sec for 3 min, briefly vortexed, put on ice for 2 min, followed by a second round of 50 oscillations/sec for 3 min in the TissueLyser. Samples were sonicated for 10 sec and subjected to centrifugation at 12,470 g for 30 min at 4 °C. The supernatant was transferred to a new microfuge tube and protein concentration was determined with Bio-Rad's Protein Assay Dye Reagent Concentrate (Bradford Assay) (5000006, Bio-Rad).

2.6.1. Immunoblotting Protocols

Traditional Western blot: Muscle tissue was combined with an equal volume of sample homogenate and Laemmli sample buffer (Laemmli 1970), containing 5% 2-mercaptoethanol, then further diluted in sample buffer to a final concentration of 1 mg/mL. Samples of 10 μ g of *Crym* tg TA homogenate and 40 μ g of control TA homogenate were loaded onto 4-12% Bis-Tris gels (NuPAGE NP0321PK2, Thermo Fisher), electrophoresed for 1 h at 170 V, and transferred to nitrocellulose for 2 h at 22 V. Blots were blocked for 3 h in blocking solution (3% milk in TBS containing 0.1% Tween-20 and 10 mM azide). Monoclonal mouse anti- μ -crystallin (SC-376687, Santa Cruz Biotechnology, Inc., Dallas, TX) and monoclonal rabbit anti-lysyl-tRNA synthetase antibodies (#129080, Abcam, Cambridge, United Kingdom), used as a loading control, were diluted 1:1000 in blocking buffer and incubated overnight at room temperature.

Lysyl-tRNA synthetase, encoded by the *Kars* gene, was used as the protein loading control because the expression of its mRNA showed minimal variance among mice and across genotypes unlike many other common control proteins (Supplemental Document 1). (At the time we did these studies, we did not have proteomic data.) After extensive washing, the membranes were incubated for 2 h with HRP conjugated goat anti-rabbit or goat anti-mouse secondary antibody diluted 1:10,000 in blocking solution. After extensive washing, chemiluminescence was visualized with the Super Signal West Femto Maximum Sensitivity Kit (#34095, Thermo Fisher) and imaged with a BioRad ChemiDoc XRS and image lab software (#1708265, BioRad).

Capillary-based Western blot (Wes): Wes analysis was performed according to the manufacturer's instructions for the 12-230 kDa protein separation module (#SM-W004; Protein Simple, San Jose, CA) to provide an automated alternative to the traditional Western Blot. Instrument settings were as follows; stacking and separation time, 30 min; separation voltage, 375 V; time for antibody blocking, 30 min; incubation with primary antibody time, 60 min; incubation with secondary antibody time, 30 min; luminol/peroxide chemiluminescence detection time, 15 min (HDR exposure). Protein extracted from whole tissue lysates (gastrocnemius, TA, soleus, diaphragm, heart, kidney, cerebral cortex, quadriceps, liver) from 3 male *Crym* tg and 3 control were prepared with 2x Laemmli Sample Buffer (#1610737; Bio-Rad, Hercules, CA) to generate an overall sample protein concentration of 1.0 mg/mL for each sample generated. The primary antibody to μ -crystallin (see above) was diluted 1:25 in Protein Simple's Antibody Diluent 2. A primary antibody to a control protein, aconitase-2 (ab129069; Abcam,

United Kingdom), was used at 1:200. We chose aconitase-2 as the protein loading control because this protein is abundantly expressed in many tissues, showed very little variability in expression in mice of the same genotype and between *Crym* tg and controls, as assayed by whole proteome LC.MS/MS (data not shown), and because the molecular mass of this protein is distinct from that of μ -crystallin. The primary and control antibodies were multiplexed. Samples were run as technical duplicates. Compass software (Compass for SW 4.0 Mac Beta; Protein Simple) was used to visualize the electropherograms and to analyze peaks of interest for area under the curve (AUC). The peak signal-to-noise ratio was set at ≥ 10 automatically by the software. Due to slight capillary-to-capillary variations in molecular weight readout, identified peaks at a molecular weight of interest were allowed a 10% range in molecular weight (as automatically set by the Wes system). AUC was analyzed with individual t-tests per tissue following the Benjamini, Krieger and Yekutieli FDR approach at $Q = 1\%$.

2.6.2. RNA and cDNA Preparation

Tissue from 3-month old *Crym* tg and control mice were removed, snap frozen in liquid nitrogen and stored at -80°C .

RNA was extracted using the following protocol. Tissue was placed in a 2 mL tube with 1 mL of TRIzol Reagent (15596026; Thermo Fisher Scientific) and two 5 mm steel beads (69989; Qiagen, Hilden, Germany), loaded into a TissueLyser LT (Qiagen) and run at 50 oscillations/sec for 2 min. Samples were checked for complete homogenization after 2 min and, if incompletely homogenized, run again in 30 sec cycles with checks for complete homogenization after each cycle. Samples were vortexed

briefly, inverted to mix at room temperature for 5 min, and subjected to centrifugation at 12,000 g for 10 min at 4 °C. Supernatant was removed into a new 1.5 mL RNase-free tube and 200 µL of chloroform was added. After vortexing for 15 sec, the sample remained at room temperature for 3 min. After a second centrifugation, at 12,000 g for 15 min at 4 °C, the top (clear) layer was removed into a new 1.5 mL RNase free tube and 500 µL of ice-cold isopropanol was added. Tubes were vortexed and inverted several times to mix, and then left at room temperature for 10 min. Centrifugation at 12,000 g for 10 min at 4 °C generated a white pellet of RNA, which was washed with 1 mL of ice-cold 75% ethanol and collected again by centrifugation (7,500 g for 5 min at 4 °C). After drying at room temperature , the pellet was dissolved in 25-35 µL of RNase-, DNase-free water at 60 °C for 10 min. RNA samples were stored at -80 °C until use.

cDNA was generated with the QuantiTect Reverse Transcription Kit (205313; Qiagen). RT-qPCR was performed on a CFX Connect thermal cycler (Bio-Rad) using the cDNA and PrimeTime Gene Expression Master Mix (1055772; IDT, Coralville, IA) in 20 µL reaction volumes in a BioRad CFX Connect thermal cycler following the manufacturer's protocol for the PrimeTime qPCR Probe Assays (IDT) except for the extension of the number of amplification cycles to 60. Primers are listed below.

IDT PrimeTime RT-qPCR Probe-Based Assay.

Crym₂: Forward: 5'-GAGATGTTTCGGGTCTGTTCAT-3'.

Probe: 5'-/FAM/TCATCACAG/ZEN/TCACCATGGCAACAGA/3IABkFQ/-3'.

Reverse: 5'-GGCTTTACCCATTCACCAAATAA-3'.

Nom1: Forward: 5'-TAAACCCAGAGTTCACTTCCTAC-3'.

Probe: 5'-/5HEX/TCGTCTTCA/ZEN/GTTTCCATCAACAGTGCA/3IABkFQ/-3'.

Reverse: 5'-CCTTCTCGCAACATTCCCA-3'.

Tert: Forward: 5'-CTCCTTTCCTCTAGGGCTATCT-3'.

Probe: 5'-/HEX/TCTCTGTCT/ZEN/CCCTTACCCACAGCT/3IABkFQ/-3'.

Reverse: 5'-AGTGCTGACATCTCATTCCCTTC-3'.

Relative tissue specific expression of *Crym*, standard deviations, and p values were calculated according to Taylor et al. (Taylor et al. 2019). *Nom1* was used as the control gene to measure *Crym* expression by qPCR.

2.7. Proteomic and Transcriptomic Comparison of Skeletal Muscle of *Crym* tg and Control Mice

Skeletal muscle samples were harvested from six 3-month-old, male, *Crym* tg and control littermate mice. All of the mice were perfused with cold PBS prior to muscle collection except for one of the 6 control samples. Samples, comprising half of the left TA muscle, divided longitudinally, were homogenized by bead beating (see above). Sample preparation for proteomics and nano ultra-performance liquid chromatography-tandem mass spectrometry were performed as described (Kim et al. 2019). Spectra were searched against a UniProt mouse reference proteome using Sequest HT algorithm described by Eng et al. (Eng et al. 2008) and MS Amanda algorithm developed by Dorfer et al. (Dorfer et al. 2014). Search configuration, false discovery control and quantitation were as described (Kim et al. 2019).

RNA extraction and RNA-seq was performed by Genewiz (South Plainfield, NJ) on 20 mg samples of TA muscles from 3-month-old mice from 3 *Crym* tg littermate and 3 control littermate mice. Genewiz generated FASTQ files of the raw RNA-seq data, after removing transcripts that mapped to introns and transcripts that mapped to multiple genes. p-Values for comparisons of genes expressed in *Crym* tg and control mice were also from Genewiz.

2.9. Ca²⁺ Transients

The amplitude of Ca²⁺ transients was recorded as described (Lukyanenko, Muriel, and Bloch 2017). In brief, isolated FDB fibers were loaded with Rhod-2AM (Thermo Fisher Scientific, Waltham, MA). Trains of voltage-induced Ca²⁺ transients were induced by field stimulation (A-M Systems, Carlsborg, WA). Rhod-2 was visualized with the Zeiss 510 Duo confocal microscope (Carl Zeiss). Image J 1.31v (NIH) was used for image analysis. The values reported were measured as the difference between maximal fluorescence intensity (F_{max}) and background fluorescence (F_0), normalized to F_0 . Quantitative data are shown as mean \pm SE. A Student's t-test was used to compare the data with $p < 0.05$ considered statistically significant.

2.9.1. Metabolic Chambers

Data were from two different cohorts of 4 *Crym* tg and 4 C57BL/6J control mice housed in an Oxymax/CLAMS (Columbus Instruments, Columbus, OH) open circuit indirect calorimeter, in two separate experiments. Measurements for RER, Accumulated CO₂, Delta CO₂, CO₂ Out, Heat, Delta O₂, Feed Weight, Volume CO₂, Accumulated O₂,

Feed Accumulation, Z Total, Volume O₂, O₂ Out, X Total, X Ambulatory, Flow, O₂ In, and CO₂ In were taken directly or calculated every 18 min for approximately 92 h. Z Total and X Total refer to the total number of times an animal disrupted the infrared (IR) beam in the Z and X axis, respectively, while X Ambulatory refers to the number of times an animal disrupted at least two consecutive IR beams. Complete measurements were compiled and 24 h worth of measurements were analyzed, starting at the first dark cycle after a 24 h period of acclimation. Values were normalized to total body weight and analyzed separately for light and dark periods. Outliers were identified with the ROUT method (Motulsky and Brown 2006) at Q = 1%, with GraphPad Prism version 6.0e for Mac (GraphPad Software, La Jolla, CA). Averages were then calculated for all measurements except for Feed Weight, Feed Accumulation, Z Total, X Total, and X Ambulatory, for which the sums were determined. Each average or sum for each mouse was tested for significance, grouped as a genotype with an unpaired, parametric t-test with Welch's Correction.

2.9.2. Diet Studies

Crym tg and control male and female mice at approximately 14 weeks old were placed on one of five diets (Supplemental Document 5). The number of mice on a particular diet varied from 5 to 16, due to the occasional death of a mouse, unrelated to the experiment, or to our inability to weigh them on a particular date. The diets were “normal” diet (2018SX, Envigo Madison, WI), high fat diet (D12492), low fat diet (D12450J), high simple carbohydrate diet (D15040205), or high complex carbohydrate diet (D12450K), all from Research Diets Inc. (New Brunswick, NJ) unless otherwise

specified. Mouse weight (anaesthetized with 2.5% isoflurane) and food weight were recorded every Monday, Wednesday, and Friday for approximately 60 d. Water was provided *ad libitum*.

Mouse weights were normalized to their starting body weight. Using the Real Statistics Resource Pack software (Release 6.8) (Zaiontz 2020) to run the Mauchly and John-Nagao-Sugiura tests, we found that all of the groups violated at least one test for sphericity ($\alpha = 0.05$). We therefore used GraphPad Prism 8.2.0 for Mac to apply the Greenhouse and Geisser epsilon correction factor to either a two-way repeated measures (RM) ANOVA or a mixed-effects model, specifically a compound symmetry covariance matrix fit with Restricted Maximum Likelihood (REML) if data were missing for certain dates ($\alpha = 0.05$). When we observed significance with the two-way RM ANOVA or mixed-effects model (REML), we performed multiple post-hoc unpaired, two-tailed t tests assuming heteroscedasticity at $\alpha = 0.05$ to determine which data points showed significant differences between *Crym* tg and control mice.

2.9.3. T₃, T₄, TSH Levels

Homogenates of TA muscles and serum from four *Crym* tg and four control mice were sent to the clinical diagnostic service at Vanderbilt University (Nashville, TN) for analysis of T₃, T₄ and TSH.

2.9.4. Statistics

T₃, T₄ and TSH levels were analyzed by a two-tailed t-test with Welch's correction. The thyroid hormone mass (in ng/mL) was divided by total protein (in ng/mL)

and used to determine the percent of total thyroid hormone per total protein in a milliliter of serum or homogenized muscle. The negative log base 10 of the percent of total protein for each value was determined and used to calculate the average and standard deviation.

2.9.5. Materials

Unless otherwise stated, all biologics were from Sigma-Aldrich and all salts were from Thermo Fisher.

3. Results

We created a transgenic mouse in which murine *Crym* is expressed at high levels in skeletal muscle, comparable to those seen in some human muscle biopsies, and assessed the effects an abundance of μ -crystallin would have on muscle structure and function, and on metabolism. The *Crym* transgene was encoded in a plasmid under the control of the human slow troponin I enhancer and the human skeletal actin promoter with the polyadenylation sequence of bovine growth hormone mRNA (Supplemental Figure 1A). After oocyte injection, the plasmid inserted randomly into intron 12 of the *Cntn6* gene on murine chromosome 6 (Supplemental Figure 1B), as determined by sequencing (Supplemental Figure 1C). The mice were bred to homozygosity and genotyping of the mice showed that there was a single insertion in the genome resulting in two copies of the *Crym* transgene in the diploid mouse genome (Supplemental Figure 2). Back-crossing *Crym* tg with control mice yielded the expected Mendelian inheritance pattern (Supplementary Table 1). *Cntn6* was not significantly differentially expressed in control

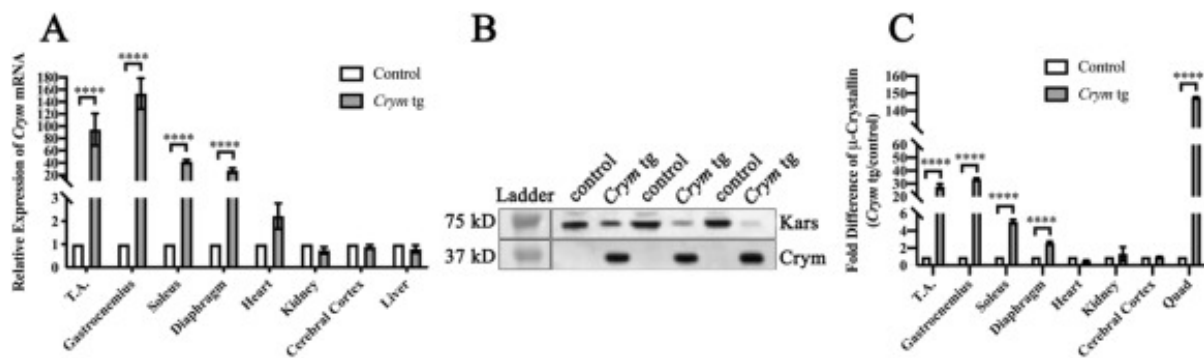
and *Crym* tg mice and showed little to no expression as assayed by RNA-seq in both. This indicates that the gene was not disrupted by the transgene's insertion.

3.1. RT-qPCR, Western Blot, and Immunofluorescence

RT-qPCR of several skeletal muscles showed moderate to large increases in *Crym* mRNA in male *Crym* tg mice compared to male controls (Figure 1A). Because many canonical control genes were significantly differentially expressed, we compared RNA-seq and LC.MS/MS data (Supplemental Document 1 and 3 respectively) to identify gene products with the smallest coefficient of variation. We used RefFinder (Xie et al. 2012) to evaluate the most promising control genes among biological and technical replicates of various tissues (data not shown). We found that *Nom1* was optimal, as it showed the most stability. Using *Nom1* mRNA as a standard, we observed large increases in the *Crym* mRNA levels in skeletal muscles of the *Crym* tg mice, compared both to controls and to heart muscle and non-muscle tissues. Notably, different skeletal muscles in the tg mice differed significantly in their relative expression of *Crym*. We found no significant differences in *Crym* mRNA levels in non-skeletal muscle tissues in tg and controls (Figure 1A).

Figure 1. Increased *Crym* mRNA and μ -crystallin protein levels in *Crym* tg vs. control mice. A. *Crym* expression in several skeletal muscles and other tissues were analyzed from 3 *Crym* tg and 3 control mice. All analyses were in technical triplicate, except for soleus and diaphragm. B. Western blot of μ -crystallin in *Crym* tg and control TA muscle extracts. Control mice had 40 μ g of TA homogenate per lane, and *Crym* tg

lanes had 10 μ g of TA homogenates per lane. We were unable to detect μ -crystallin reliably in controls in these blots. C. μ -Crystallin was quantitated with Protein Simple's Wes instrument. Areas under the curve, generated from electropherograms of μ -crystallin expression, were normalized to aconitase-2 expression (n = 3, in technical duplicate) in several muscles and other tissues. Multiple individual t-tests using the Benjamini, Krieger and Yekutieli FDR approach at Q = 1% determined statistical significance (**** = p<0.0001). The results show that *Crym* tg skeletal muscle express high levels of *Crym* mRNA and protein compared to controls and to other tissues analyzed.

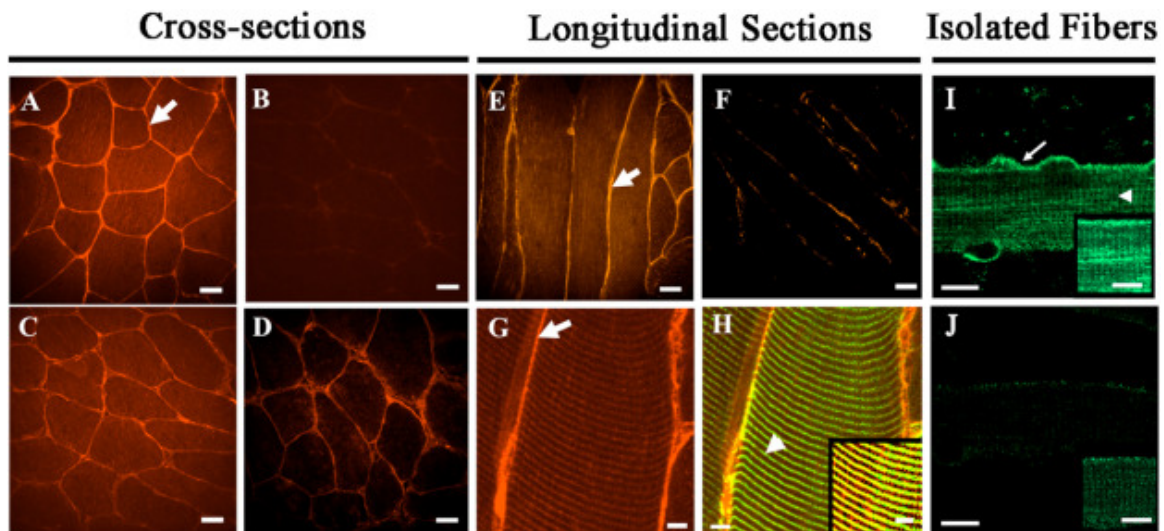


Immunoblotting confirmed that μ -crystallin (*Crym*) was present in elevated to highly elevated amounts in transgenic skeletal muscles compared to controls (Figure 1B). We used capillary-based immunoblotting in a Wes apparatus (Figure 1C) to quantitate the differences, with aconitase 2 as a loading control, and determined that transgenic skeletal muscles contain 2.6 to 147.5-fold more μ -crystallin than controls, depending on the muscle. Remarkably, although all skeletal muscles we assayed showed increased levels of μ -crystallin, their relative amounts varied considerably (Figure 1C), consistent with our qRT-PCR results. These differences were highly significant (p<0.0001).

We also examined the distribution of μ -crystallin in transgenic muscle. In cross-sections of TA and flexor digitorum brevis (FDB) muscle, immunolabeling for μ -crystallin was concentrated near the sarcolemma (Figure 2, arrows) but was also present in the myoplasm. Soleus cross sections did not show a similar concentration of μ -crystallin near the sarcolemma compared to controls (Figure 2C, D), perhaps because they express lower amounts of the protein. Longitudinal sections of TA muscle and isolated FDB myofibers also showed high levels of μ -crystallin at or near the sarcolemma (Figure 2E, G, I), but in addition revealed a faint striated distribution in the myoplasm (Figure 2H, I), which in TA muscles colocalized with desmin at the level of the Z-disk (Figure 2H, arrowhead). We did not observe immunolabeling for μ -crystallin in the capillaries or connective tissue surrounding myofibers. These results as well as results from qPCR and Wes data (Figures 1A and 1C respectively) indicate that μ -crystallin is expressed at elevated levels in myofibers of the transgenic mice but not in other cell types in muscle or other tissues.

Figure 2. Immunolabeling of μ -crystallin in control and *Crym* tg skeletal muscles. A-D, Cross (A-D), longitudinal sections (E-H), of *Crym* tg (A, C, E, G, H) and control (B, D, F) TA (A, B, E-H) and soleus muscles (C, D) were stained with anti- μ -crystallin antibody and Alexa Fluor-568-conjugated secondary antibody. In G-H, longitudinal sections of *Crym* tg TA muscle (G, μ -crystallin only) were colabeled with anti-desmin and Alexa Fluor-488-conjugated secondary antibody (H, yellow color shows colabeled structures). I, J, Flexor digitorum brevis (FDB) myofibers in culture from *Crym* tg (I) and control mice (J) were labeled with anti- μ -crystallin antibody and

Alexa-Fluor 488-conjugated secondary antibody. The results show that μ -crystallin was detected at higher levels in tg muscles than in controls. In TA muscle and FDB myofibers it was enriched at the levels of the sarcolemma (arrows, A,E,G, I) and Z-disks, colabeled with desmin (arrowhead, H) or shown without desmin colabel (arrowhead, I). Inset panels (H-J) are brightened and magnified. *Crym* tg (I) and control (J) FDB images were brightened and magnified equivalently. A-F, scale bars = 20 μ m; G, H, scale bars = 5 μ m; I, J, scale bars = 10 μ m.



3.2. Hormone levels

We compared the levels of different hormones involved in thyroid hormone signaling in *Crym* tg and control mice. We found significantly more T_3 in the TA muscle (~190 fold more) of *Crym* tg mice and significantly less T_4 in the serum (~1.2 fold less) compared to controls ($p < 0.001$ and $p < 0.05$, respectively). Thyroid stimulating hormone (TSH) was not significantly different in serum (Table 1) of *Crym* tg and control mice and, as expected, was not detected in muscle. Intramuscular T_4 and serum T_3 also did not

differ significantly between *Crym* tg and controls. Thus, the large increase in μ -crystallin in murine skeletal muscle is associated with an even larger increase in muscle T₃.

Table 1. T₃, T₄, and TSH in TA muscle and serum in *Crym* tg and control

mice. Hormone levels were determined by a clinical diagnostic laboratory. Muscle T₃ was significantly higher in *Crym* tg compared to controls while serum T₄ was significantly lower in *Crym* tg compared to controls. TSH was not significantly different in serum and was not detected in muscle (n = 4). Significance was calculated using a two-tailed Student's t-test with Welch's Correction ($\alpha = 0.05$).

TA Muscle

	Control				<i>Crym tg</i>						
	Perce	-	Std.	Std.	n	Perce	-	Std.	Std.	n	p
	nt	Log(Perc	Dev.	Dev.		nt	Log(Perc	Dev.	Dev.		Valu
	Mean	ent		(-		Mean	ent		(-		es
	(ng/m	Mean)		Log)		(ng/m	Mean)		Log)		
	g					g					
	protei					protei					
	n)					n)					
T ₃	5.801	8.252	1.940	0.13	4	1.115	6.070	1.065	0.34	4	0.000
	E-09		E-09	0		E-06		E-06	1		3
T ₄	1.008	5.294	1.084	0.70	4	2.392	5.939	2.610	0.67	4	0.231
	E-07		E-07	1		E-08		E-08	0		4
TS	N.D.	N.D.	N/A	N/A	4	N.D.	N.D.	N/A	N/A	4	N/A

H

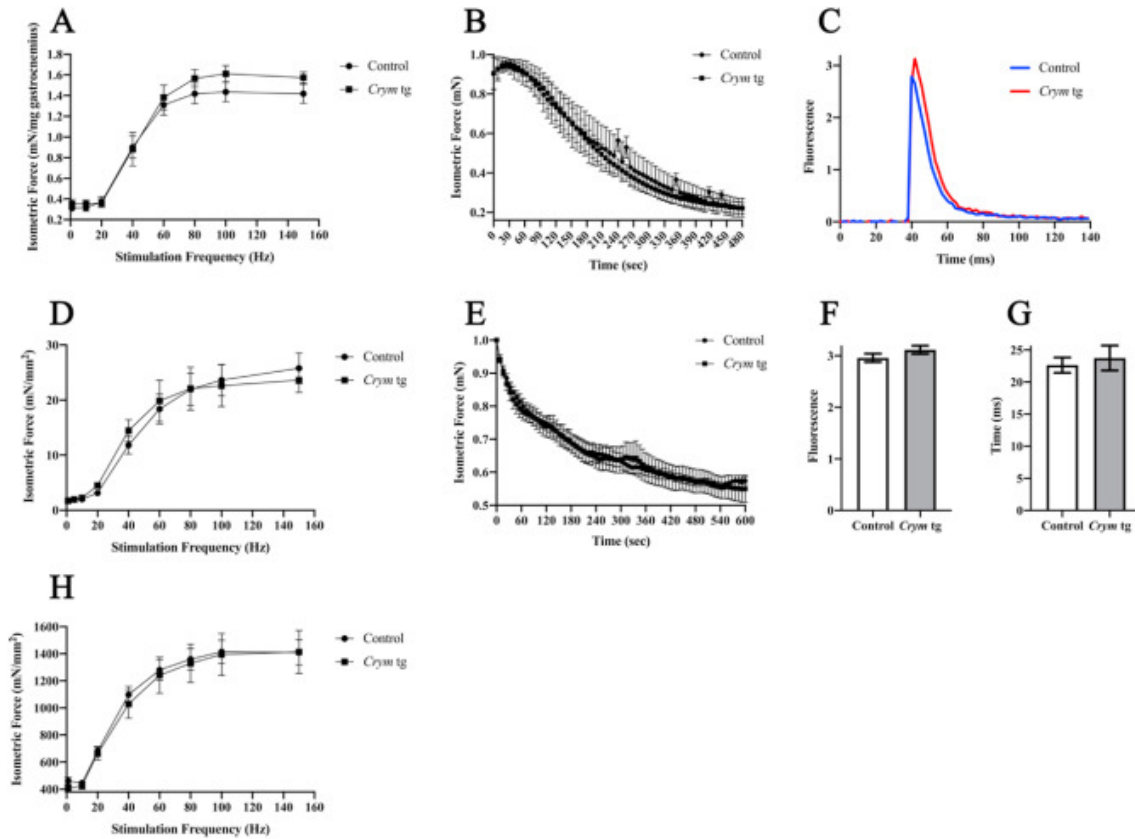
Table 1 continued

	Serum										
	Control					<i>Crym tg</i>					
	Perce	-	Std.	Std.	n	Perce	-	Std.	Std.	n	p
	nt	Log(Perc	Dev.	Dev.	nt	nt	Log(Perc	Dev.	Dev.	nt	Valu
	Mean	ent		(-	Mean	ent		(-		es	
	(ng/m	Mean)		Log)	(ng/m	Mean)		Log)			
	g				g						
	protei				protei						
	n)				n)						
T ₃	2.672	5.577	3.826	0.06	4	2.325	5.635	1.865	0.03	4	0.173
	E-06		E-07	3		E-06		E-07	6		2
T ₄	1.146	3.941	5.530	0.02	4	9.417	4.028	1.076	0.05	4	0.033
	E-04		E-06	1		E-05		E-05	1		9
TS	1.546	2.816	2.652	0.07	4	1.376	2.885	5.664	0.15	4	0.614
H	E-03		E-04	6		E-03		E-04	7		9

3.2.1. Morphology and physiology

When we performed different morphological and physiological assays of the structure and function of the transgenic mice, we found no significant differences between *Crym* tgs and controls. The fiber sizes, distribution of fiber sizes, fiber types by immunohistochemistry of myosin heavy chains, weights, and the frequency of centrally nucleated fibers (CNFs) were not significantly altered in the TA muscles of *Crym* tgs (Supplemental Figures 4, 5C, 9C-D). Specific isometric force of contraction, maximal rate of twitch force contraction/relaxation, grip strength, maximum treadmill running speed, and distance run were also indistinguishable between *Crym* tg and controls (Figure 3A, B; Supplemental Figure 6; Supplemental Figure 10). Fatiguability in the *Crym* tg mice showed a trend towards being slower than in controls, but this did not rise to the level of significance (Figure 3B). At the single myofiber level, voltage-induced Ca^{2+} transients, maximal amplitudes of transients and transient decay rates, all measured with the Ca^{2+} -sensitive fluorescent indicator, Rhod2, under conditions that measure changes in cytoplasmic and not mitochondrial Ca^{2+} (26), were identical in the two strains of mice (Figure 3C, F, G). Fat staining with BODIPY (493/503) was also the same (Supplemental Figure 7). However, we did find that *Crym* tg gastrocnemius muscles and mesenchymal fat pads weighed slightly more than their control counterparts ($p < 0.05$; Supplemental Figure 3). By these measures, the overexpression of *Crym* and the resulting accumulation of T_3 in myofibers has minimal effects on the structure or function of murine skeletal muscle.

Figure 3. Contractile properties of Crym tg muscle. Force frequency curves (A, B, D, E, H) of gastrocnemius (A, B), soleus (D, E), and extensor digitorum longus (Freake and Oppenheimer) (H). Force was normalized to gastrocnemius muscle weight (A) or to soleus or EDL cross-sectional area (D, H). For fatigue, force was normalized to peak force (B, E). Ca²⁺ transients in isolated myofibers (C, F, G). C. Representative Ca²⁺ transient evoked by a voltage pulse, visualized with Rhod2. Blue, control; red, *Crym tg*. F. Maximal amplitudes of the Ca²⁺ transients. (n = 100). G. Mean time constants for the decay of the transients (n = 100). Statistics utilized the Student's t-test for Ca²⁺ measurements (F, G) or the Holm-Šídák test on the gastrocnemius (n = 5; A, B), soleus (control n = 4, *Crym tg* n = 5; D, E), or EDL (control n = 6, *Crym tg* n = 5; H) at $\alpha = 0.05$. All error bars show standard error. The results show no statistically significant differences in any of these measurements.



3.2.2. Fiber Types

We applied a machine learning approach to obtain more quantitative information about the soleus muscles in the *Crym tg* mouse. We did not find any significant differences in the fiber type populations or total number of fibers of *Crym tg* soleus muscles (782 ± 219 fibers) compared to controls (933 ± 442). Furthermore, our results obtained by determining fiber type visually closely matched the results we determined computationally (Supplemental Figures 4C, 5C, 9A-B; Supplemental Document 4). We did discover significant differences in a few metrics, however. In particular, the minimal Feret's diameter of *Crym tg* Type I, I/Ib, I/Ib/IIa, IIa, IIa/IIb, IIb, and all fiber types in aggregate were significantly smaller than control fibers of the same types while Type I/IIa and IIX fibers were not significantly altered in minimal Feret's diameter. *Crym tg*

Type I, IIb, and IIa/IIb fibers were significantly more circular than controls, whereas Type I/IIb, IIx, and all fiber types in the *Crym* tg in aggregate were less circular than controls (Supplemental Document 4). Using visual evaluation only, we did not observe any significant differences in myosin-specific fiber type labeling in TA or gastrocnemius muscle cross sections between *Crym* tg mice and controls (Supplemental Figures 5 and 9; the sizes of these muscles were too large to analyze by machine learning with our equipment). Our results indicate that, although the fiber types in *Crym* tg and control soleus muscles are indistinguishable, several properties differ significantly between the two genotypes.

3.3. Metabolism

As T₃ can have a profound effect on metabolism, we subjected *Crym* tg and control mice to metabolic studies in Comprehensive Lab Monitoring System (CLAMS) cages. We determined 18 metabolic traits and found that 6 and 4 traits (Supplemental Table 2) were significantly different between *Crym* tg and control mice during the light and dark cycles, respectively. The respiratory exchange ratio (RER), a measure of the oxidative preference for carbohydrates vs fats, was significantly different during both the light and dark cycles, with essentially no change in the overall energy expenditure (Table 2). Table 2 shows the mean RER of the *Crym* tg and control mice, compared to standardized values (Lusk 1924). The results show that the oxidative metabolism in the transgenic mice has partially shifted away from the use of carbohydrates as an energy source and towards fats. The difference from controls is 13.7%. Other traits that also differed significantly between *Crym* tg and control mice in both light and dark periods

were Delta CO₂, and Accumulated CO₂ (Supplemental Table 2). Thus, overexpression of *Crym* in skeletal muscle has a significant effect on murine preference for fat as a fuel source for energy metabolism.

Table 2. Mean RER and corresponding carbohydrate and fat usage. Mean RER was determined by averaging calculated RER values for each genotype (n = 8). The closest standard RER value (taken from Lusk, G (41)) was determined and carbohydrate vs fat utilization as energy sources from the standard RER value are listed.

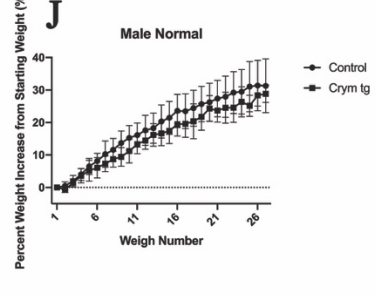
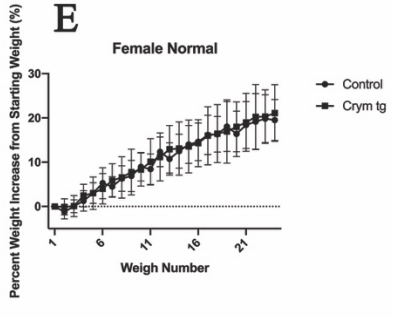
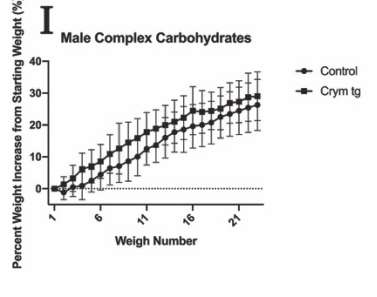
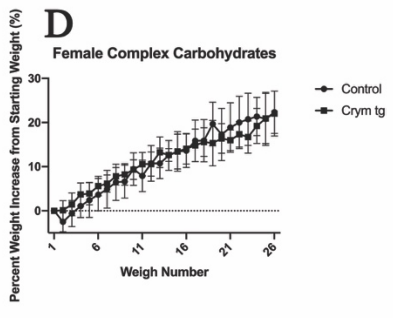
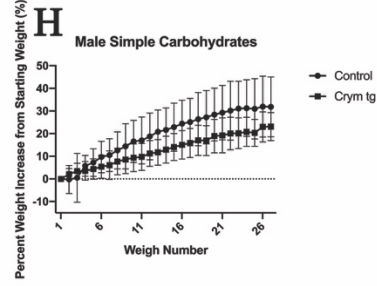
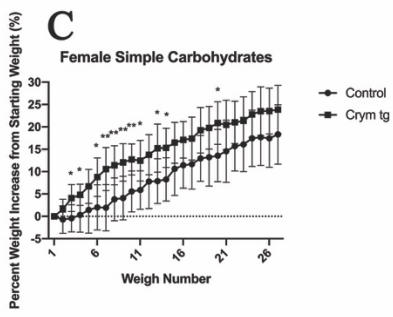
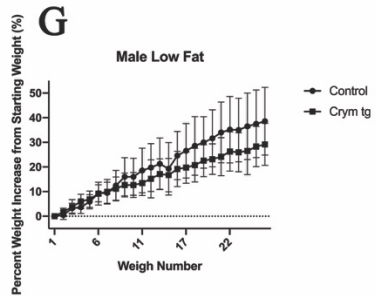
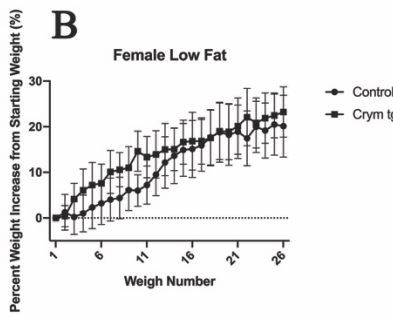
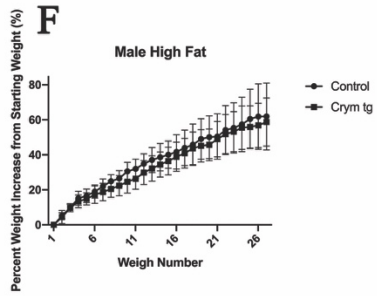
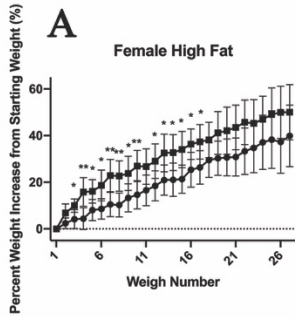
			Percentage of total oxygen consumed		Percentage of total heat produced by:		Calories per liter of O ₂	
	Mean RER	Closest Standard RER Value	Carbohydrate	Fat	Carbohydrate	Fat	Number	Log ₁₀
Control	0.916	0.92	72.7	27.3	74.1	25.9	4.948	0.69447
<i>Crym</i> tg	0.879	0.88	59	41	60.8	39.2	4.899	0.69012

3.3.1. Diet Study

As the *Crym* tg mice prefer fats to carbohydrates as an energy source, we fed *Crym* tg and control mice high fat, low fat, high simple carbohydrate, high complex carbohydrate and

normal control diets and measured their weight gain over a period of 2 months. We observed significant increases in normalized body weight of female *Crym tg* mice on the high simple carbohydrate and high fat diets, compared to controls. Female *Crym tg* mice on the other diets and male *Crym tg* mice on all 5 of the diets did not gain significantly more or less weight than controls (Figure 4).

Figure 4. Weight gain of *Crym tg* and control mice on various diets. *Crym tg* and control mice were placed on different diets and weighed over the course of 60 days. Female (A-D) and male (F-I) *Crym tg* and control mice were placed on diet containing high fat (A, F), low fat (B, G), high simple carbohydrates (C, H), high complex carbohydrates (D, I), or on a normal diet (E, J) for 60 days. Mice were weighed three times a week and the percent weight increase from their starting weight was determined. Female *Crym tg* mice on high fat or high simple carbohydrate diets gained weight significantly more rapidly than controls. We did not observe any other significant results using a two-way repeated measures ANOVA or mixed-effects model (* = $p < 0.05$, ** = $p < 0.001$, $n = 5-16$; see Supplemental Document 5 also).



3.3.2. Global gene expression (RNA-seq)

The expression of a large number of genes can be affected by T₃ (Supplemental Document 2), which is thought to act largely through thyroid responsive elements (TREs). As T₃ is present in much higher levels in *Crym* tg mice, we had RNA-seq performed on TA muscle samples from 3 *Crym* tg and 3 control mice and measured more than 13,000 transcripts from approximately 8.4x10⁸ reads. All samples had an average Q score >37 with approximately 87% of bases having a Q score greater than 30. After removing transcripts that aligned to introns or that mapped to multiple genes, and after Benjamini-Hochberg False Discovery Rate (FDR) correction, we found that 566 genes were significantly different between *Crym* tg and controls at $\alpha = 0.05$ (Supplemental Document 1). Gene ontology (GO) analysis revealed a relative decrease in the expression of genes encoding proteins involved in glycolysis and glycogen metabolism and in fast contractile speeds, and an increase in the expression of genes associated with oxidative metabolism and slower contraction (Tables 3, Supplemental Table 6). STRING network analysis also showed clusters of genes involved in ubiquitination, filament associated genes, and the innate immune system (Supplemental Figure 8). After Benjamini-Hochberg FDR correction, DAVID chromosome annotation showed significantly more ($p = 5.7E-7$) differentially expressed transcripts arising from chromosome 6 than would be expected. Notably, only 7 of the 566 DEGs contained putative TREs (Supplemental Table 3).

Table 3. Changes in gene expression related to glycolytic and oxidative pathways and fiber type. Genes related to the glycolytic and oxidative metabolic pathways were

determined by assessing root ontological terms for DEGs (n = 566) processed using PANTHER. Enrichment of ontological terms was determined by $p < 0.05$ after Bonferroni correction of Fisher's exact p-values. Fiber contraction speed genes were determined by cross referencing a putative fiber type-specific list of genes (18). Genes that shared both glycolytic and β -oxidative ontologies were removed from the analysis. The results show that *Crym* tg muscle exhibit changes in gene expression consistent with a shift to a slower contractile, more oxidative state.

Glycolytic Pathway		Oxidative Pathway		Fast Contractile		Slow Contractile	
Genes		Genes		Genes		Genes	
#	#	#	#	#	#	#	#
increase	decrease	increase	decrease	increase	decrease	increase	decrease
d	d	d	d	d	d	d	d
5	11	29	20	10	43	54	8

In addition to its ability to bind T_3 , μ -crystallin is a ketimine reductase, with its activity inhibited by T_3 binding (Hallen et al. 2011). Although this activity is likely inhibited by the high intracellular levels of T_3 in *Crym* tg muscle, five genes involved in lysine degradation (a pathway including substrates that μ -crystallin acts on in its capacity as a ketimine reductase), showed significant changes in expression in the *Crym* tg muscle compared to controls, with *Aldh2*, *Ogdh* and *Dlst* increasing in expression and *Sccpdh* and *Setd7* decreasing in expression.

3.3.3. Global protein expression (LC.MS/MS)

Proteomic analysis used liquid chromatography-tandem mass spectrometry (LC.MS/MS) followed by bioinformatic assessment (Supplemental Document 3). GO analysis was performed on the 85 significantly differentially expressed proteins using the PANTHER Classification System which resulted in 7 statistically significant ontological classes. Four of the terms related to muscle while one was for oxidation-reduction process (Table 4). Eleven proteins that were significantly differentially expressed in *Crym* tg mice compared to controls were associated with the “oxidation-reduction process” gene ontology. Five of those proteins increased in expression in *Crym* tg mice compared to controls while 6 decreased (Supplemental Table 5). Although the gene products revealed by LC.MS/MS and RNA-seq showed minimal overlap, the significant ontological terms in the proteomic study were similar to those found in the transcriptomic study.

Table 4. Significant biological GO terms. Ontological terms were derived from a list of 85 differentially expressed proteins via LC.MS/MS proteomics comparing *Crym* tg mice to controls. The results are consistent with the *Crym* tg skeletal muscle undergoing a shift towards a slower contractile, more oxidative state.

Term	Count	p-value	Fold Enrichment
oxidation-reduction process	11	3.700E-04	3.976
cardiac muscle contraction	4	9.580E-04	20.363
cardiac myofibril assembly	3	1.034E-03	61.088
detection of muscle stretch	2	1.605E-02	122.176
protein refolding	2	3.576E-02	54.300
cardiac muscle hypertrophy	2	3.576E-02	54.300
regulation of mitotic spindle assembly	2	4.740E-02	40.725

4. Discussion

As imbalances in T_3 , such as hypothyroidism or hyperthyroidism, can result in a variety of maladies, thyroid hormone levels are carefully controlled under normal conditions. Regulation of thyroid hormone levels are affected by the feedback loop of thyrotropin releasing hormone (TRH), TSH, T_4 , somatostatin (Pirahanchi and Jialal 2019; Siler et al. 1974), monocarboxylate thyroid hormone transporters (especially MCT8/10) (van Mullem et al. 2016), and deiodinases (*DIO1-3*) that convert T_4 transported into the cell into T_3 and other metabolites (Bianco and Kim 2006). μ -Crystallin binds T_3 (Hashizume, Miyamoto, Ichikawa, Yamauchi, Sakurai, et al. 1989; Tata 1958) and its absence has been shown to increase efflux of T_3 from the cell significantly (Suzuki et al. 2007). This information, paired with the fact that *CRYM* levels can vary greatly in human muscle (Klooster et al. 2009), raises the question: what effects does μ -crystallin have in

those individuals where it is highly expressed? To address this, we generated a skeletal muscle specific transgenic mouse, *Crym* tg, in which *Crym* mRNA and protein are expressed in skeletal muscle at high levels comparable to those seen in some humans (Homma et al. 2012; Klooster et al. 2009; Reed et al. 2007). We find that when *Crym* is overexpressed, metabolism shifts away from carbohydrate use toward fat use, with concomitant shifts in the expression of genes from glycolysis toward β -oxidation and from fast contractile toward slow contractile gene products.

Expression of *CRYM* in human skeletal muscle from 430 individuals in the GTEx database show about 20% of individuals expressing *CRYM* at relatively high levels while the majority of people express little to no *CRYM*. RT-qPCR and Western blot data [(Klooster et al. 2009); see also (Homma et al. 2012)] show a similar percentage of individuals expressing high levels of *CRYM*, 30-40 times higher than low expressers. Though a marked variability in *CRYM* expression has been observed, to the best of our knowledge no data so far correlates human *CRYM* expression to energy expenditure, locomotive ability, or body composition. We have confirmed this in our own laboratory (Reed et al., unpublished). *Crym* tg mice produce approximately 94-fold more *Crym* mRNA as assayed by RT-qPCR and ~28 times more μ -crystallin protein in their TA muscles compared to control C57BL/6J mice. Thus, the *Crym* tg mouse model reproduces key features of human high expressers, producing *Crym* at levels that vastly outstrip control mice or human low expressers.

The enhancer from the *TNNI1* gene that we used to increase expression of the *Crym* transgene is a slow skeletal muscle specific gene (Sheng and Jin 2016) while the promoter, taken from the human skeletal actin gene (*ACTA1*), shows expression in both

fast and slow type fibers (Ciciliot et al. 2013). To our knowledge, muscle-specific differences in gene expression driven by the skeletal actin promoter have not been documented, though it is regulated by a number of factors, including adrenergic signaling (Bishopric and Kedes 1991). Indeed, thyroid hormone itself can reduce skeletal actin expression, but only when it is introduced exogenously at levels several orders of magnitude greater than those reached in either control or *Crym* tg TA muscles (Collie and Muscat 1992; Gustafson, Markham, and Morkin 1986). Studies of skeletal actin protein do not show differences in expression that depend on the muscle or fiber type composition, however (Giger et al. 2009; Pette and Staron 1997), suggesting that differences in the activity of the actin promoter may not account for our results. Less is known about the activity of the *TNNI1* enhancer element, but, paradoxically, soleus and diaphragm, which are more slowly contracting in mice than other skeletal muscles (Luff 1981) have lower levels of *Crym* expression at the mRNA and protein level compared to other skeletal muscles in *Crym* tg mice, although they are elevated compared to controls. Thus, although unexpected, our results clearly show that the same promoter/enhancer pair can drive different levels of transgene expression in different muscle groups.

As expected from the high levels of *Crym* expressed in the muscles of the transgenic mice, we observed a large accumulation of intracellular T_3 (~190-fold) in the TA muscle compared to controls. μ -Crystallin promotes accumulation of T_3 in the cytoplasm in part by sequestering the hormone. Levels of total T_3 in control mouse serum are unchanged in the transgenic mouse. At these levels, μ -crystallin in the muscle should be close to saturated with bound T_3 . The same should be true for the C57BL/6J control muscle.

Although we cannot explain the 5-fold higher enrichment in the T₃ level compared to μ -crystallin protein (the stoichiometry of binding is 1:1 (Hallen and Cooper 2017)), we propose that μ -crystallin may promote the influx and slow the efflux of thyroid hormones by interacting directly with the T₃ transporters at the cell surface (Friesema et al. 2008; Mori et al. 2002). This would be consistent with our finding μ -crystallin at the sarcolemma of *Crym* tg muscle (Figure 2A, E, G, I).

It is also not clear why serum T₄ is decreased in *Crym* tg mice compared to controls. TSH levels are unchanged between *Crym* tg and control mice, so T₄ production should be unimpaired. Lower serum T₄ may result from its increased intramuscular conversion into T₃ and its intracellular storage once it is bound to μ -crystallin in the myoplasm. Thus, the higher levels of μ -crystallin are likely to create a “sink” for T₃ within the cell that is filled by mass action of T₄ transported from the serum into the myoplasm, followed by its intracellular deiodination. Additional studies will be needed to determine why T₄ decreases in the serum, why T₃ accumulates to such high levels in the muscles of the transgenic mice, and whether the levels of intracellular T₃ accumulation vary with the levels of expression of μ -crystallin in different muscles.

We did not see any significant differences in the numbers of any fiber type or in the total number of fibers when we compared soleus muscles of *Crym* tg mice to controls. Similarly, we also saw no differences in fiber type between control and *Crym* tg TA and gastrocnemius muscles. Staining for myosin heavy chains is only one metric used to quantify fiber type as slow twitch or fast twitch, however. Future studies using ATPase staining (Brooke and Kaiser 1970), succinic dehydrogenase staining (Bancroft and

Gamble 2008), or α -glycerophosphate dehydrogenase staining (Dubowitz, Sewry, and Oldfors 2013) may present a more complete picture of any, potentially subtle, fiber type changes that occur due to the overexpression of μ -crystallin in skeletal muscle. Despite this superficial similarity, we did find differences in the minimal Feret's diameter and the circularity of particular fiber types, among other significantly different morphological characteristics, although we cannot ascribe any physiological significance to these differences. Because we see a shift towards β -oxidation as determined by RER, and slow twitch fibers preferentially utilize β -oxidation compared to fast twitch fibers (Kalmar, Blanco, and Greensmith 2012) while also having a smaller size (Schiaffino and Reggiani 2011), soleus myofibers may be shifting towards a slower twitch phenotype. Remarkably, notwithstanding the large changes in the levels of thyroid hormones that we have measured, we see very few other changes in the structure or function of the hindlimb muscles in mice. Like the fiber types, central nucleation and fat deposition are essentially unchanged. Physiologically, overall muscle function and the function of individual muscles and muscle fibers are indistinguishable between transgenic and control samples. Thus μ -crystallin's effects on muscle structure and function are not readily apparent, despite its massive effect on the distribution of T_3 . This is consistent with our observation that most changes in gene expression that we measure in transgenic muscle are quite modest – usually less than 50% higher or lower than controls. Whether the similarities between control and tg muscle are sustained when mice are stressed by changes in diet, or by injury or disease, must still be determined.

Because T_3 has profound effects on metabolism, we also studied the *Crym* tg mice in metabolic cages. We found that, under normal resting conditions, RER, a measure of

preference for sources of metabolic energy, was significantly different between the *Crym* tg mice and controls. The difference in RER corresponds to a 13.7% increase in utilization of fat as an energy source over carbohydrates in *Crym* tg mice compared to controls.

Consistent with the changes we observed in RER, GO analysis of RNA-seq data on *Crym* tg and controls showed an increase in expression of genes associated with β -oxidation and a decrease in genes associated with glycolysis. As the murine TA muscle is comprised almost entirely of fast twitch fibers, which are primarily glycolytic (Kalmar, Blanco, and Greensmith 2012), we compared our 566 significantly differentially expressed genes to a list of 1343 fast and slow fiber type genes generated by Drexler et al. (Drexler et al. 2012). We found that 106 or ~19% of the genes altered in expression in the *Crym* tg mice encode contractile or other proteins related to fiber type (Table 3), and that the expression of genes associated with fast fiber types significantly decreased while that of genes associated with slow fiber types significantly increased (Table 3). By contrast, proteomic studies results revealed 26 significantly differentially expressed, fiber type-specific proteins, of which 7 shifted towards a slower phenotype while 19 shifted towards a faster phenotype (Table 5). As reported (Fitts et al. 1984), high levels of TH have little effect on fast twitch muscles but cause slow twitch muscles to exhibit faster twitch characteristics. Because mice have very few slow twitch fibers and the *Crym* tg mouse is subject to far less than the thyrotoxic levels of TH used in previous rodent studies, it is perhaps not surprising that we see minimal effects of *Crym* overexpression. However, we have shown for the first time that high levels of T₃ in myocytes may cause curious transcriptional/translational shifts in which slow fiber type genes increase in

expression while fast fiber type proteins increase in expression. Future studies evaluating the regulatory steps concerning transcription and translation may determine how TH can decrease the mRNA content of genes expressed primarily in fast fiber types but increase the protein levels of fast fiber type proteins, and *vice versa*. Coupled with the shift towards a preference for fat utilization and increased expression of genes involved in β -oxidative metabolism, 11 proteins related to the metabolic oxidation-reduction process, and decreased expression of genes involved in carbohydrate metabolism, it seems likely that the accumulation of T_3 in muscle is associated with a shift towards a slower twitch, more β -oxidative phenotype.

Table 5. Proteins differentially expressed in *Crym tg* mice compared to controls by LC.MS/MS associated with muscle twitch speed. A total of 26 of the 85 differentially expressed proteins identified via LC.MS/MS proteomics are associated with fast or slow twitch speeds. The fourth column from the left lists the fiber types these proteins are normally associated with. The fifth column indicates the nature of the shift we observed in the *Crym tg*. The results show changes indicating changes in proteins associated with both slow and fast twitch fibers.

Gene	Abundance Ratio: (Crym tg)/(Control)	padj	Type of Gene	Shifted Towards
<i>Ptgr2</i>	0.001	5.06E-16	slow	fast
<i>Bdh1</i>	0.314	5.06E-16	slow	fast
<i>Rab14</i>	0.352	5.06E-16	slow	fast
<i>Ankrd2</i>	0.388	3.09E-12	slow	fast
<i>Paics</i>	0.427	1.69E-07	fast	slow
<i>Csrp3</i>	0.435	5.06E-16	slow	fast
<i>Tmem65</i>	0.563	5.03E-04	slow	fast
<i>Cryab</i>	0.576	3.48E-07	slow	fast
<i>Dnaja4</i>	0.605	2.78E-03	slow	fast
<i>Gbe1</i>	0.639	1.10E-04	slow	fast
<i>Fhl1</i>	0.672	1.10E-03	slow	fast
<i>Palmd</i>	0.676	1.36E-03	slow	fast
<i>Sdhc</i>	0.705	6.11E-03	slow	fast
<i>Hspb6</i>	0.711	8.19E-03	slow	fast
<i>Hspb1</i>	0.732	1.96E-02	slow	fast

Table 5 continued

<i>Pfn1</i>	0.747	3.07E-02	slow	fast
<i>Gstm2</i>	1.351	1.08E-02	fast	fast
<i>Casq2</i>	1.363	8.62E-03	slow	slow
<i>Myh7b</i>	1.381	5.68E-03	slow	slow
<i>Idh2</i>	1.389	4.59E-03	slow	slow
<i>Selenbp2</i>	1.403	3.13E-03	slow	slow
<i>Kera</i>	1.445	1.12E-03	fast	fast
<i>Fbp2</i>	1.724	9.86E-08	fast	fast
<i>Myl2</i>	2.672	5.06E-16	slow	slow
<i>Gpt</i>	1000	5.06E-16	slow	slow
<i>Lta4h</i>	1000	5.06E-16	fast	fast

Earlier studies used thyrotoxic doses of T₃ and T₄ in rats to alter skeletal muscles. These doses induced a shift in slow twitch soleus muscle from slow to faster characteristics, but without accompanying changes in contractile velocity. They had no effect on fast twitch extensor digitorum longus muscles (Fitts et al. 1984). Consistent with our observations, these results suggest that the contractile properties of muscle may not always correspond to its histochemical and biochemical properties, at least when thyroid hormones are elevated. The levels reached in *Crym* tg muscle are considerably

below thyrotoxic levels, however. A later study examined the properties of muscle in mice lacking thyroid hormone receptors and, again, found changes in soleus but not EDL (Johansson et al. 2003). In this case, however, soleus muscles in the knockouts showed even slower twitch characteristics than in controls, consistent with changes seen in hypothyroid mice. These results suggest that any elevation in T_3 related to transgenic expression of *Crym* is more likely to appear in slow twitch than in fast twitch muscles. Given the fact that only ~60% of murine soleus muscles are slow and the effects of *Crym* overexpression are subtler than either thyrotoxicosis or the complete ablation of the thyroid hormone receptor, significant differences in the physiological properties of *Crym* tg muscles might not be expected. This is congruent with our observation that the changes in gene expression of the myosin heavy and light chains in TA muscle are relatively small and inconsistent (Supplemental Table 4). While we do not see any changes in fiber type as measured by myosin heavy chain presence in soleus muscle, we do see smaller Type I/IIb and IIa fibers consistent with a shift towards a slower muscle twitch phenotype.

We saw significantly greater rates of increase in body weight of female *Crym* tg compared to control mice on high fat or high simple carbohydrate diets (Figure 4A, C). There may be a sexually dimorphic effect that higher levels of μ -crystallin has on metabolism because we did not observe a similar significant increase in body weight of *Crym* tg males on these diets (Figure 4F-J). Indeed Chen et al. found that mice with two X chromosomes had “accelerated weight gain on a high fat diet” and up to a 2-fold increase in adiposity compared to XY mice (Chen et al. 2012) showing a clear sexual

dimorphism for fat storage. Thus, μ -crystallin may affect metabolism in a sexually dimorphic way.

The changes that we have observed are novel. To the best of our knowledge, the only comprehensive studies of thyroid hormone-dependent gene expression in mice to date were performed in liver tissue, though an older study has been reported on skeletal muscle in men (Clément et al. 2002). There are 5,129 significantly differentially expressed genes shared across three whole genome microarrays comparing hyperthyroid mouse liver to euthyroid or hypothyroid mouse liver (GEO DataSets ID: 200068803, 200065947, 200021307). Of the 566 significant DEGs we identified by RNA-seq, 211 showed changes in these studies of liver. 107 were significantly increased in expression while 104 were significantly decreased in expression (Supplemental Document 2). Notably, however, only a small subset of these DEGs are known to contain TREs (Supplemental Table 3). Despite the fact that T_3 is highly elevated in the TA muscles of *Crym* tg mice, the changes in mRNA and protein levels are modest. This is in keeping with earlier studies of the relatively modest effects of more extreme changes in thyroid hormone signaling in rodent muscle (Fitts et al. 1984; Johansson et al. 2003).

The shift in gene expression and metabolism in *Crym* tg mice may also be relevant to human physiology and perhaps to the pathophysiology of FSHD. CRYM levels in human muscles vary widely (Klooster et al. 2009), but no distinctive physiological differences have been linked to this variability. Such differences may appear in muscle stressed by disease, however. In particular, *CRYM* is likely to be linked directly or indirectly to FSHD (Reed et al. 2007; Vanderplanck et al. 2011). DUX4 expressed in FSHD muscle increases CRYM expression (Vanderplanck et al. 2011), and

μ -crystallin in mice promotes a shift in RER and gene expression consistent with a shift toward a slower fiber type, which if pronounced enough would generate less force upon contraction. Notably, force generated by fast twitch muscle fibers is significantly reduced in FSHD (Lassche et al. 2013). Although *Crym* tg mice do not show a decrease in force, the changes we document in TA muscle could be associated with such a decrease if it manifests over decades, the time course of the disease in man.

In summary, we found that the expression of high levels of μ -crystallin in murine skeletal muscle greatly increases T₃ levels in muscle, shifts metabolism to favor the use of fat over carbohydrates as an energy source, and enhances the expression of genes typical of slow skeletal muscle. Remarkably, the morphological and physiological characteristics of the muscle are not significantly altered. We therefore propose that the higher levels of μ -crystallin seen in some humans regulate gene expression and metabolism in similar, subtle ways. We speculate that individuals showing high levels of μ -crystallin expression in muscle will be more resistant to diabetes and obesity, and that mechanisms that up-regulate μ -crystallin will be beneficial in treating these conditions.

Credit authorship contribution statement

Christian J. Kinney: Data curation, oversaw the RNA-seq experiments, the quantitation of the western blots, and generated the data in Figures 1 and 4 and Tables 2, 3, and 4, Suppl. Figs. 6-9, and Suppl. Tables 2-6. He contributed to the data in Table 5, Suppl. Figs. 1-3, 4A, and 5. He prepared the manuscript and all the supplemental documents. He wrote the paper with Dr. Bloch. **Andrea O'Neill:** Data curation, generated the data shown in Figure 2, Suppl. Figs. 4-7 and 9, and contributed to the data in Figure 4 and

Suppl. Fig. 3 and 9. She also maintained the transgenic mouse line and supervised its breeding. **Kaila Noland:** Data curation, generated the data in Figure 1, Suppl. Table 1, Suppl. Fig. 2, and contributed to the data in Figure 4 and Suppl. Fig. 3. **Weiliang Huang:** generated the proteomic data shown in Table 5 and Suppl. Doc. 3. **Joaquin Muriel:** identified the site in chromosome 6 harboring the transgene, shown in Suppl. Fig. 1. **Valeriy Lukyanenko:** Data curation, generated the data for Figure 3, panels C, F, and G. **Maureen A. Kane:** Data curation, worked with Dr. Huang to generate the proteomic data (Table 5 and Suppl. Doc. 3). **Christopher W. Ward:** Data curation, generated the data for Figure 3, panels A, B, D, E, H, and Suppl. Fig. 10. **Alyssa F. Collier:** Data curation, generated the data in Table 1. **Joseph A. Roche:** Data curation, worked with A. Collier to generate the data in Table 1 and performed preliminary characterization of the twitch properties of transgenic muscle. **John C. McLenithan:** Data curation, worked with C. Kinney, K. Noland and A. O'Neill to generate the data in Suppl. Fig. 3 and with C. Kinney to generate the data in Table 2.. **Patrick W. Reed:** prepared the plasmid vector for transgenesis, worked with Ms. O'Neill to breed the homozygous transgenic line, and performed many of the preliminary characterizations of transgenic muscle. **Robert J. Bloch:** coordinated the work, directed Mr. Kinney, Ms. O'Neill, Ms. Noland, Ms. Collier and Dr. Reed, and arranged the collaborations with Drs. Huang, Kane, Ward, and McLenithan. He wrote the paper with Mr. Kinney.

Declaration of interests

The authors declare that they have no known competing financial interests or personal relationships that could have appeared to influence the work reported in this paper.

The authors declare that they have no known competing financial interests or personal relationships that could have appeared to influence the work reported in this paper.

Supplementary data

<https://www.sciencedirect.com/science/article/pii/S2665944121000079>

Funding

This work was initially supported by a subcontract to RJB from 5 U54 HD060848 (Dr. C. Emerson, Jr., P.I.), and more recently by NIH grants to RJB (2RO1 AR064268 minority supplement for CK) and to PWR (1R21 AR057519). We also acknowledge the generous support of the Kahlert Foundation for our research, and funding from the Graduate School, University of Maryland, Baltimore, for KN's stipend.

Bibliography

Abe, Satoko, Toyomasa Katagiri, Akihiko Saito-Hisaminato, Shin-ichi Usami, Yasuhiro Inoue, Tatsuhiko Tsunoda, and Yusuke Nakamura. 2003. 'Identification of CRYM as a candidate responsible for nonsyndromic deafness, through cDNA microarray analysis of human cochlear and vestibular tissues', *The American Journal of Human Genetics*, 72: 73-82.

Aguet, François, Dimitri Van De Ville, and Michael Unser. 2008. 'Model-based 2.5-D deconvolution for extended depth of field in brightfield microscopy', *IEEE Transactions on Image Processing*, 17: 1144-53.

Bancroft, John D, and Marilyn Gamble. 2008. *Theory and practice of histological techniques* (Elsevier health sciences).

Beslin, Aline, Marie-Pierre Vié, Jean-Paul Blondeau, and Jacques Francon. 1995. 'Identification by photoaffinity labelling of a pyridine nucleotide-dependent tri-iodothyronine-binding protein in the cytosol of cultured astroglial cells', *Biochemical Journal*, 305: 729-37.

Bianco, Antonio C, and Brian W Kim. 2006. 'Deiodinases: implications of the local control of thyroid hormone action', *The Journal of clinical investigation*, 116: 2571-79.

Bishopric, Nanette H, and Larry Kedes. 1991. 'Adrenergic regulation of the skeletal alpha-actin gene promoter during myocardial cell hypertrophy', *Proceedings of the National Academy of Sciences*, 88: 2132-36.

Borel, Franck, Isma Hachi, Andres Palencia, Marie-Claude Gaillard, and Jean-Luc Ferrer. 2014. 'Crystal structure of mouse mu-crystallin complexed with NADPH and the T3 thyroid hormone', *The FEBS journal*, 281: 1598-612.

Briguet, Alexandre, Isabelle Courdier-Fruh, Mark Foster, Thomas Meier, and Josef P Magyar. 2004. 'Histological parameters for the quantitative assessment of muscular dystrophy in the mdx-mouse', *Neuromuscular disorders*, 14: 675-82.

Brooke, Michael L H, and Kenneth K Kaiser. 1970. 'Three" myosin adenosine triphosphatase" systems: the nature of their pH lability and sulfhydryl dependence', *Journal of Histochemistry & Cytochemistry*, 18: 670-72.

Burks, Tyesha N, Eva Andres-Mateos, Ruth Marx, Rebeca Mejias, Christel Van Erp, Jessica L Simmers, Jeremy D Walston, Christopher W Ward, and Ronald D Cohn. 2011. 'Losartan restores skeletal muscle remodeling and protects against disuse atrophy in sarcopenia', *Science translational medicine*, 3: 82ra37-82ra37.

Chen, Xuqi, Rebecca McClusky, Jenny Chen, Simon W Beaven, Peter Tontonoz, Arthur P Arnold, and Karen Reue. 2012. 'The number of x chromosomes causes sex differences in adiposity in mice', *PLoS Genet*, 8: e1002709.

Ciciliot, Stefano, Alberto C Rossi, Kenneth A Dyar, Bert Blaauw, and Stefano Schiaffino. 2013. 'Muscle type and fiber type specificity in muscle wasting', *The international journal of biochemistry & cell biology*, 45: 2191-99.

Clément, Karine, Nathalie Viguerie, Maximilian Diehn, Ash Alizadeh, Pierre Barbe, Claire Thalamas, John D Storey, Patrick O Brown, Greg S Barsh, and Dominique Langin.

2002. 'In vivo regulation of human skeletal muscle gene expression by thyroid hormone', *Genome research*, 12: 281-91.

Collie, ES, and George E Muscat. 1992. 'The human skeletal alpha-actin promoter is regulated by thyroid hormone: identification of a thyroid hormone response element', *Cell growth & differentiation: the molecular biology journal of the American Association for Cancer Research*, 3: 31-42.

Dixit, Manjusha, Eugénie Anseau, Alexandra Tassin, Sara Winokur, Rongye Shi, Hong Qian, Sébastien Sauvage, Christel Mattéotti, Anne M van Acker, and Oberdan Leo. 2007. 'DUX4, a candidate gene of facioscapulohumeral muscular dystrophy, encodes a transcriptional activator of PITX1', *Proceedings of the National Academy of Sciences*, 104: 18157-62.

Dorfer, Viktoria, Peter Pichler, Thomas Stranzl, Johannes Stadlmann, Thomas Taus, Stephan Winkler, and Karl Mechtler. 2014. 'MS Amanda, a universal identification algorithm optimized for high accuracy tandem mass spectra', *Journal of proteome research*, 13: 3679-84.

Drexler, Hannes CA, Aaron Ruhs, Anne Konzer, Luca Mendler, Mark Bruckskotten, Mario Looso, Stefan Günther, Thomas Boettger, Marcus Krüger, and Thomas Braun. 2012. 'On marathons and Sprints: an integrated quantitative proteomics and

transcriptomics analysis of differences between slow and fast muscle fibers', *Molecular & Cellular Proteomics*, 11: M111. 010801.

Dubowitz, Victor, Caroline A Sewry, and Anders Oldfors. 2013. *Muscle biopsy: a practical approach: expert consult; online and print* (Elsevier Health Sciences).

Ebashi, Setsuro, Makoto Endo, and Iwao Ohtsuki. 1969. 'Control of muscle contraction', *Quarterly reviews of biophysics*, 2: 351-84.

Encarnacion-Rivera, Lucas, Steven Foltz, H Criss Hartzell, and Hyojung Choo. 2020. 'Myosoft: An automated muscle histology analysis tool using machine learning algorithm utilizing FIJI/ImageJ software', *PloS one*, 15: e0229041.

Eng, Jimmy K, Bernd Fischer, Jonas Grossmann, and Michael J MacCoss. 2008. 'A fast SEQUEST cross correlation algorithm', *Journal of proteome research*, 7: 4598-602.

Fitts, Robert H, Cheryl J Brimmer, John P Troup, and Brian R Unsworth. 1984. 'Contractile and fatigue properties of thyrotoxic rat skeletal muscle', *Muscle & Nerve: Official Journal of the American Association of Electrodiagnostic Medicine*, 7: 470-77.

Friesema, Edith CH, Jurgen Jansen, Jan-willem Jachtenberg, W Edward Visser, Monique HA Kester, and Theo J Visser. 2008. 'Effective cellular uptake and efflux of thyroid

hormone by human monocarboxylate transporter 10', *Molecular endocrinology*, 22: 1357-69.

Gagne, Remi, James R Green, Hongyan Dong, Mike G Wade, and Carole L Yauk. 2013. 'Identification of thyroid hormone receptor binding sites in developing mouse cerebellum', *BMC genomics*, 14: 341.

Giger, Julia M, Paul W Bodell, Ming Zeng, Kenneth M Baldwin, and Fadia Haddad. 2009. 'Rapid muscle atrophy response to unloading: pretranslational processes involving MHC and actin', *Journal of Applied Physiology*, 107: 1204-12.

Gunning, Peter, P Ponte, H Blau, and L Kedes. 1983. 'alpha-skeletal and alpha-cardiac actin genes are coexpressed in adult human skeletal muscle and heart', *Molecular and cellular biology*, 3: 1985-95.

Gustafson, Thomas A, Bruce E Markham, and Eugene Morkin. 1986. 'Effects of thyroid hormone on alpha-actin and myosin heavy chain gene expression in cardiac and skeletal muscles of the rat: measurement of mRNA content using synthetic oligonucleotide probes', *Circulation research*, 59: 194-201.

Hallen, André, and Arthur JL Cooper. 2017. 'Reciprocal control of thyroid binding and the pipecolate pathway in the brain', *Neurochemical research*, 42: 217-43.

Hallen, André, Arthur JL Cooper, Joanne F Jamie, Paul A Haynes, and Robert D Willows. 2011. 'Mammalian forebrain ketimine reductase identified as μ -crystallin; potential regulation by thyroid hormones', *Journal of neurochemistry*, 118: 379-87.

Hallen, André, Arthur JL Cooper, Joanne F Jamie, and Peter Karuso. 2015. 'Insights into enzyme catalysis and thyroid hormone regulation of cerebral ketimine reductase/ μ -crystallin under physiological conditions', *Neurochemical research*, 40: 1252-66.

Hashizume, Kiyoshi, T Miyamoto, Kazuo Ichikawa, Keishi Yamauchi, Akihiro Sakurai, Hiromi Ohtsuka, Mutsuhiro Kobayashi, Yutaka Nishii, and Takashi Yamada. 1989. 'Evidence for the presence of two active forms of cytosolic 3, 5, 3'-triiodo-L-thyronine (T3)-binding protein (CTBP) in rat kidney. Specialized functions of two CTBPs in intracellular T3 translocation', *Journal of Biological Chemistry*, 264: 4864-71.

Homma, Sachiko, Jennifer CJ Chen, Fedik Rahimov, Mary Lou Beermann, Kendal Hanger, Genila M Bibat, Kathryn R Wagner, Louis M Kunkel, Charles P Emerson Jr, and Jeffrey Boone Miller. 2012. 'A unique library of myogenic cells from facioscapulohumeral muscular dystrophy subjects and unaffected relatives: family, disease and cell function', *European Journal of Human Genetics*, 20: 404-10.

Johansson, Catarina, Per Kristian Lunde, Sten Göthe, Jan Lännergren, and Håckan Westerblad. 2003. 'Isometric force and endurance in skeletal muscle of mice devoid of all known thyroid hormone receptors', *The Journal of physiology*, 547: 789-96.

Kalmar, Bernadett, Gonzalo Blanco, and Linda Greensmith. 2012. 'Determination of muscle fiber type in rodents', *Current protocols in mouse biology*, 2: 231-43.

Kammoun, Malek, I Cassar-Malek, Bruno Meunier, and Brigitte Picard. 2014. 'A simplified immunohistochemical classification of skeletal muscle fibres in mouse', *European journal of histochemistry: EJH*, 58.

Kim, Dongwon, Ruosi Chen, Mary Sheu, Noori Kim, Sooah Kim, Nasif Islam, Eric M Wier, Gaofeng Wang, Ang Li, and Angela Park. 2019. 'Noncoding dsRNA induces retinoic acid synthesis to stimulate hair follicle regeneration via TLR3', *Nature Communications*, 10: 2811.

Kim, Robert Y, Robin Gasser, and Graeme J Wistow. 1992. ' μ -crystallin is a mammalian homologue of *Agrobacterium* ornithine cyclodeaminase and is expressed in human retina', *Proceedings of the National Academy of Sciences*, 89: 9292-96.

Klooster, Rinse, Kirsten Straasheijm, Bharati Shah, Janet Sowden, Rune Frants, Charles Thornton, Rabi Tawil, and Silvère Van Der Maarel. 2009. 'Comprehensive expression analysis of FSHD candidate genes at the mRNA and protein level', *European Journal of Human Genetics*, 17: 1615.

Kobayashi, Mutsuhiro, Kiyoshi Hashizume, Satoru Suzuki, Kazuo Ichikawa, and Teiji Takeda. 1991. 'A Novel NADPH-Dependent Cytosolic 3, 5, 3'-Triiodo-LThyronine-Binding Protein (CTBP; 5. IS) in Rat Liver: A Comparison with 4.7 S NADPH-Dependent CTBP', *Endocrinology*, 129: 1701-08.

Laemmli, Ulrich K. 1970. 'Cleavage of structural proteins during the assembly of the head of bacteriophage T4', *nature*, 227: 680-85.

Larsen, P Reed, J Enrique Silva, and Michael M Kaplan. 1981. 'Relationships between circulating and intracellular thyroid hormones: physiological and clinical implications', *Endocrine Reviews*, 2: 87-102.

Lassche, Saskia, Ger JM Stienen, Tom C Irving, Silvère M Van Der Maarel, Nicol C Voermans, George W Padberg, Henk Granzier, Baziel GM van Engelen, and Coen AC Ottenheijm. 2013. 'Sarcomeric dysfunction contributes to muscle weakness in facioscapulohumeral muscular dystrophy', *Neurology*, 80: 733-37.

Luff, AR. 1981. 'Dynamic properties of the inferior rectus, extensor digitorum longus, diaphragm and soleus muscles of the mouse', *The Journal of physiology*, 313: 161-71.

Lukyanenko, Valeriy, Joaquin M Muriel, and Robert J Bloch. 2017. 'Coupling of excitation to Ca²⁺ release is modulated by dysferlin', *The Journal of physiology*, 595: 5191-207.

Lusk, Graham. 1924. 'Animal calorimetry twenty-fourth paper. Analysis of the oxidation of mixtures of carbohydrate and fat', *Journal of Biological Chemistry*, 59: 41-42.

Mori, Jun-ichirou, Satoru Suzuki, Mitsuhiro Kobayashi, Takeshi Inagaki, Ai Komatsu, Teiji Takeda, Takahide Miyamoto, Kazuo Ichikawa, and Kiyoshi Hashizume. 2002. 'Nicotinamide adenine dinucleotide phosphate-dependent cytosolic T3 binding protein as a regulator for T3-mediated transactivation', *Endocrinology*, 143: 1538-44.

Motulsky, Harvey J, and Ronald E Brown. 2006. 'Detecting outliers when fitting data with nonlinear regression—a new method based on robust nonlinear regression and the false discovery rate', *BMC bioinformatics*, 7: 123.

Ohkubo, Yohsuke, Takashi Sekido, Shin-ichi Nishio, Keiko Sekido, Junichiro Kitahara, Satoru Suzuki, and Mitsuhiro Komatsu. 2019. 'Loss of μ -crystallin causes PPAR γ activation and obesity in high-fat diet-fed mice', *Biochemical and biophysical research communications*, 508: 914-20.

Olojo, Rotimi O, Andrew P Ziman, Erick O Hernández-Ochoa, Paul D Allen, Martin F Schneider, and Christopher W Ward. 2011. 'Mice null for calsequestrin 1 exhibit deficits in functional performance and sarcoplasmic reticulum calcium handling', *PloS one*, 6: e27036.

Pette, Dirk, and Robert S Staron. 1997. 'Mammalian skeletal muscle fiber type transitions.' in, *International Review of Cytology* (Elsevier).

Pirahanchi, Y., and I. Jialal. 2019. 'Physiology, Thyroid Stimulating Hormone (TSH).' in, *StatPearls* (StatPearls Publishing LLC.: Treasure Island (FL)).

Reed, Patrick W, Andrea M Corse, Neil C Porter, Kevin M Flanigan, and Robert J Bloch. 2007. 'Abnormal expression of mu-crystallin in facioscapulohumeral muscular dystrophy', *Experimental neurology*, 205: 583-86.

Sandler, Ben, Paul Webb, James W Apriletti, B Russell Huber, Marie Togashi, Suzana T Cunha Lima, Sanja Juric, Stefan Nilsson, Richard Wagner, and Robert J Fletterick. 2004. 'Thyroxine-thyroid hormone receptor interactions', *Journal of Biological Chemistry*, 279: 55801-08.

Schiaffino, Stefano, and Carlo Reggiani. 2011. 'Fiber types in mammalian skeletal muscles', *Physiological reviews*, 91: 1447-531.

Schindelin, Johannes, Ignacio Arganda-Carreras, Erwin Frise, Verena Kaynig, Mark Longair, Tobias Pietzsch, Stephan Preibisch, Curtis Rueden, Stephan Saalfeld, and Benjamin Schmid. 2012. 'Fiji: an open-source platform for biological-image analysis', *Nature methods*, 9: 676-82.

Seko, Daiki, Shizuka Ogawa, Tao-Sheng Li, Akihiro Taimura, and Yusuke Ono. 2015.

' μ -Crystallin controls muscle function through thyroid hormone action', *The FASEB Journal*, 30: 1733-40.

Sheng, Juan-Juan, and Jian-Ping Jin. 2016. 'TNNI1, TNNI2 and TNNI3: Evolution, regulation, and protein structure–function relationships', *Gene*, 576: 385-94.

Siler, TM, SSC Yen, W Vale, and R Guillemin. 1974. 'Inhibition by somatostatin on the release of TSH induced in man by thyrotropin-releasing factor', *The Journal of Clinical Endocrinology & Metabolism*, 38: 742-45.

Spangenburg, Espen E, Stephen JP Pratt, Lindsay M Wohlers, and Richard M Lovering. 2011. 'Use of BODIPY (493/503) to visualize intramuscular lipid droplets in skeletal muscle', *Journal of Biomedicine and Biotechnology*, 2011.

Suzuki, Satoru, Nobuyoshi Suzuki, Jun-ichirou Mori, Aki Oshima, Shinichi Usami, and Kiyoshi Hashizume. 2007. ' μ -Crystallin as an intracellular 3, 5, 3'-triiodothyronine holder in vivo', *Molecular endocrinology*, 21: 885-94.

Tata, Jamshed R. 1958. 'A cellular thyroxine-binding protein fraction', *Biochimica et biophysica acta*, 28: 91-94.

Tawil, Rabi, Silvère M Van Der Maarel, and Stephen J Tapscott. 2014.

'Facioscapulohumeral dystrophy: the path to consensus on pathophysiology', *Skeletal muscle*, 4: 12.

Taylor, Sean C, Katia Nadeau, Meysam Abbasi, Claude Lachance, Marie Nguyen, and Joshua Fenrich. 2019. 'The ultimate qPCR experiment: producing publication quality, reproducible data the first time', *Trends in biotechnology*, 37: 761-74.

van Mullem, Alies A, Anja LM van Gucht, W Edward Visser, Marcel E Meima, Robin P Peeters, and Theo J Visser. 2016. 'Effects of thyroid hormone transporters MCT8 and MCT10 on nuclear activity of T3', *Molecular and cellular endocrinology*, 437: 252-60.

Vanderplanck, Céline, Eugénie Anseau, Sébastien Charron, Nadia Stricwant, Alexandra Tassin, Dalila Laoudj-Chenivresse, Steve D Wilton, Frédérique Coppée, and Alexandra Belayew. 2011. 'The FSHD atrophic myotube phenotype is caused by DUX4 expression', *PloS one*, 6: e26820.

Xie, Fuliang, Peng Xiao, Dongliang Chen, Lei Xu, and Baohong Zhang. 2012.

'miRDeepFinder: a miRNA analysis tool for deep sequencing of plant small RNAs', *Plant molecular biology*, 80: 75-84.

Zaiontz, Charles. 2020. "Real Statistics Resource Pack software (Release 6.8)." In. www.real-statistics.com.

Discussion and Conclusion

μ -Crystallin plays an important physiological role, as is demonstrated by the effects of overexpressing, ablating, or mutating the protein. Three mutations in human *CRYM* are responsible for non-syndromic deafness, while overexpressing or ablating mouse μ -crystallin causes changes in metabolism and alters the fiber sizes of soleus and tibialis anterior muscle fibers respectively. μ -Crystallin is also strictly spatiotemporally restricted, especially in the brain, where it is frequently used as a marker for layer V neurons in the cerebral cortex. Given this strict spatiotemporal restriction of expression it is curious that there is a wide range of expression in human skeletal muscle. Most individuals express low levels of *CRYM*, whereas some people (~15% of the population) express significantly higher levels. Understanding the function of μ -crystallin is beneficial to understanding how mutations in the gene cause disease and what the implications of expressing high or low levels of the protein are. I have performed a series of experiments in a mouse model in which *Crym* is specifically overexpressed in skeletal muscle, the *Crym* tg, in order to answer these questions and advance our understanding of this potentially important gene.

My studies are the first to characterize a mouse model of overexpressing μ -crystallin. In *Crym* tg mice we observe shifts in the transcriptome and the fiber size of soleus muscle fibers concomitant with a shift towards a more oxidative, slow twitch phenotype. In addition, female *Crym* tg mice gain weight faster than control mice on high fat or high simple carbohydrate diets. These results along with previous research on μ -crystallin implicate the protein in the modulation of metabolism.

Although many aspects of μ -crystallin have been elucidated, questions still remain as to its functions, including its ability to bind T_3 and NADPH, and its activity as a ketimine reductase. Future studies may explore the cause of the varied expression of *CRYM* in human muscle. A population specific SNP near the promoter of *CRYM* may affect the binding of transcription factors and subsequent expression of the gene. Other studies may explore why *CRYM* is so regionally restricted in areas of the brain and kidney. Finally, because μ -crystallin can alter metabolism, *CRYM* may find utility as a therapeutic in certain metabolic disorders such as obesity and diabetes.

Chapter 3: CRISPR-Cas12a in Dysferlin Null Mice

Introduction

Dysferlin (gene *DYSF* in humans) has been reported to promote repair of the plasma membrane after myofiber injury (Bansal et al. 2003; Bittel et al. 2020). Others have reported that its primary role may be in regulating Ca^{2+} release at the triad junction of skeletal muscle (Kerr, Ward, and Bloch 2014; Kerr et al. 2013; Lukyanenko, Muriel, and Bloch 2017). Mutations in *DYSF* can cause several myopathies: Miyoshi muscular dystrophy-1 (Liu et al. 1998), distal myopathy with anterior tibial onset (Illa et al. 2001), and limb-girdle muscular dystrophy type 2B (Bashir et al. 1998).

In A/J mice a 5-6 kb ETn retrotransposon incorporated into intron 4 of mouse *Dysf*, ablating expression of the dysferlin protein (Ho et al. 2004). A/J mice are useful for studying dysferlinopathies, but healthy mice that express normal levels of dysferlin must be used as controls in experiments studying A/J mice, and such controls are not readily available. (The A/JCr mouse, maintained at NCI Frederick, diverged from the A/J strain more than 30 years ago). An A/J mouse model in which the inhibitory ETn retrotransposon could be removed conditionally would be ideal because one leg could be maintained as dysferlin null while the other could be rescued and allowed to produce dysferlin, as in healthy mice. In order to design such a mouse, I designed primers to sequence across the retrotransposon.

Ho et al. were unable to PCR amplify across the retrotransposon insertion in the *Dysf* gene of A/J mice, likely owing to the fact that insertion is relatively long (Ho et al.

2004), 5-6 kb, has low complexity (Vlangos et al. 2013), and is repetitive (Maksakova and Mager 2005). These factors make it very difficult for DNA polymerase to amplify the region with high fidelity. I surmounted this problem by optimizing the DNA polymerase and reagents used in the PCR reaction. In order to cut out the ETn retrotransposon in the A/J mice, I leveraged the unique properties of CRISPR-Cas12a. Cas12a is a site-directed RNA and DNA cleaving enzyme (Fonfara et al. 2016; Zetsche et al. 2015). The protospacer-adjacent motif (PAM) sequence of Cas12a is T-rich, as opposed to the G-rich PAMs of most other Cas nucleotide cleaving enzymes such as Cas9 (Zetsche et al. 2015). Because Cas12a can cleave both DNA and RNA, I generated a plasmid that encoding the Cas12a enzyme as well as a strand of RNA that was cleaved multiple times by Cas12a generating multiple gRNAs, enabling multiplexed genome editing using only a single plasmid.

With the correct PCR master mix reagents and DNA polymerase, I was able to amplify the ETn retrotransposon to measure if genome editing with CRISPR-Cas12a was successful. Through methodical experimentation I determined the best polymerase, PCR master mix reagents, and optimal DNA targeting crRNAs. These experiments are important steps towards generating a retrotransposon excising system for the A/J dysferlinopathy mouse model.

Methods

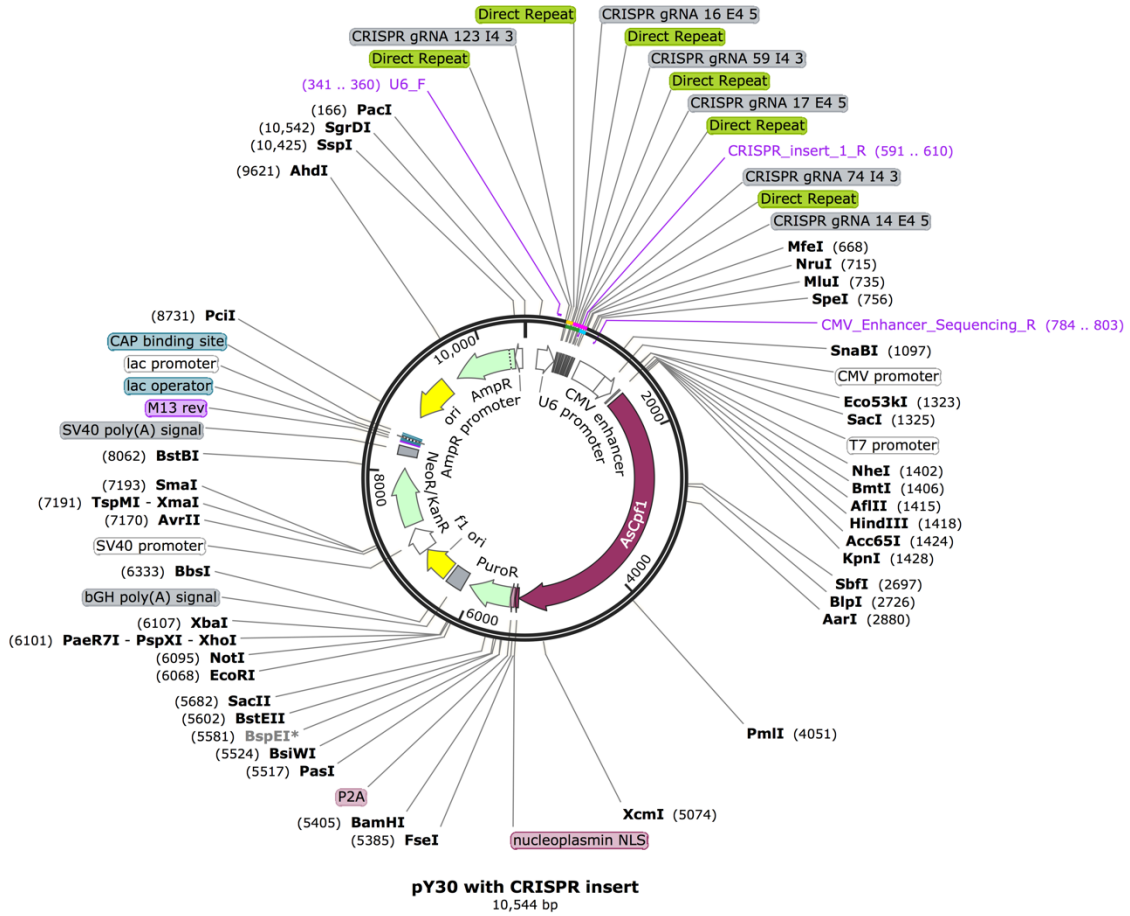
CRISPR-Cas12a Plasmid

Six gRNA sequences, used to direct Cas12a to a cut site, were determined by selecting for the gRNA sequences with the highest activity score and lowest off-target score in DESKGEN (www.deskgen.com), the highest CINDEL score in CINDEL (www.big.hanyang.ac.kr/cindel/), the lowest number of off targets in GuideScan (www.guidescan.com/), and the highest off-target score in Benchling (www.benchling.com). The six selected gRNAs are listed below. The six gRNAs, along with direct repeat sequences, which are used to direct Cas12a to cut RNA and which were located before the first gRNA and in between every gRNA (Figure 5), were compiled and split amongst 4 single stranded DNA (ssDNA) oligonucleotides and ordered from IDT (Coralville, IA). Briefly, 40 μL of 1X T4 DNA Ligase Reaction Buffer (B0202S, New England Biolabs) was added to 4 nanomoles of each lyophilized oligonucleotide. 4 μL of each oligonucleotide were combined into a single tube with 5 μL of T4 Polynucleotide Kinase at 10,000 units/mL (M0201S, New England Biolabs) and 19 μL of 1X T4 DNA Ligase Reaction Buffer and mixed. The tube was placed in a thermal cycler set to 37 °C for 30 min, 95 °C for 5 min followed by a -5 °C/min ramp down to 25 °C. The resultant “sticky ended” assembled gRNA and direct repeat oligonucleotide was purified using a PureLink PCR Purification Kit (K310001, Invitrogen). The recipient pY30 plasmid (Plasmid #84745, Addgene, Watertown, MA) was linearized using BsmBI restriction enzyme (R0580, New England Biolabs) following the manufacturers protocol. The insert was then ligated into the vector by combining in a tube 10 μL of T7 DNA Ligase Reaction Buffer 2X, 1 μL T7 DNA Ligase at 3,000,000 units/mL (M0318S, New England Biolabs), vector and insert DNA in a 1:3 molar ratio, and water to 20 μL , then incubated at room temperature for 30 mins to generate the assembled plasmid (Figure A).

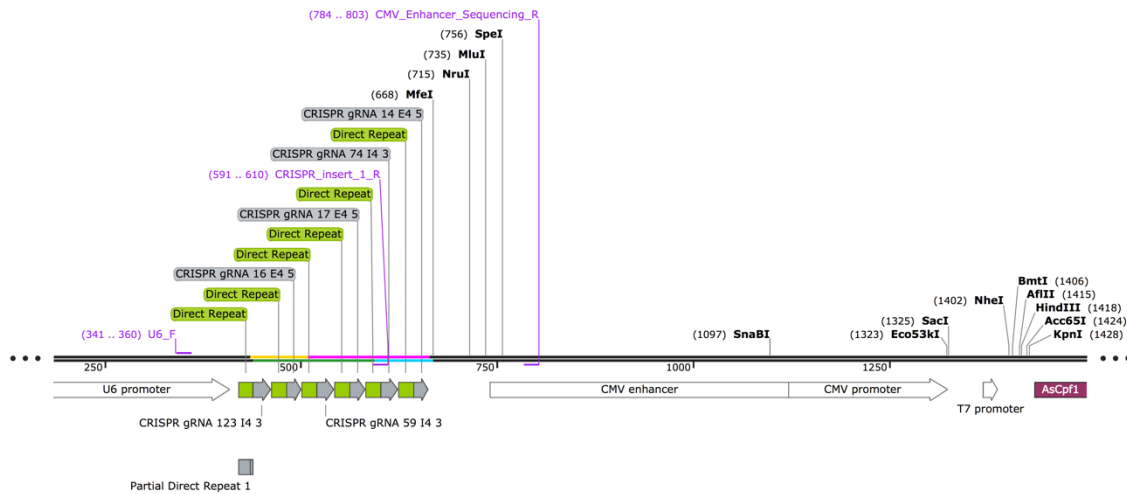
Figure 5. Maps of multiplexed CRISPR-Cas12a plasmid. A. Antibiotic resistance genes used for selection as well as their commensurate promoters and bacterial origin of replication sequences are included in order to propagate the plasmid in bacteria. B. gRNAs and direct repeats were ligated into the plasmid to generate individual gRNAs used to edit the DNA sequence surrounding the retrotransposon in the *A/J Dysf* gene. Cas12a is referred to as AsCpf1 in this schematic. A U6 promoter is used to drive expression of the multiplexed gRNAs while a CMV enhancer and CMV/T7 promoter drive expression of Cas12a.

Figure 5

A.



B.



CRISPR-Cas12a gRNAs:

123 I4 3: TCAGAGTCTTTTATCACAGCACC

16 E4 5: GAAGCTGGCAGAGAGGCTGG

59 I4 3: ACCTTCACACACACACACACA

17 E4 5: TGAAGCTGGCAGAGAGGCTG

74 I4 3: CGTGATGCTGGGATTGAACCCAG

14 E4 5: CAGAGAGGCTGGGGGTGGCA

Direct Repeat:

AATTCTACTCTTGTAGAT

Electroporation of Murine Soleus Muscle

2 male C57BL6/J mice were electroporated, as described (DiFranco et al. 2011), after being injected in their soleus muscles with the multiplexed gRNA pY30 plasmid and 1

male C57BL6/J mouse was electroporated after being injected in its soleus muscles with the untargeted pY30 plasmid to act as a control.

A male A/J mouse was also electroporated with the *Dysf* gRNA targeted pY30 plasmid following the same described protocol.

Genomic DNA Extraction and PCR Amplification

A male *Crym* tg mouse (notated as “C”) and two male C57BL/6J mice (notated as “4” and “6”) were tail snipped. Genomic DNA (gDNA) was extracted from mouse tail snips using a PureLink Genomic DNA Mini Kit (K182002, Invitrogen, Carlsbad, CA) with a protocol modified only by substituting DirectPCR Lysis Reagent (Tail) (102-T, Viagen Biotech, Los Angeles, CA) in place of PureLink® Genomic Digestion Buffer.

Four polymerases were tested for their ability to amplify long sections of low complexity, GC-rich, repetitive DNA. GoTaq Green Master Mix (M712, Promega, Madison, WI), LongAmp Taq 2X Master Mix (M0287, New England Biolabs, Ipswich, MA), Q5 Hot Start High-Fidelity 2X Master Mix (M0494, New England Biolabs), and Platinum SuperFi PCR Master Mix (12358010, Thermo Fisher Scientific, Waltham, MA) were used to amplify an approximately 5 kb length of genomic DNA spanning the distal end of intron 3 in the mouse *Dysf* gene until the distal end of intron 4 (*Dysf_F* and *Dysf_R* primers). In order to increase the specificity of the amplification, nested primers were used for some reactions (indicated by the first letter starting with an “N”). Nested PCR amplifications were done first with the nested primers listed below following the manufacturers protocol for the master mixes with the modification of the temperature of the annealing step (see below) and then a 0.5 μ L aliquot of the first round reaction was

used as the input DNA for the second round of amplification with the non-nested primers listed below at the below annealing temperatures.

Nested_Dysf_F: TAGGACCCACAGAACAGGACT

Nested_Dysf_R: CCCACCCCAGATCCAAACAA

Dysf_F: CGGTGACAAGTGTGGTCTCA

Dysf_R: CCTTAAGCGTTCCTGGGAGT

Annealing Temperatures:

Nested_Dysf: GoTaq Green Master Mix: 60.5 °C

LongAmp Taq 2X Master Mix: 58.0 °C

Q5 Hot Start High-Fidelity 2X Master Mix: 68.0 °C

Platinum SuperFi PCR Master Mix: 65.3 °C

Dysf: GoTaq Green Master Mix: 59.0 °C

LongAmp Taq 2X Master Mix: 59.0 °C

Q5 Hot Start High-Fidelity 2X Master Mix: 68.0 °C

Platinum SuperFi PCR Master Mix: 64.7 °C

PCR products were run on a 1.5% agarose gel with ethidium bromide at approximately 150 volts until the ethidium bromide band reached one quarter of the way up from the bottom of the gel. Gels were imaged on a UV transilluminator (Figure 6).

The best polymerase was Platinum SuperFi which produced specific bands without any smearing in the gel blot. It was used with a modified master mix of Dr. Peter Jones' "Death Mix." Briefly, 12.5 μ L of Platinum SuperFi Master Mix, 5 μ L of GC Enhancer, 1.87 μ L of 13.4 mM dithiothreitol, 0.5 μ L of 5 mM 7-deaza-dGTP, 20 ng of gDNA, 1.25 μ L of 10 μ M forward primer, 1.25 μ L of 10 μ M reverse primer, and water to 25 μ L were mixed together and used in each reaction. The thermal cycling conditions followed the polymerase master mix manufacturers "Long PCR" protocol.

Figure 6

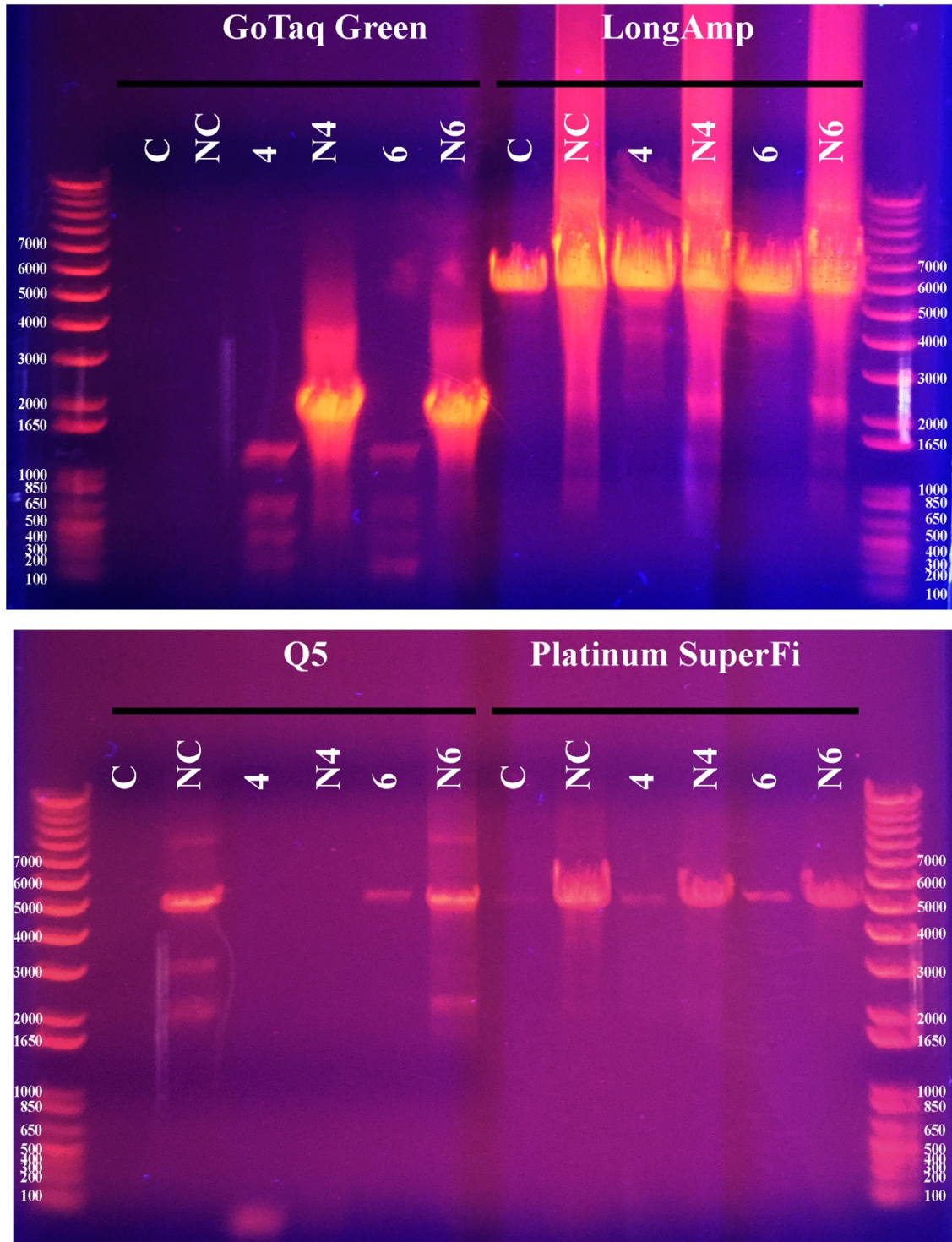


Figure 6. Various polymerases were tested for their ability to amplify a long, repetitive, low complexity retrotransposon in the A/J *Dysf* gene. GoTaq Green,

LongAmp, Q5, and Platinum SuperFi polymerase were evaluated in nested (N) and non-nested PCR reactions using genomic DNA from 1 male *Crym* tg mouse (C) and 2 male C57BL/6J mice (4 and 6) for their ability to amplify an approximately 5 kb section of DNA in the murine *Dysf* gene. Platinum SuperFi polymerase amplified the desired section of DNA with the fewest off-target amplicons. Its nested PCR reactions resulted in a greater abundance of amplicon.

Genome Editing of Retrotransposon in the *Dysf* Gene of A/J Mice

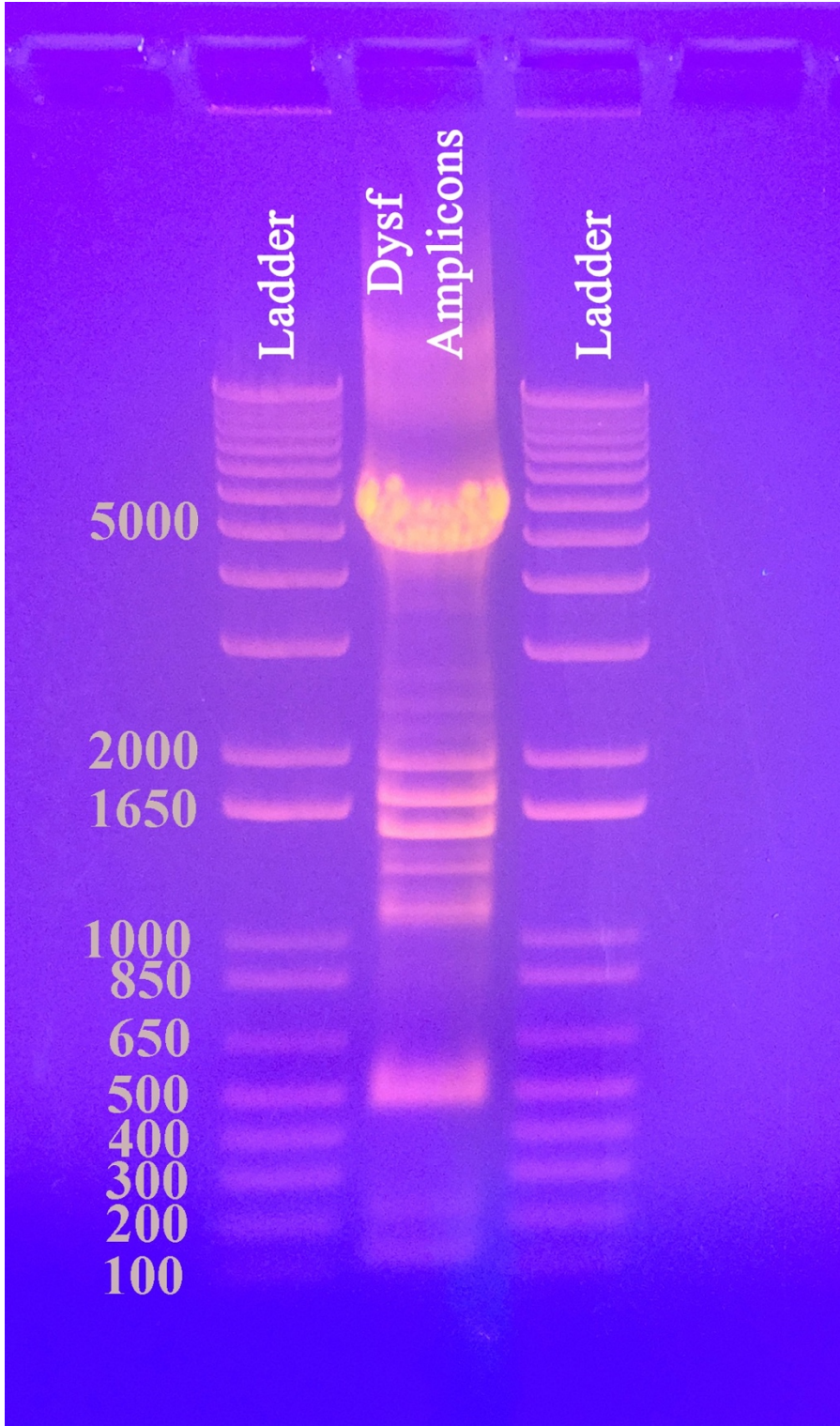
Soleus muscle was harvested 3 weeks after electroporating an A/J mouse with the assembled *Dysf* targeting pY30 plasmid and another A/J mouse with the unmodified pY30 plasmid. Genomic DNA was extracted and purified as previously described and the large region surrounding the ETn retrotransposon in A/J mice was amplified using the nested PCR protocol and the modified Death Mix with Platinum SuperFi polymerase. The control genomic DNA was amplified using the same conditions in the first lane but was also amplified by modifying the annealing temperature of the *Dysf* primers from 64.7 °C to 61.2 °C (Figure 7B). The resultant amplicons were electrophoresed on a gel also as previously described (Figure 7). Selected bands from the CRISPR edited A/J genomic DNA were gel purified using a GeneJET Gel Extraction kit (K0691, Thermo Fisher Scientific, Waltham, MA) and then sequenced using the *Dysf*_F and *Dysf*_R primers through the University of Maryland, Baltimore Genomics Core Facility.

Figure 7. *Dysf* amplicons after electroporation of A/J FDB with a *Dysf* CRISPR based genome editing plasmid or control CRISPR plasmid. A. The most prevalent band at ~5.2 kb corresponds to the amplicon band size of uncut *Dysf* while the sequence

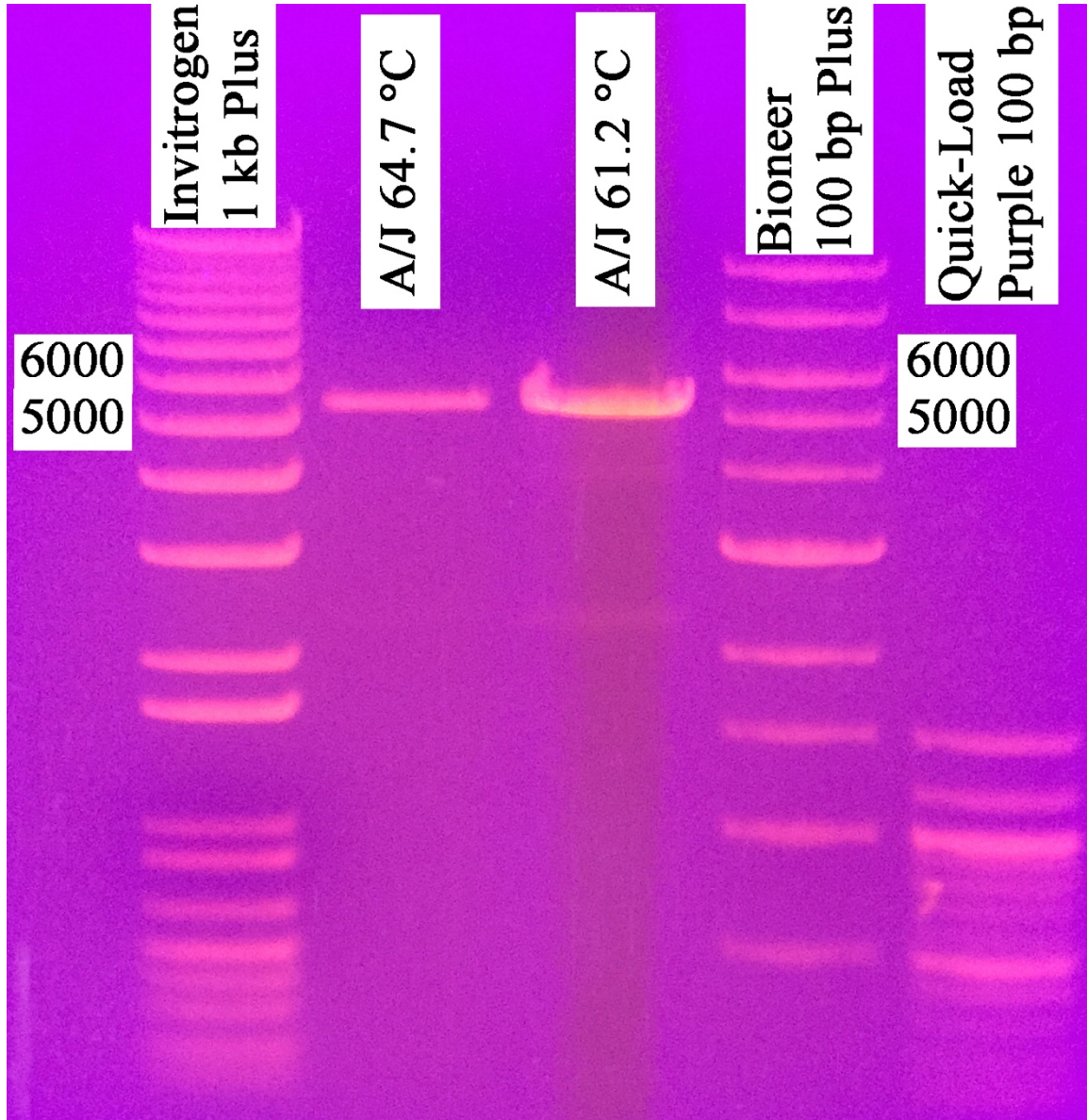
of the ~1700 bp and ~500 bp bands correspond to sequences surrounding the inserted retrotransposon in the *Dysf* gene of A/J mice. Several other uncharacterized bands are present possibly from the generation of other indels. **B.** Several different ladders were used as indicated in lanes 1, 4, and 5 as well as two annealing temperatures for the *Dysf* primers, 64.7 °C in lane 2 and 61.2 °C in lane 3. No additional bands were observed.

Figure 7

A.



B.



Results

Multiple bands were observed in the DNA gel after amplification of the ETn insertion site in *Dysf*. The two bands present in the highest concentration, excluding uncut DNA at 5,266 bp long, were at ~1700 bp and ~500 bp. Alignment of the DNA sequence from the

~1700 bp band with the mouse reference genome (GRCm38/mm10) indicated that approximately 4 kb of DNA was deleted including exon 4 and a portion of intron 4. The 500 bp band aligned to DNA in the mouse reference genome indicating an even larger deletion of approximately 4.7 kb, also spanning exon 4 and portions of intron 3 and 4. Only the original unedited ~5.2 kb retrotransposon insertion was present in the genomic DNA of the A/J mouse electroporated with the pY30 plasmid lacking gRNAs (Figure 7B).

Discussion

At the time of these experiments multiplex genome editing using CRISPR-Cas12a had only been demonstrated for three months prior (Zetsche et al. 2017). The nature of using a new technology along with targeting its use to a complex region of the genome necessitated the multiple iterative “mini-experiments” such as optimizing the PCR polymerase and reaction conditions. However, after these optimizations genome editing via CRISPR-Cas12a was successful in some myonuclei.

To my knowledge no one has been able to amplify the ETn retrotransposon inserted into the *Dysf* gene in A/J mice, though at least one lab has tried (Ho et al. 2004). The length, complexity, and repetitiveness of the region makes it difficult to PCR amplify. Through extensive experimentation I determined an optimal PCR master mix and DNA polymerase to use for amplifying this difficult DNA in the genome in A/J mice.

The multiple bands seen in Figure 7 are likely a product of several factors. First the brightest band at ~5.2 kb is the size of DNA in A/J mice that hasn't been cut.

Although I aimed to electroporate every nucleus in the soleus of the mouse, inevitably not every nucleus received a copy of the *Dysf* targeting plasmid or for other efficiency reasons DNA cleavage in some myonuclei did not occur. No DNA template was provided to be inserted during DNA repair through homologous recombination so it's also possible that cleavage occurred in the *Dysf* gene and the cleaved fragment was then re-ligated back into the genome. The fragments of varying sizes are likely indels that occurred after the cleavage and repair of the cleaved DNA. I successfully removed the disruptive ETn retrotransposon because the sequences of the 500 bp and 1700 bp bands corresponded to regions surrounding the ETn retrotransposon insertion site. Future studies may select an optimal gRNA and use a DNA template to restore the WT *Dysf* sequence.

There are many programs that can be used bioinformatically to inform researchers of the best gRNAs to use with Cas12a to cut DNA but these programs all operate on predictions. The only way to definitively know that a gRNA will cut DNA is to test it *in vitro/in vivo*. This can be a laborious process testing many individual gRNAs for efficacy. I surmounted this issue by performing gene editing in multiplex with 6 bioinformatically optimal gRNAs targeted to a region surrounding the ETn retrotransposon insertion site in the *Dysf* gene of A/J mice. After PCR amplifying the region and examining the resultant DNA bands on an electrophoretic gel, the brightest bands can be isolated. These bands of DNA indicate the most abundant DNA sequences present in the genome edited mouse muscle, and by proxy, the best performing gRNA sequences. Further isolation and sequencing of the abundant amplicons purified from the DNA gel can be used to backtrack to the gRNAs that likely caused the cut. Because the region to be excised by CRISPR-Cas12a, the ETn retrotransposon in the *Dysf* gene of A/J mice, was particularly

challenging to amplify, I had to develop additional protocols and reagent mixtures. A nested PCR using the experimentally determined most efficacious polymerase, and an optimized PCR master mix was required to amplify across the region. This was done in order to generate indel amplicons generated by the CRISPR genome editing, and consequently the gRNAs that are optimal for removing the ETn retrotransposon in the *Dysf* gene of A/J mice. To the best of my knowledge, this was the first time the ETn retrotransposon in the *Dysf* gene of A/J mice has been amplified and the first time multiplexed CRISPR-Cas12a was performed in myocytes. These techniques pave the way for other researchers to quickly evaluate a selection of gRNAs for functional efficacy in targeting DNA and for amplifying long, repetitive, low-complexity sections of DNA.

Chapter 4: Sonoporation of Murine Muscle

Introduction

Sonoporation is a method used for introducing foreign elements such as DNA into a cell by altering the cell membrane permeability via the use of sound (Fechheimer et al. 1987; Fechheimer et al. 1986). Many methods exist to introduce exogenous DNA into a cell, such as viruses, electroporation, and microparticle injection, to name only a few (Keown, Campbell, and Kucherlapati 1990). These methods have a variety of pros and cons. Most common forms of viral transduction are limited by the size of the plasmid the viral hosts can carry (Latchman 2001) and by host immune responses against the viral vector (Shirley et al. 2020), while the biolistic technology required for microparticle injection is specialized and the procedure is invasive (Johnston and Tang 1993). Microinjection is a low-throughput technology (Capecchi 1980) and electroporation can cause physiological changes to myofibers even after a year post-electroporation (Roche et al. 2011). Sonoporation can accommodate macromolecules and large plasmids, is non-immunogenic, non-invasive, spatiotemporally controlled, and is readily accessible (Miller, Pislaru, and Greenleaf 2002).

I was interested in introducing a large plasmid *in vivo* in murine muscle. I selected sonoporation as the method to do so. The plasmid, described in the previous chapter, is a CRISPR-Cas12a system used to conditionally rescue A/J mice from their dysferlinopathy in certain muscles, leaving muscles in other regions of the body dysferlinopathic. Using such a system I planned on studying the effects of potential treatments for

dysferlinopathic mice, inhibiting or rescuing the mouse's production of dysferlin in hind limb muscles of one or both legs, before and after administration of the plasmid via sonoporation.

For sonoporation, I used plasmid reporters conjugated to size-isolated microbubbles. Microbubbles are small bubbles of various gases and coatings. They are FDA-approved for use in humans to improve contrast on ultrasound images and may be administered intravenously (Chong, Papadopoulou, and Dayton 2018). Ultrasonic irradiation of microbubbles can cause the expansion and compression of the microbubble, eventually causing bursting. This push and pull of the bubble near cell surfaces can cause the formation of pores to open in the cell membrane. Microstreaming, that is the rapid flow of fluids, may also occur when the microbubble bursts, with speeds reaching 700 m/s. These microjets may effectively inject the plasmid into nearby cells (Fan, Kumon, and Deng 2014; Hernot and Klibanov 2008). The use of microbubble-assisted sonoporation in murine skeletal muscle has been shown to significantly increase the transfection efficiency compared to intramuscular injection (Burke et al. 2012).

I worked with Dr. Victor Frenkel and Dr. Pavlos Anastasiadis to design and implement a pilot experiment to explore the feasibility of microbubble-facilitated gene transfer via sonoporation. I sought to answer the question of whether murine hindlimb muscles could be transfected with a plasmid using sonoporation. Because other forms of transduction or transfection have a variety of downsides to their use, sonoporation, if efficacious for the delivery of exogenous DNA into cells, would represent a great benefit due to the ease of use, low cost, and potentially high efficacy of introducing foreign DNA

into animal models of disease, and perhaps in the future even for the application of gene therapies in humans.

Methods

Cationic microbubbles, 4-5 μm in diameter (SIMB4-5, Advanced Microbubbles, Newark, CA) were conjugated with two different plasmids: a Venus-Dysferlin plasmid (Lukyanenko, Muriel, and Bloch 2017) and E2-Crimson plasmid (Strack et al. 2009) kindly gifted to me by Dr. Alexandros Pouloupoulos. Plasmid DNA was loaded onto the microbubbles (MB) by mixing 40 μg of plasmid suspended in water with the microbubbles. The microbubble-plasmid solution was allowed to incubate on ice for 20-40 mins. The solution was spun in a centrifuge at 200-500g for 5-10 mins and the bottom aqueous infranatant was removed and discarded. Sterile phosphate-buffered saline (PBS) was mixed with the mixture such that the microbubble-DNA conjugate composed 25% of the volume, yielding 6.25×10^6 MB/mL. Male (6) and female (4) C57BL6/J mice, three months of age, were anaesthetized with isoflurane and their legs were depilated with Nair. A 1 F mouse tail vein catheter (MTV-01, SAI Infusion Technologies, Lake Villa, IL) was inserted into the tail vein of each mouse. A volume of tap water large enough to cover the body of the mice was degassed under vacuum for 3 hours and then heated via microwave to 37 °C to act as a medium between the ultrasonic transducer and the mouse muscle, as well as to keep the mice warm. The ultrasonic transducer was placed 4 centimeters above the right tibialis anterior (TA) muscle. A 300 μL aliquot of PBS-Venus-Dysferlin-cDNA-microbubble solution was injected into the tail veins of 3 of the

male mice and 4 female mice while an equivalent volume of PBS was injected into the tail vein of 3 of the male mice. The mice were then sonoporated with a 1 MHz unfocused transducer. A pulse, consisting of 5 sets of 300 consecutive 1 MHz sinusoids of 1V or 0.4 V peak-to-peak amplitude separated by 100 ms, was applied every 10 seconds for 5 mins. Mice were removed from the water bath, dried and allowed to recover under a heat lamp.

Mice were imaged using an IVIS Spectrum In Vivo Imaging System (124262, PerkinElmer, Waltham, PA) at 4 days post-sonoporation. Imaging was performed at an excitation wavelength of 535 nm and recorded at an emission wavelength of 560 nm (Figure 8). One female mouse labeled “Female CRISPR” in Figure 8 was imaged as part of a separate, unrelated experiment. Mice were euthanized at 9 days post-sonoporation and left and right TA muscles were collected, snap frozen, sectioned, and placed on microscope slides, as described (Kinney et al. 2020). Sections were immunohistochemically stained with rabbit-anti-dystrophin (PAS-16734; Thermo Fisher Scientific) to label the plasma membrane as well as anti-Venus (SAB4301138; Millipore Sigma, Burlington, MA), both diluted 1:100 in Mouse-On-Mouse (M.O.M.) diluent (BMK-2202; Vector labs, Burlingame, CA) and mounted in Vectashield + DAPI (H-1500; Vector Laboratory). Sections were imaged by confocal microscopy with a Zeiss 510 Duo microscope (Carl Zeiss, Oberkochen, Germany).

Results

Little to no fluorescence was visible in the hindlimbs of experimental mice that had been sonoporated with the Venus-Dysferlin plasmid at day 4. Control mice appear to have a

similar level of fluorescence compared to experimental mice. High levels of autofluorescence are visible in some mice, with no significant differences in Venus fluorescence apparent in mice given the Venus-Dysferlin plasmid compared to controls (Figure 8).

Day 4 ex: 535 em: 560

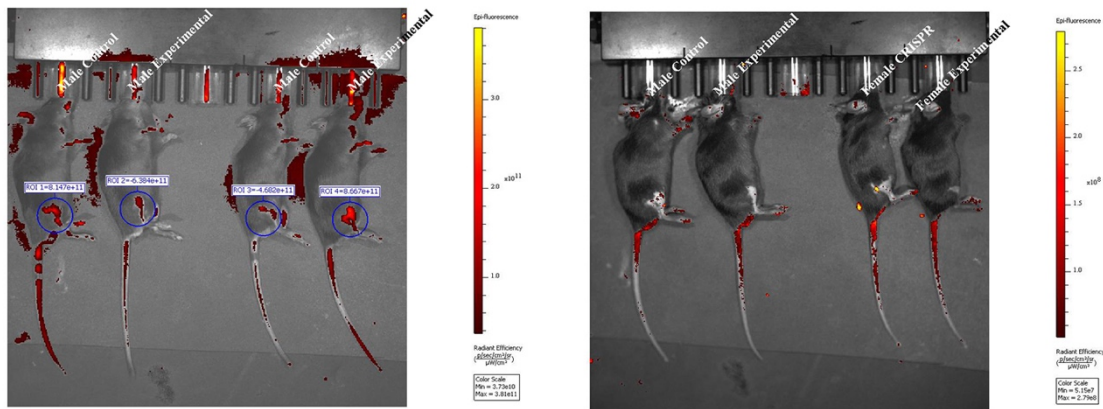


Figure 8. Representative heat map in vivo imaging of E2-Crimson, a far red shifted fluorophore, in the right TA of mice, expressed from a sonoporated plasmid. A representative IVIS Spectrum image of male and female mice at 4 and 9 days after sonoporation is shown. Mice designated as “Experimental” were sonoporated with a reporter plasmid (E2-Crimson) while mice designated as “Control” were sonoporated with PBS. A female “CRISPR” mouse that is unrelated is shown as well. Mice were imaged on Day 4 and 9 at an excitation wavelength of 535 nm and at an emission wavelength of 560 nm on Day 4 and 520 nm on Day 9. No significant fluorescent signal was observed from any mice at any time point though an abundance of background signal was observed.

Discussion

In order to examine a potentially less invasive, less immunogenic method for transfecting mice with large plasmids, I experimented with sonoporation. Unfortunately, this method did not yield the results I expected: little to no transfection occurred, as evidenced by the low level of fluorescence observed in the hind limbs of mice post-sonoporation.

Efficient transfection of skeletal muscle via ultrasonic sonoporation have been previously shown (Burke et al. 2012), it's possible that the inefficient transfection I observed was due to the difference in methods. Clearance of the microbubbles by the liver could also be another possible reason for why no transfection occurred.

Microbubbles are rapidly cleared from the blood when injected peripherally.

Accordingly, some researchers inject the microbubbles intraportally in the hepatic vein (Shen et al. 2008). Still another possible reason is user error. The procedures are relatively complex with proper positioning of the transducer and mouse being crucial to successfully transmitting the ultrasound waves. Injection of the mouse tail vein is also a difficult skill to master. Finally, any number of earlier, more basic steps such as conjugation of the plasmid to the microbubbles or purification of the plasmid for example may have gone awry due to human error.

Future studies may first attempt replicating past successful transfections. Intraportal injection may also increase transfection efficiency. If successful, sonoporation would represent a non-invasive, non-immunogenic, size unlimited method for transfecting foreign DNA into skeletal muscle.

Chapter 5: Discussion

Effects of Increased μ -Crystallin Expression in Murine Skeletal Muscle

μ -Crystallin is a potent thyroid hormone binding protein (Kinney and Bloch 2021). Thyroid hormone receptors bind T_3 only 5 times more strongly than μ -crystallin does (Kinney et al. 2020). Thyroid hormones influence a wide variety of physiological processes from metabolism (Larsen, Silva, and Kaplan 1981) to thermogenesis (Freaker and Oppenheimer 1995). Because thyroid hormones have such robust and wide-ranging effects on the body, the variance in healthy thyroid hormone levels is small (Hollowell et al. 2002). Hypo- or hyperthyroidism can result from a lack or surplus of thyroid hormone, leading to a variety of maladies (Taylor et al. 2018). In contrast to the tightly controlled thyroid hormone levels, *CRYM* mRNA and protein levels have been shown to vary significantly, up to 30-40 fold in skeletal muscle (Kinney et al. 2020). Given the tight control over thyroid hormone levels in the body and the disease-causing consequences of deviating from healthy levels, coupled with the high binding affinity of μ -crystallin for thyroid hormones, I wondered what effects μ -crystallin might have on individuals who express high levels of the protein in their muscle. To answer that question, I utilized a transgenic mouse, the *Crym* tg mouse, genetically engineered to overexpress μ -crystallin specifically in its skeletal muscles.

Crym tg mice on average express *Crym* mRNA and protein in skeletal muscle at levels at least 27.5 and 2.6 times those observed in control mice respectively.

Concurrently, we also observed 192.2 fold greater intramuscular levels (in TA) of T_3 and

1.2 fold less serum T₄ in *Crym* tg mice compared to controls. In order to determine what effects this large increase in μ -crystallin and T₃ is having on the mice we performed various physiologic, morphologic, and cellular measurements on the *Crym* tg mice.

We found that *Crym* tg mice are very similar to their control counterparts. Importantly, however, *Crym* tg mice shift their metabolism towards a preference for fats as an energy source. This discovery, initially observed through the use of metabolic cages, was replicated in various other experiments including RNA-seq and LC.MS/MS proteomics, fiber type analysis, and diet studies. Individually, the results I observed in many of these studies showed small, but significant, changes compared to control mice. Overall, however, we observed a 13.7% increase in preference for fat over carbohydrates in *Crym* tg mice compared to controls. This is a large alteration in energy expenditure and supports μ -crystallin's function as a binding protein of the strong metabolic regulators, T₃ and T₄. These results help to resolve the role that *CRYM* plays in muscle, particularly for individuals who express high levels of the protein. Future studies may explore the exact mechanism by which μ -crystallin drives an increased preference for fat utilization, what factors determine the level of expression of *CRYM*, and whether various health metrics, particularly body composition, is correlated with *CRYM* expression.

Increased levels of *CRYM* in people may cause them to burn more fat and may play a role protecting them from obesity and related metabolic disorders. By increasing the amount of fat utilized as an energy source in people their body composition may be altered to become leaner and their BMI may decrease. This decrease in fat content among individuals who are overweight or obese would improve their overall health leading to an improvement in their quality of life as well as a potentially longer lifespan. Modulation of

CRYM may play an important role in the fat content of people and consequently, their health, quality of life, and lifespan.

Generation of a Multiplexed gRNA CRISPR-Cas12a Cassette

In addition to working with *Crym* tg mice, I also tried to generate a CRISPR based system to excise a retrotransposon that disrupts the *Dysf* gene of A/J mice. This insertion prevents the production of dysferlin and consequently causes a murine dysferlinopathy. A system for easily removing the pathogenic retrotransposon sequence would enhance the utility of the A/J mouse model system by allowing experiments to occur on the same mouse, *in vivo*, in the presence or absence of endogenous dysferlin. The system I designed functioned as a trial cassette for putative gRNAs. Bioinformatically informed gRNA selection is infamously inexact. By using a cassette with many potential gRNAs I could test several gRNAs for efficacy, instead of one by one. This system would be of great utility towards determining the optimal gRNAs to rescue A/J mice, as well as to the wider scientific field of genomic engineering.

I successfully generated a single, large plasmid containing the coding sequence for the Cas12a genome editing protein and a contiguous gRNA oligonucleotide that targeted regions surrounding the retrotransposon insertion site in the *Dysf* gene of A/J mice. In the course of designing this CRISPR cassette I encountered unexpected challenges in amplifying the genomic region of the lesion in the *Dysf* gene of A/J mice. This difficult-to-amplify region required a specific mixture of PCR reagents, determined through informed trial and error, to amplify the long genomic DNA. After determining

the correct mixture of PCR reagents, I used electroporation to insert the CRISPR-Cas12a and putative gRNAs into the mouse. I observed indels surrounding the *Dysf* retrotransposon insertion site only in mice that were electroporated with the plasmid containing *Dysf* targeting gRNAs. Future experiments with this plasmid may involve optimizing the efficacy of genome editing *in vitro*.

Sonoporation of Murine Skeletal Muscle

It's possible to decrease the size of the aforementioned genome editing plasmid by removing bacterial sequences and determining the minimal functional sequence for the various components contained in the plasmid, but there is a limit to how small such a plasmid can be and still remain effective. Plasmid size is important because many *in vivo* genome editing applications require the use of viruses that can only contain a certain amount of extraneous DNA. In order to surmount the problems presented by a limited viral vector loading size, I explored using sonoporation to introduce large exogenous plasmids into mice, such as the CRISPR cassette I designed.

Plasmids conjugated to microbubbles injected intravenously can be sonoporated into muscle and other tissue using ultrasound. Microbubbles are effectively size unlimited vectors for transmitting foreign DNA into cells. Multiple plasmids will bind onto a comparatively large cationic microbubble. These microbubbles are then injected intravenously and ultrasound is applied to the desired organ to transfect. The rapid expansion and contraction of the bubble in the blood stream causes the microbubble to burst, “shooting” the plasmid into nearby cells.

Before attempting to use a much larger and more complex plasmid such as the CRISPR cassette I generated, I tried using the system with a simple plasmid expressing the far red shifted fluorescent marker E2-Crimson. The light from far red shifted fluorophores doesn't dissipate as readily as the emissions of other shorter wavelength fluorophores do when passing through tissue (Strack et al. 2009). With the kind help of Dr. Victor Frenkel and his lab, I sonoporated mice with a reporter plasmid expressing E2-Crimson. Unfortunately, I did not observe fluorescence in the hind limbs of sonoporated mice. This may have been due to a variety of factors ranging from a difference in protocols, compared to sonoporation that has been previously shown in skeletal muscle, to human error in the preparation of the plasmid or injection/sonoporation of the mice. Because plasmid size should not be a limiting factor in tissue transfections, sonoporation remains an interesting method for use *in vivo* and *in vitro*. Future studies may explore the best techniques for performing sonoporation in muscle and the best formulation of microbubble vectors for large plasmids, as there are many different sizes and compositions of microbubbles.

Conclusions

Increased expression of μ -crystallin in murine skeletal muscle results in a shift in metabolism from glycolysis of carbohydrates towards the β -oxidation of fat. These results may be important towards management of obesity, diabetes, and other metabolically related disorders. CRISPR-Cas12a is an effective system for conducting multiplexed screens of gRNAs for optimal targeting efficiency. Simplifying the use of CRISPR-

Cas12a enhances the ability of researchers to quickly and easily determine an optimal gRNA for a variety of CRISPR based applications like genome editing or epigenomic therapeutics. Finally, sonoporation offers an attractive approach to transfecting specific organs after a minimally invasive intravenous injection of microbubble-conjugated DNA, though the exact methods for doing this with murine skeletal muscle will require refinement.

Bibliography

Abdalla, Sherine M, and Antonio C Bianco. 2014. 'Defending plasma T3 is a biological priority', *Clinical endocrinology*, 81: 633-41.

Abe, Satoko, Toyomasa Katagiri, Akihiko Saito-Hisaminato, Shin-ichi Usami, Yasuhiro Inoue, Tatsuhiko Tsunoda, and Yusuke Nakamura. 2003. 'Identification of CRYM as a candidate responsible for nonsyndromic deafness, through cDNA microarray analysis of human cochlear and vestibular tissues', *The American Journal of Human Genetics*, 72: 73-82.

Aguet, François, Dimitri Van De Ville, and Michael Unser. 2008. 'Model-based 2.5-D deconvolution for extended depth of field in brightfield microscopy', *IEEE Transactions on Image Processing*, 17: 1144-53.

Ahmed, Jehangir N, Koula EM Diamand, Helen M Bellchambers, and Ruth M Arkell. 2020. 'Systematized reporter assays reveal ZIC protein regulatory abilities are Subclass-

specific and dependent upon transcription factor binding site context', *Scientific reports*, 10: 1-14.

Apriletti, James W, Ralff CJ Ribeiro, Richard L Wagner, Weijun Feng, Paul Webb, Peter J Kushner, Brian L West, Stefan Nilsson, Thomas S Scanlan, and Robert J Fletterick. 1998. 'Molecular and structural biology of thyroid hormone receptors', *Clinical and Experimental Pharmacology and Physiology*, 25: S2-S11.

Arion, Dominique, Travis Unger, David A Lewis, Pat Levitt, and Károly Mirnics. 2007. 'Molecular evidence for increased expression of genes related to immune and chaperone function in the prefrontal cortex in schizophrenia', *Biological psychiatry*, 62: 711-21.

Bancroft, John D, and Marilyn Gamble. 2008. *Theory and practice of histological techniques* (Elsevier health sciences).

Bansal, Dimple, Katsuya Miyake, Steven S Vogel, Séverine Groh, Chien-Chang Chen, Roger Williamson, Paul L McNeil, and Kevin P Campbell. 2003. 'Defective membrane repair in dysferlin-deficient muscular dystrophy', *nature*, 423: 168-72.

Bashir, Rumaisa, Stephen Britton, Tom Strachan, Sharon Keers, Elizabeth Vafiadaki, Majlinda Lako, Isabelle Richard, Sylvie Marchand, Nathalie Bourg, and Zohar Argov. 1998. 'A gene related to *Caenorhabditis elegans* spermatogenesis factor *fer-1* is mutated in limb-girdle muscular dystrophy type 2B', *Nature genetics*, 20: 37-42.

Beasley, Clare L, Kyla Pennington, Aine Behan, Robin Wait, Michael J Dunn, and David Cotter. 2006. 'Proteomic analysis of the anterior cingulate cortex in the major psychiatric disorders: evidence for disease-associated changes', *Proteomics*, 6: 3414-25.

Beckett, Geoffrey J, and John R Arthur. 1994. '3 The iodothyronine deiodinases and 5'-deiodination', *Baillière's clinical endocrinology and metabolism*, 8: 285-304.

Bello, F, and AG Bakari. 2012. 'Hypothyroidism in adults: A review and recent advances in management', *J Diabetes Endocrinol*, 3: 57-69.

Beslin, Aline, Marie-Pierre Vié, Jean-Paul Blondeau, and Jacques Francon. 1995. 'Identification by photoaffinity labelling of a pyridine nucleotide-dependent tri-iodothyronine-binding protein in the cytosol of cultured astroglial cells', *Biochemical Journal*, 305: 729-37.

Béziat, Vivien, Juan Li, Jian-Xin Lin, Cindy S Ma, Peng Li, Aziz Bousfiha, Isabelle Pellier, Samaneh Zoghi, Safa Baris, and Sevgi Keles. 2018. 'A recessive form of hyper-IgE syndrome by disruption of ZNF341-dependent STAT3 transcription and activity', *Science immunology*, 3.

Bianco, Antonio C, and Brian W Kim. 2006. 'Deiodinases: implications of the local control of thyroid hormone action', *The Journal of clinical investigation*, 116: 2571-79.

Bishopric, Nanette H, and Larry Kedes. 1991. 'Adrenergic regulation of the skeletal alpha-actin gene promoter during myocardial cell hypertrophy', *Proceedings of the National Academy of Sciences*, 88: 2132-36.

Bittel, Daniel C, Goutam Chandra, Laxmi Tirunagri, Arun B Deora, Sushma Medikayala, Luana Scheffer, Aurelia Defour, and Jyoti K Jaiswal. 2020. 'Annexin A2 mediates dysferlin accumulation and muscle cell membrane repair', *Cells*, 9: 1919.

Borel, Franck, Isma Hachi, Andres Palencia, Marie-Claude Gaillard, and Jean-Luc Ferrer. 2014. 'Crystal structure of mouse mu-crystallin complexed with NADPH and the T3 thyroid hormone', *The FEBS journal*, 281: 1598-612.

Brent, Gregory A. 2012. 'Mechanisms of thyroid hormone action', *The Journal of clinical investigation*, 122: 3035-43.

Briguet, Alexandre, Isabelle Courdier-Fruh, Mark Foster, Thomas Meier, and Josef P Magyar. 2004. 'Histological parameters for the quantitative assessment of muscular dystrophy in the mdx-mouse', *Neuromuscular disorders*, 14: 675-82.

Brochier, Camille, Marie-Claude Gaillard, Elsa Diguët, Nicolas Caudy, Carole Dossat, Béatrice Ségurens, Patrick Wincker, Emmanuel Roze, Jocelyne Caboche, and Philippe Hantraye. 2008. 'Quantitative gene expression profiling of mouse brain regions reveals

differential transcripts conserved in human and affected in disease models', *Physiological genomics*, 33: 170-79.

Brooke, Michael H, and Kenneth K Kaiser. 1970. 'Three' myosin adenosine triphosphatase" systems: the nature of their pH lability and sulfhydryl dependence', *Journal of Histochemistry & Cytochemistry*, 18: 670-72.

Burke, Caitlin W, Jung Soo Suk, Anthony J Kim, Yu-Han J Hsiang, Alexander L Klibanov, Justin Hanes, and Richard J Price. 2012. 'Markedly enhanced skeletal muscle transfection achieved by the ultrasound-targeted delivery of non-viral gene nanocarriers with microbubbles', *Journal of controlled release*, 162: 414-21.

Burks, Tyesha N, Eva Andres-Mateos, Ruth Marx, Rebeca Mejias, Christel Van Erp, Jessica L Simmers, Jeremy D Walston, Christopher W Ward, and Ronald D Cohn. 2011. 'Losartan restores skeletal muscle remodeling and protects against disuse atrophy in sarcopenia', *Science translational medicine*, 3: 82ra37-82ra37.

Capecchi, Mario R. 1980. 'High efficiency transformation by direct microinjection of DNA into cultured mammalian cells', *Cell*, 22: 479-88.

Casas, Francois, Muriel Busson, Stephanie Grandemange, Pascal Seyer, Angel Carazo, Laurence Pessemesse, Chantal Wrutniak-Cabello, and Gerard Cabello. 2006.

'Characterization of a novel thyroid hormone receptor α variant involved in the regulation of myoblast differentiation', *Molecular endocrinology*, 20: 749-63.

Casas, François, Pierrick Rochard, Anne Rodier, Isabelle Cassar-Malek, Sophie Marchal-Victorion, Rudolf J Wiesner, Gérard Cabello, and Chantal Wrutniak. 1999. 'A variant form of the nuclear triiodothyronine receptor c-ErbA α 1 plays a direct role in regulation of mitochondrial RNA synthesis', *Molecular and cellular biology*, 19: 7913-24.

Chassande, Olivier, Alexandre Fraichard, Karine Gauthier, Frédéric Flamant, Claude Legrand, Pierre Savatier, Vincent Laudet, and Jacques Samarut. 1997. 'Identification of transcripts initiated from an internal promoter in the c-erbA α locus that encode inhibitors of retinoic acid receptor- α and triiodothyronine receptor activities', *Molecular endocrinology*, 11: 1278-90.

Chen, Xuqi, Rebecca McClusky, Jenny Chen, Simon W Beaven, Peter Tontonoz, Arthur P Arnold, and Karen Reue. 2012. 'The number of x chromosomes causes sex differences in adiposity in mice', *PLoS Genet*, 8: e1002709.

Chong, Wui K, Virginie Papadopoulou, and Paul A Dayton. 2018. 'Imaging with ultrasound contrast agents: current status and future', *Abdominal Radiology*, 43: 762-72.

Chopra, Inder J. 1977. 'A study of extrathyroidal conversion of thyroxine (T4) to 3, 3', 5-triiodothyronine (T3) in vitro', *Endocrinology*, 101: 453-63.

Ciciliot, Stefano, Alberto C Rossi, Kenneth A Dyar, Bert Blaauw, and Stefano Schiaffino. 2013. 'Muscle type and fiber type specificity in muscle wasting', *The international journal of biochemistry & cell biology*, 45: 2191-99.

Clément, Karine, Nathalie Viguerie, Maximilian Diehn, Ash Alizadeh, Pierre Barbe, Claire Thalamas, John D Storey, Patrick O Brown, Greg S Barsh, and Dominique Langin. 2002. 'In vivo regulation of human skeletal muscle gene expression by thyroid hormone', *Genome research*, 12: 281-91.

Close, R. 1965. 'Force: velocity properties of mouse muscles', *nature*, 206: 718-19.

Collie, ES, and George E Muscat. 1992. 'The human skeletal alpha-actin promoter is regulated by thyroid hormone: identification of a thyroid hormone response element', *Cell growth & differentiation: the molecular biology journal of the American Association for Cancer Research*, 3: 31-42.

Daoud, Hussein, Paul N Valdmanis, Francois Gros-Louis, Véronique Belzil, Dan Spiegelman, Edouard Henrion, Ousmane Diallo, Anne Desjarlais, Julie Gauthier, and William Camu. 2011. 'Resequencing of 29 candidate genes in patients with familial and sporadic amyotrophic lateral sclerosis', *Archives of neurology*, 68: 587-93.

Dème, Danièle, Enzo Fimiani, Jacques Pommier, and Jacques Nunez. 1975. 'Free diiodotyrosine effects on protein iodination and thyroid hormone synthesis catalyzed by thyroid peroxidase', *European journal of biochemistry*, 51: 329-36.

DiFranco, Marino, Philip Tran, Marbella Quinonez, and Julio L Vergara. 2011. 'Functional expression of transgenic α 1sDHPR channels in adult mammalian skeletal muscle fibres', *The Journal of physiology*, 589: 1421-42.

Dixit, Manjusha, Eugénie Anseau, Alexandra Tassin, Sara Winokur, Rongye Shi, Hong Qian, Sébastien Sauvage, Christel Mattéotti, Anne M van Acker, and Oberdan Leo. 2007. 'DUX4, a candidate gene of facioscapulohumeral muscular dystrophy, encodes a transcriptional activator of PITX1', *Proceedings of the National Academy of Sciences*, 104: 18157-62.

Dorfer, Viktoria, Peter Pichler, Thomas Stranzl, Johannes Stadlmann, Thomas Taus, Stephan Winkler, and Karl Mechtler. 2014. 'MS Amanda, a universal identification algorithm optimized for high accuracy tandem mass spectra', *Journal of proteome research*, 13: 3679-84.

Drexler, Hannes CA, Aaron Ruhs, Anne Konzer, Luca Mendler, Mark Bruckskotten, Mario Looso, Stefan Günther, Thomas Boettger, Marcus Krüger, and Thomas Braun. 2012. 'On marathons and Sprints: an integrated quantitative proteomics and

transcriptomics analysis of differences between slow and fast muscle fibers', *Molecular & Cellular Proteomics*, 11: M111. 010801.

Dubowitz, Victor, Caroline A Sewry, and Anders Oldfors. 2013. *Muscle biopsy: a practical approach: expert consult; online and print* (Elsevier Health Sciences).

Ducros, Genevieve, and Teresa Trippenbach. 1991. 'Respiratory effects of lactic acid injected into the jugular vein of newborn rabbits', *Pediatric research*, 29: 548-52.

Ebashi, Setsuro, Makoto Endo, and Iwao Ohtsuki. 1969. 'Control of muscle contraction', *Quarterly reviews of biophysics*, 2: 351-84.

Eckey, Maren, Udo Moehren, and Aria Baniahmad. 2003. 'Gene silencing by the thyroid hormone receptor', *Molecular and cellular endocrinology*, 213: 13-22.

Encarnacion-Rivera, Lucas, Steven Foltz, H Criss Hartzell, and Hyojung Choo. 2020. 'Myosoft: An automated muscle histology analysis tool using machine learning algorithm utilizing FIJI/ImageJ software', *PloS one*, 15: e0229041.

Eng, Jimmy K, Bernd Fischer, Jonas Grossmann, and Michael J MacCoss. 2008. 'A fast SEQUEST cross correlation algorithm', *Journal of proteome research*, 7: 4598-602.

Fan, Zhenzhen, Ronald E Kumon, and Cheri X Deng. 2014. 'Mechanisms of microbubble-facilitated sonoporation for drug and gene delivery', *Therapeutic delivery*, 5: 467-86.

Fechheimer, M, C Denny, RF Murphy, and DL Taylor. 1986. 'Measurement of cytoplasmic pH in *Dictyostelium discoideum* by using a new method for introducing macromolecules into living cells', *European journal of cell biology*, 40: 242-47.

Fechheimer, Marcus, John F Boylan, Sandra Parker, Jesse E Siskin, Gordhan L Patel, and Stephen G Zimmer. 1987. 'Transfection of mammalian cells with plasmid DNA by scrape loading and sonication loading', *Proceedings of the National Academy of Sciences*, 84: 8463-67.

Fekete, Csaba, Joseph Kelly, Emese Mihály, Sumit Sarkar, William M Rand, Gábor Légrádi, Charles H Emerson, and Ronald M Lechan. 2001. 'Neuropeptide Y has a central inhibitory action on the hypothalamic-pituitary-thyroid axis', *Endocrinology*, 142: 2606-13.

Fekete, Csaba, and Ronald M Lechan. 2007. 'Negative feedback regulation of hypophysiotropic thyrotropin-releasing hormone (TRH) synthesizing neurons: role of neuronal afferents and type 2 deiodinase', *Frontiers in neuroendocrinology*, 28: 97-114.

Fekete, Csaba, Emese Mihály, Lu-Guang Luo, Joseph Kelly, Jes Thorn Clausen, QuanFu Mao, William M Rand, Larry Gene Moss, Michael Kuhar, and Charles H Emerson. 2000. 'Association of cocaine-and amphetamine-regulated transcript-immunoreactive elements with thyrotropin-releasing hormone-synthesizing neurons in the hypothalamic paraventricular nucleus and its role in the regulation of the hypothalamic–pituitary–thyroid axis during fasting', *Journal of Neuroscience*, 20: 9224-34.

Fekete, Csaba, Sumit Sarkar, William M Rand, John W Harney, Charles H Emerson, Antonio C Bianco, and Ronald M Lechan. 2002. 'Agouti-related protein (AGRP) has a central inhibitory action on the hypothalamic-pituitary-thyroid (HPT) axis; comparisons between the effect of AGRP and neuropeptide Y on energy homeostasis and the HPT axis', *Endocrinology*, 143: 3846-53.

Figuroa-Romero, Claudia, Junguk Hur, J Simon Lunn, Ximena Paez-Colasante, Diane E Bender, Raymond Yung, Stacey A Sakowski, and Eva L Feldman. 2016. 'Expression of microRNAs in human post-mortem amyotrophic lateral sclerosis spinal cords provides insight into disease mechanisms', *Molecular and Cellular Neuroscience*, 71: 34-45.

Fink, Kathren L, Stephen M Strittmatter, and William BJ Cafferty. 2015. 'Comprehensive corticospinal labeling with mu-crystallin transgene reveals axon regeneration after spinal cord trauma in *ngr1*^{-/-} mice', *Journal of Neuroscience*, 35: 15403-18.

- Fitts, Robert H, Cheryl J Brimmer, John P Troup, and Brian R Unsworth. 1984. 'Contractile and fatigue properties of thyrotoxic rat skeletal muscle', *Muscle & Nerve: Official Journal of the American Association of Electrodiagnostic Medicine*, 7: 470-77.
- Fonfara, Ines, Hagen Richter, Majda Bratovič, Anaïs Le Rhun, and Emmanuelle Charpentier. 2016. 'The CRISPR-associated DNA-cleaving enzyme Cpf1 also processes precursor CRISPR RNA', *nature*, 532: 517-21.
- Fornes, Oriol, Jaime A Castro-Mondragon, Aziz Khan, Robin Van der Lee, Xi Zhang, Phillip A Richmond, Bhavi P Modi, Solenne Correard, Marius Gheorghe, and Damir Baranašić. 2020. 'JASPAR 2020: update of the open-access database of transcription factor binding profiles', *Nucleic acids research*, 48: D87-D92.
- Francelle, Laetitia, Laurie Galvan, Marie-Claude Gaillard, Martine Guillermier, Diane Houitte, Gilles Bonvento, Fanny Petit, Caroline Jan, Noëlle Dufour, and Philippe Hantraye. 2015. 'Loss of the thyroid hormone-binding protein Crym renders striatal neurons more vulnerable to mutant huntingtin in Huntington's disease', *Human molecular genetics*, 24: 1563-73.
- Freake, Hedley C, and Jack H Oppenheimer. 1995. 'Thermogenesis and thyroid function', *Annual review of nutrition*, 15: 263-91.

Frey-Jakobs, Stefanie, Julia M Hartberger, Manfred Fliegau, Claudia Bossen, Magdalena L Wehmeyer, Johanna C Neubauer, Alla Bulashevskaya, Michele Proietti, Philipp Fröbel, and Christina Nöltner. 2018. 'ZNF341 controls STAT3 expression and thereby immunocompetence', *Science immunology*, 3.

Friesema, Edith CH, Roelof Docter, Ellis PCM Moerings, Bruno Stieger, Bruno Hagenbuch, Peter J Meier, Eric P Krenning, Georg Hennemann, and Theo J Visser. 1999. 'Identification of thyroid hormone transporters', *Biochemical and biophysical research communications*, 254: 497-501.

Friesema, Edith CH, Jurgen Jansen, Jan-willem Jachtenberg, W Edward Visser, Monique HA Kester, and Theo J Visser. 2008. 'Effective cellular uptake and efflux of thyroid hormone by human monocarboxylate transporter 10', *Molecular endocrinology*, 22: 1357-69.

Fukada, Yasuyo, Kenichi Yasui, Michio Kitayama, Koji Doi, Toshiya Nakano, Yasuhiro Watanabe, and Kenji Nakashima. 2007. 'Gene expression analysis of the murine model of amyotrophic lateral sclerosis: studies of the Leu126delTT mutation in SOD1', *Brain research*, 1160: 1-10.

Gallagher, David T, HG Monbouquette, I Schröder, Hugh Robinson, Marcia J Holden, and NN Smith. 2004. 'Structure of alanine dehydrogenase from *Archaeoglobus*: active

site analysis and relation to bacterial cyclodeaminases and mammalian mu crystallin', *Journal of molecular biology*, 342: 119-30.

Gardiner-Garden, M, and M Frommer. 1987. 'CpG islands in vertebrate genomes', *Journal of molecular biology*, 196: 261-82.

Giger, Julia M, Paul W Bodell, Ming Zeng, Kenneth M Baldwin, and Fadia Haddad. 2009. 'Rapid muscle atrophy response to unloading: pretranslational processes involving MHC and actin', *Journal of Applied Physiology*, 107: 1204-12.

Graupner, Gerhart, Ken N Wills, Maty Tzukerman, Xiao-kun Zhang, and Magnus Pfahl. 1989. 'Dual regulatory role for thyroid-hormone receptors allows control of retinoic-acid receptor activity', *nature*, 340: 653-56.

Gunning, Peter, P Ponte, H Blau, and L Kedes. 1983. 'alpha-skeletal and alpha-cardiac actin genes are coexpressed in adult human skeletal muscle and heart', *Molecular and cellular biology*, 3: 1985-95.

Gustafson, THOMAS A, BRUCE E Markham, and EUGENE Morkin. 1986. 'Effects of thyroid hormone on alpha-actin and myosin heavy chain gene expression in cardiac and skeletal muscles of the rat: measurement of mRNA content using synthetic oligonucleotide probes', *Circulation research*, 59: 194-201.

Hallen, André, and Arthur JL Cooper. 2017. 'Reciprocal control of thyroid binding and the pipecolate pathway in the brain', *Neurochemical research*, 42: 217-43.

Hallen, André, Arthur JL Cooper, Joanne F Jamie, Paul A Haynes, and Robert D Willows. 2011. 'Mammalian forebrain ketimine reductase identified as μ -crystallin; potential regulation by thyroid hormones', *Journal of neurochemistry*, 118: 379-87.

Hallen, André, Arthur JL Cooper, Joanne F Jamie, and Peter Karuso. 2015. 'Insights into enzyme catalysis and thyroid hormone regulation of cerebral ketimine reductase/ μ -crystallin under physiological conditions', *Neurochemical research*, 40: 1252-66.

Hallen, André, Arthur JL Cooper, Jason R Smith, Joanne F Jamie, and Peter Karuso. 2015. 'Ketimine reductase/CRYM catalyzes reductive alkylamination of α -keto acids, confirming its function as an imine reductase', *Amino acids*, 47: 2457-61.

Harris, Mark, Carl Aschkenasi, Carol F Elias, Annie Chandrankunnel, Eduardo A Nillni, Christian Bjørbæk, Joel K Elmquist, Jeffrey S Flier, and Anthony N Hollenberg. 2001. 'Transcriptional regulation of the thyrotropin-releasing hormone gene by leptin and melanocortin signaling', *The Journal of clinical investigation*, 107: 111-20.

Hashizume, Kiyoshi, Mutsuhiro Kobayashi, and Takahide Miyamoto. 1986. 'Active and inactive forms of 3, 5, 3'-triiodo-L-thyronine (T3)-binding protein in rat kidney cytosol:

possible role of nicotinamide adenine dinucleotide phosphate in activation of T3 binding', *Endocrinology*, 119: 710-19.

Hashizume, Kiyoshi, T Miyamoto, Kazuo Ichikawa, Keishi Yamauchi, Akihiro Sakurai, Hiromi Ohtsuka, Mutsuhiro Kobayashi, Yutaka Nishii, and Takashi Yamada. 1989.

'Evidence for the presence of two active forms of cytosolic 3, 5, 3'-triiodo-L-thyronine (T3)-binding protein (CTBP) in rat kidney. Specialized functions of two CTBPs in intracellular T3 translocation', *Journal of Biological Chemistry*, 264: 4864-71.

Hashizume, Kiyoshi, Takahide Miyamoto, Kazuo Ichikawa, Keishi Yamauchi, Mutsuhiro Kobayashi, Akihiro Sakurai, Hiromi Ohtsuka, Yutaka Nishii, and Takashi Yamada. 1989.

'Purification and characterization of NADPH-dependent cytosolic 3, 5, 3'-triiodo-L-thyronine binding protein in rat kidney', *Journal of Biological Chemistry*, 264: 4857-63.

Hashizume, Kiyoshi, Takahide Miyamoto, Mutsuhiro Kobayashi, Satoru Suzuki, Kazuo Ichikawa, Keishi Yamauchi, Hiromi Ohtsuka, and Teiji Takeda. 1989. 'Cytosolic 3, 5, 3'-triiodo-L-thyronine (T3)-binding protein (CTBP) regulation of nuclear T3 binding: evidence for the presence of T3-CTBP complex-binding sites in nuclei', *Endocrinology*, 124: 2851-56.

Hashizume, Kiyoshi, Takahide Miyamoto, Keishi Yamauchi, Kazuo Ichikawa, Mutsuhiro Kobayashi, Hiromi Ohtsuka, Akihiro Sakurai, Satoru Suzuki, and Takashi Yamada. 1989. 'Counterregulation of nuclear 3, 5, 3'-triiodo-L-thyronine (T3) binding by oxidized and

reduced-nicotinamide adenine dinucleotide phosphates in the presence of cytosolic T3-binding protein in vitro', *Endocrinology*, 124: 1678-83.

Hernot, Sophie, and Alexander L Klibanov. 2008. 'Microbubbles in ultrasound-triggered drug and gene delivery', *Advanced drug delivery reviews*, 60: 1153-66.

Heuer, Heike, Martin K-H Schäfer, Dajan O'Donnell, Philippe Walker, and Karl Bauer. 2000. 'Expression of thyrotropin-releasing hormone receptor 2 (TRH-R2) in the central nervous system of rats', *Journal of Comparative Neurology*, 428: 319-36.

Hinaux, Helene, Maryline Blin, Julien Fumey, Laurent Legendre, Aurelie Heuze, Didier Casane, and Sylvie Retaux. 2015. 'Lens defects in *A. styanax mexicanus* Cavefish: Evolution of crystallins and a role for alphaA-crystallin', *Developmental neurobiology*, 75: 505-21.

Ho, Mengfatt, Cristina M Post, Leah R Donahue, Hart GW Lidov, Roderick T Bronson, Holly Goolsby, Simon C Watkins, Gregory A Cox, and Robert H Brown Jr. 2004. 'Disruption of muscle membrane and phenotype divergence in two novel mouse models of dysferlin deficiency', *Human molecular genetics*, 13: 1999-2010.

Hodges, Angela, Andrew D Strand, Aaron K Aragaki, Alexandre Kuhn, Thierry Sengstag, Gareth Hughes, Lyn A Elliston, Cathy Hartog, Darlene R Goldstein, and Doris

Thu. 2006. 'Regional and cellular gene expression changes in human Huntington's disease brain', *Human molecular genetics*, 15: 965-77.

Hodin, Richard A, Mitchell A Lazar, Bruce I Wintman, Douglas S Darling, Ronald J Koenig, P Reed Larsen, David D Moore, and William W Chin. 1989. 'Identification of a thyroid hormone receptor that is pituitary-specific', *Science*, 244: 76-79.

Hollowell, Joseph G, Norman W Staehling, W Dana Flanders, W Harry Hannon, Elaine W Gunter, Carole A Spencer, and Lewis E Braverman. 2002. 'Serum TSH, T4, and thyroid antibodies in the United States population (1988 to 1994): National Health and Nutrition Examination Survey (NHANES III)', *The Journal of Clinical Endocrinology & Metabolism*, 87: 489-99.

Homma, Sachiko, Jennifer CJ Chen, Fedik Rahimov, Mary Lou Beermann, Kendal Hanger, Genila M Bibat, Kathryn R Wagner, Louis M Kunkel, Charles P Emerson Jr, and Jeffrey Boone Miller. 2012. 'A unique library of myogenic cells from facioscapulohumeral muscular dystrophy subjects and unaffected relatives: family, disease and cell function', *European Journal of Human Genetics*, 20: 404-10.

Hommyo, Reiji, Satoshi O Suzuki, Nona Abolhassani, Hideomi Hamasaki, Masahiro Shijo, Norihisa Maeda, Hiroyuki Honda, Yusaku Nakabeppu, and Toru Iwaki. 2018. 'Expression of CRYM in different rat organs during development and its decreased

expression in degenerating pyramidal tracts in amyotrophic lateral sclerosis', *Neuropathology*, 38: 247-59.

Illa, Isabel, Carme Serrano-Munuera, Eduard Gallardo, Adriana Lasa, Ricardo Rojas-García, Jaume Palmer, Pia Gallano, Montserrat Baiget, Chie Matsuda, and Robert H Brown. 2001. 'Distal anterior compartment myopathy: a dysferlin mutation causing a new muscular dystrophy phenotype', *Annals of Neurology: Official Journal of the American Neurological Association and the Child Neurology Society*, 49: 130-34.

Imai, Hiroki, Kouichi Ohta, Akiko Yoshida, Satoru Suzuki, Kiyoshi Hashizume, Shinichi Usami, and Takanobu Kikuchi. 2010. ' μ -crystallin, new candidate protein in endotoxin-induced uveitis', *Investigative ophthalmology & visual science*, 51: 3554-59.

Jansen, Jurgen, Edith CH Friesema, Carmelina Milici, and Theo J Visser. 2005. 'Thyroid hormone transporters in health and disease', *Thyroid*, 15: 757-68.

Jhanwar, Suresh C, RSK Chaganti, and Carlo M Croce. 1985. 'Germ-line chromosomal localization of humanc-erb-A oncogene', *Somatic cell and molecular genetics*, 11: 99-102.

Johansson, Catarina, Per Kristian Lunde, Sten Göthe, Jan Lännergren, and Håckan Westerblad. 2003. 'Isometric force and endurance in skeletal muscle of mice devoid of all known thyroid hormone receptors', *The Journal of physiology*, 547: 789-96.

Johnston-Wilson, NL, CD Sims, JP Hofmann, L Anderson, AD Shore, EF Torrey, and Robert H Yolken. 2000. 'Disease-specific alterations in frontal cortex brain proteins in schizophrenia, bipolar disorder, and major depressive disorder', *Molecular psychiatry*, 5: 142-49.

Johnston, Stephen A, and De-Chu Tang. 1993. 'The use of microparticle injection to introduce genes into animal cells in vitro and in vivo', *Genetic engineering*: 225-36.

Joshi, Shreyas S, Mansi Sethi, Martin Striz, Neil Cole, James M Denegre, Jennifer Ryan, Michael E Lhamon, Anuj Agarwal, Steve Murray, and Robert E Braun. 2019. 'Noninvasive sleep monitoring in large-scale screening of knock-out mice reveals novel sleep-related genes', *bioRxiv*: 517680.

Kalmar, Bernadett, Gonzalo Blanco, and Linda Greensmith. 2012. 'Determination of muscle fiber type in rodents', *Current protocols in mouse biology*, 2: 231-43.

Kalyanaraman, Hema, Raphaela Schwappacher, Jisha Joshua, Shunhui Zhuang, Brian T Scott, Matthew Klos, Darren E Casteel, John A Frangos, Wolfgang Dillmann, and Gerry R Boss. 2014. 'Nongenomic thyroid hormone signaling occurs through a plasma membrane-localized receptor', *Science signaling*, 7: ra48-ra48.

Kammoun, Malek, I Cassar-Malek, Bruno Meunier, and Brigitte Picard. 2014. 'A simplified immunohistochemical classification of skeletal muscle fibres in mouse', *European journal of histochemistry: EJH*, 58.

Keown, Wayne A, Colin R Campbell, and Raju S Kucherlapati. 1990. 'Methods for introducing DNA into mammalian cells', *Methods in enzymology*, 185: 527-37.

Kerr, Jaclyn P, Christopher W Ward, and Robert J Bloch. 2014. 'Dysferlin at transverse tubules regulates Ca²⁺ homeostasis in skeletal muscle', *Frontiers in physiology*, 5: 89.

Kerr, Jaclyn P, Andrew P Ziman, Amber L Mueller, Joaquin M Muriel, Emily Kleinhans-Welte, Jessica D Gumerson, Steven S Vogel, Christopher W Ward, Joseph A Roche, and Robert J Bloch. 2013. 'Dysferlin stabilizes stress-induced Ca²⁺ signaling in the transverse tubule membrane', *Proceedings of the National Academy of Sciences*, 110: 20831-36.

Kim, Dongwon, Ruosi Chen, Mary Sheu, Noori Kim, Sooah Kim, Nasif Islam, Eric M Wier, Gaofeng Wang, Ang Li, and Angela Park. 2019. 'Noncoding dsRNA induces retinoic acid synthesis to stimulate hair follicle regeneration via TLR3', *Nature Communications*, 10: 2811.

Kim, Robert Y, Robin Gasser, and Graeme J Wistow. 1992. 'mu-crystallin is a mammalian homologue of Agrobacterium ornithine cyclodeaminase and is expressed in human retina', *Proceedings of the National Academy of Sciences*, 89: 9292-96.

Kinney, Christian J, and Robert J Bloch. 2021. 'μ-Crystallin: A Thyroid Hormone Binding Protein', *Endocrine Regulations*.

Kinney, Christian J, Andrea O'Neill, Kaila Noland, Weiliang Huang, Joaquin M Muriel, Valeriy Lukyanenko, Maureen A Kane, Christopher W Ward, Alyssa F Collier, Joseph A Roche, John C McLenithan, Patrick W Reed, and Robert J Bloch. 2020. 'μ-Crystallin in Mouse Skeletal Muscle Promotes a Shift from Glycolytic toward Oxidative Metabolism', *Current Reseach in Physiology*.

Kinney, Christian J., Andrea O'Neill, Kaila Noland, Weiliang Huang, Joaquin Muriel, Valeriy Lukyanenko, Maureen A. Kane, Christopher W. Ward, Alyssa F. Collier, Joseph A. Roche, John C. McLenithan, Patrick W. Reed, and Robert J. Bloch. 2021. 'μ-Crystallin in Mouse Skeletal Muscle Promotes a Shift from Glycolytic toward Oxidative Metabolism', *Current Research in Physiology*, 4: 47-59.

Klooster, Rinse, Kirsten Straasheijm, Bharati Shah, Janet Sowden, Rune Frants, Charles Thornton, Rabi Tawil, and Silvere Van Der Maarel. 2009. 'Comprehensive expression analysis of FSHD candidate genes at the mRNA and protein level', *European Journal of Human Genetics*, 17: 1615.

Kobayashi, Mutsuhiro, Kiyoshi Hashizume, Satoru Suzuki, Kazuo Ichikawa, and Teiji Takeda. 1991. 'A Novel NADPH-Dependent Cytosolic 3, 5, 3'-Triiodo-LThyronine-Binding Protein (CTBP; 5. IS) in Rat Liver: A Comparison with 4.7 S NADPH-Dependent CTBP', *Endocrinology*, 129: 1701-08.

Kubota, Ken, Hidemasa Uchimura, Tomoaki Mitsuhashi, Shoo Cheng Chiu, Nobuaki Kuzuya, and Shigenobu Nagataki. 1984. 'Effects of intrathyroidal metabolism of thyroxine on thyroid hormone secretion: increased degradation of thyroxine in mouse thyroids stimulated chronically with thyrotrophin', *European Journal of Endocrinology*, 105: 57-65.

Laemmli, Ulrich K. 1970. 'Cleavage of structural proteins during the assembly of the head of bacteriophage T4', *nature*, 227: 680-85.

Larsen, P Reed, J Enrique Silva, and Michael M Kaplan. 1981. 'Relationships between circulating and intracellular thyroid hormones: physiological and clinical implications', *Endocrine Reviews*, 2: 87-102.

Lassche, Saskia, Ger JM Stienen, Tom C Irving, Silvère M Van Der Maarel, Nicol C Voermans, George W Padberg, Henk Granzier, Baziel GM van Engelen, and Coen AC Ottenheijm. 2013. 'Sarcomeric dysfunction contributes to muscle weakness in facioscapulohumeral muscular dystrophy', *Neurology*, 80: 733-37.

Latchman, David S. 2001. 'Gene delivery and gene therapy with herpes simplex virus-based vectors', *Gene*, 264: 1-9.

Légrádi, Gábor, Charles H Emerson, Rexford S Ahima, Jeffrey S Flier, and Ronald M Lechan. 1997. 'Leptin prevents fasting-induced suppression of prothyrotropin-releasing hormone messenger ribonucleic acid in neurons of the hypothalamic paraventricular nucleus', *Endocrinology*, 138: 2569-76.

Lein, Ed S, Michael J Hawrylycz, Nancy Ao, Mikael Ayres, Amy Bensinger, Amy Bernard, Andrew F Boe, Mark S Boguski, Kevin S Brockway, and Emi J Byrnes. 2007. 'Genome-wide atlas of gene expression in the adult mouse brain', *nature*, 445: 168-76.

Liu, Jing, Masashi Aoki, Isabel Illa, Chenyan Wu, Michel Fardeau, Corrado Angelini, Carmen Serrano, J Andoni Urtizberea, Faycal Hentati, and Mongi Ben Hamida. 1998. 'Dysferlin, a novel skeletal muscle gene, is mutated in Miyoshi myopathy and limb girdle muscular dystrophy', *Nature genetics*, 20: 31-36.

Liu, X, S Wei, S Deng, D Li, K Liu, B Shan, Y Shao, W Wei, J Chen, and L Zhang. 2019. 'Genome-wide identification and comparison of mRNA s, lnc RNA s and circ RNA s in porcine intramuscular, subcutaneous, retroperitoneal and mesenteric adipose tissues', *Animal genetics*, 50: 228-41.

Liu, Yan-Yun, Anna Milanesi, and Gregory A Brent. 2020. 'Thyroid Hormones.' in, *Hormonal Signaling in Biology and Medicine* (Elsevier).

Lonsdale, John, Jeffrey Thomas, Mike Salvatore, Rebecca Phillips, Edmund Lo, Saboor Shad, Richard Hasz, Gary Walters, Fernando Garcia, and Nancy Young. 2013. 'The genotype-tissue expression (GTEx) project', *Nature genetics*, 45: 580-85.

Luff, AR. 1981. 'Dynamic properties of the inferior rectus, extensor digitorum longus, diaphragm and soleus muscles of the mouse', *The Journal of physiology*, 313: 161-71.

Lukyanenko, Valeriy, Joaquin M Muriel, and Robert J Bloch. 2017. 'Coupling of excitation to Ca²⁺ release is modulated by dysferlin', *The Journal of physiology*, 595: 5191-207.

Lusk, Graham. 1924. 'Animal calorimetry twenty-fourth paper. Analysis of the oxidation of mixtures of carbohydrate and fat', *Journal of Biological Chemistry*, 59: 41-42.

Maksakova, Irina A, and Dixie L Mager. 2005. 'Transcriptional regulation of early transposon elements, an active family of mouse long terminal repeat retrotransposons', *Journal of virology*, 79: 13865-74.

Mansourian, Azad Reza. 2010. 'A review on hyperthyroidism: thyrotoxicosis under surveillance', *Pakistan Journal of Biological Sciences*, 13: 1066.

Martins-de-Souza, Daniel, Wagner F Gattaz, Andrea Schmitt, Giuseppina Maccarrone, Eva Hunyadi-Gulyás, Marcos N Eberlin, Gustavo HMF Souza, Sérgio Marangoni, José C Novello, and Christoph W Turck. 2009. 'Proteomic analysis of dorsolateral prefrontal cortex indicates the involvement of cytoskeleton, oligodendrocyte, energy metabolism and new potential markers in schizophrenia', *Journal of psychiatric research*, 43: 978-86.

Martins-de-Souza, Daniel, Wagner F Gattaz, Andrea Schmitt, Christiane Rewerts, Giuseppina Maccarrone, Emmanuel Dias-Neto, and Christoph W Turck. 2009. 'Prefrontal cortex shotgun proteome analysis reveals altered calcium homeostasis and immune system imbalance in schizophrenia', *European archives of psychiatry and clinical neuroscience*, 259: 151-63.

Mendoza, Arturo, and Anthony N Hollenberg. 2017. 'New insights into thyroid hormone action', *Pharmacology & therapeutics*, 173: 135-45.

Mengeling, Brenda J, Fan Pan, and Martin L Privalsky. 2005. 'Novel mode of deoxyribonucleic acid recognition by thyroid hormone receptors: Thyroid hormone receptor β -isoforms can bind as trimers to natural response elements comprised of reiterated half-sites', *Molecular endocrinology*, 19: 35-51.

Middleton, Frank A, Karoly Mirnics, Joseph N Pierri, David A Lewis, and Pat Levitt. 2002. 'Gene expression profiling reveals alterations of specific metabolic pathways in schizophrenia', *Journal of Neuroscience*, 22: 2718-29.

Miga, Karen H, Christopher Eisenhart, and W James Kent. 2015. 'Utilizing mapping targets of sequences underrepresented in the reference assembly to reduce false positive alignments', *Nucleic acids research*, 43: e133-e33.

Mihály, Emese, Csaba Fekete, Jeffrey B Tatro, Zsolt Liposits, Ed G Stopa, and Ronald M Lechan. 2000. 'Hypophysiotropic thyrotropin-releasing hormone-synthesizing neurons in the human hypothalamus are innervated by neuropeptide Y, agouti-related protein, and α -melanocyte-stimulating hormone', *The Journal of Clinical Endocrinology & Metabolism*, 85: 2596-603.

Miklos, George L Gabor, and Ryszard Maleszka. 2004. 'Microarray reality checks in the context of a complex disease', *Nature biotechnology*, 22: 615-21.

Miller, Douglas L, Sorin V Pislaru, and James F Greenleaf. 2002. 'Sonoporation: mechanical DNA delivery by ultrasonic cavitation', *Somatic cell and molecular genetics*, 27: 115-34.

Mitchell, AM, M Tom, and RH Mortimer. 2005. 'Thyroid hormone export from cells: contribution of P-glycoprotein', *Journal of endocrinology*, 185: 93-98.

Mori, Jun-ichirou, Satoru Suzuki, Mutsuhiro Kobayashi, Takeshi Inagaki, Ai Komatsu, Teiji Takeda, Takahide Miyamoto, Kazuo Ichikawa, and Kiyoshi Hashizume. 2002.

'Nicotinamide adenine dinucleotide phosphate-dependent cytosolic T3 binding protein as a regulator for T3-mediated transactivation', *Endocrinology*, 143: 1538-44.

Morley, John E. 1979. 'Extrahypothalamic thyrotropin releasing hormone (TRH)—its distribution and its functions', *Life sciences*, 25: 1539-50.

Motulsky, Harvey J, and Ronald E Brown. 2006. 'Detecting outliers when fitting data with nonlinear regression—a new method based on robust nonlinear regression and the false discovery rate', *BMC bioinformatics*, 7: 123.

Mukai, Motoko, Kirstin Replogle, Jenny Drnevich, Gang Wang, Douglas Wacker, Mark Band, David F Clayton, and John C Wingfield. 2009. 'Seasonal differences of gene expression profiles in song sparrow (*Melospiza melodia*) hypothalamus in relation to territorial aggression', *PloS one*, 4.

O'shea, PJ, and GR Williams. 2002. 'Insight into the physiological actions of thyroid hormone receptors from genetically modified mice', *The Journal of endocrinology*, 175: 553.

Ohkubo, Yohsuke, Takashi Sekido, Shin-ichi Nishio, Keiko Sekido, Junichiro Kitahara, Satoru Suzuki, and Mitsuhsa Komatsu. 2019. 'Loss of μ -crystallin causes PPAR γ activation and obesity in high-fat diet-fed mice', *Biochemical and biophysical research communications*, 508: 914-20.

Ojha, Akanksha, and Milind Watve. 2018. 'Blind fish: An eye opener', *Evolution, Medicine, and Public Health*, 2018: 186-89.

Olojo, Rotimi O, Andrew P Ziman, Erick O Hernández-Ochoa, Paul D Allen, Martin F Schneider, and Christopher W Ward. 2011. 'Mice null for calsequestrin 1 exhibit deficits in functional performance and sarcoplasmic reticulum calcium handling', *PloS one*, 6: e27036.

Oshima, A, S Suzuki, Y Takumi, K Hashizume, S Abe, and S Usami. 2006. 'CRYM mutations cause deafness through thyroid hormone binding properties in the fibrocytes of the cochlea', *Journal of medical genetics*, 43: e25-e25.

Pantos, Constantinos, and Iordanis Mourouzis. 2018. 'Thyroid hormone receptor $\alpha 1$ as a novel therapeutic target for tissue repair', *Annals of translational medicine*, 6.

Pensato, Viviana, Stefania Magri, Eleonora Dalla Bella, Pierpaola Tannorella, Enrica Bersano, Gianni Sorarù, Marta Gatti, Nicola Ticozzi, Franco Taroni, and Giuseppe Lauria. 2020. 'Sorting rare ALS genetic variants by targeted re-sequencing panel in Italian patients: OPTN, VCP, and SQSTM1 variants account for 3% of rare genetic forms', *Journal of clinical medicine*, 9: 412.

Pette, Dirk, and Robert S Staron. 1997. 'Mammalian skeletal muscle fiber type transitions.' in, *International Review of Cytology* (Elsevier).

Phan, L, Y Jin, H Zhang, W Qiang, E Shekhtman, D Shao, D Revoe, R Villamarin, E Ivanchenko, and M Kimura. 2020. 'ALFA: Allele Frequency Aggregator', *National Center for Biotechnology Information, US National Library of Medicine. Available online: www.ncbi.nlm.nih.gov/snp/docs/gsr/alfa/(accessed on 10 March 2020).*

Pihlajamäki, Jussi, Tanner Boes, Eun-Young Kim, Farrell Dearie, Brian W Kim, Joshua Schroeder, Edward Mun, Imad Nasser, Peter J Park, and Antonio C Bianco. 2009. 'Thyroid hormone-related regulation of gene expression in human fatty liver', *The Journal of Clinical Endocrinology & Metabolism*, 94: 3521-29.

Pirahanchi, Y., and I. Jialal. 2019. 'Physiology, Thyroid Stimulating Hormone (TSH).' in, *StatPearls* (StatPearls Publishing LLC.: Treasure Island (FL).

Pirahanchi, Yasaman, Muhammad Ali Tariq, and Ishwarlal Jialal. 2020. 'Physiology, thyroid', *StatPearls [Internet]*.

Raparti, Girish, Suyog Jain, Karuna Ramteke, Mangala Murthy, Ravi Ghanghas, Sunita Ramanand, and Jaiprakash Ramanand. 2013. 'Selective thyroid hormone receptor modulators', *Indian journal of endocrinology and metabolism*, 17: 211.

Reed, Patrick W, Andrea M Corse, Neil C Porter, Kevin M Flanigan, and Robert J Bloch. 2007. 'Abnormal expression of mu-crystallin in facioscapulohumeral muscular dystrophy', *Experimental neurology*, 205: 583-86.

Roche, Joseph A, Diana L Ford-Speelman, Lisa W Ru, Allison L Densmore, Renuka Roche, Patrick W Reed, and Robert J Bloch. 2011. 'Physiological and histological changes in skeletal muscle following in vivo gene transfer by electroporation', *American Journal of Physiology-Cell Physiology*, 301: C1239-C50.

Rodríguez-Rodríguez, Adair, Iván Lazcano, Edith Sánchez-Jaramillo, Rosa María Uribe, Lorraine Jaimes-Hoy, Patricia Joseph-Bravo, and Jean-Louis Charli. 2019. 'Tanycytes and the control of thyrotropin-releasing hormone flux into portal capillaries', *Frontiers in Endocrinology*, 10: 401.

Saetre, Peter, Julia Lindberg, Jennifer A Leonard, Kerstin Olsson, Ulf Pettersson, Hans Ellegren, Tomas F Bergström, Carles Vila, and Elena Jazin. 2004. 'From wild wolf to domestic dog: gene expression changes in the brain', *Molecular brain research*, 126: 198-206.

Samocha, Kaitlin E, Elise B Robinson, Stephan J Sanders, Christine Stevens, Aniko Sabo, Lauren M McGrath, Jack A Kosmicki, Karola Rehnström, Swapan Mallick, and Andrew Kirby. 2014. 'A framework for the interpretation of de novo mutation in human disease', *Nature genetics*, 46: 944-50.

Sánchez, Edith, Rosa María Uribe, Gabriel Corkidi, R Thomas Zoeller, Miguel Cisneros, Magali Zacarias, Claudia Morales-Chapa, Jean-Louis Charli, and Patricia Joseph-Bravo. 2001. 'Differential responses of thyrotropin-releasing hormone (TRH) neurons to cold exposure or suckling indicate functional heterogeneity of the TRH system in the paraventricular nucleus of the rat hypothalamus', *Neuroendocrinology*, 74: 407-22.

Sandler, Ben, Paul Webb, James W Apriletti, B Russell Huber, Marie Togashi, Suzana T Cunha Lima, Sanja Juric, Stefan Nilsson, Richard Wagner, and Robert J Fletterick. 2004. 'Thyroxine-thyroid hormone receptor interactions', *Journal of Biological Chemistry*, 279: 55801-08.

Sap, Jan, Alberto Muñoz, Klaus Damm, Yves Goldberg, Jacques Ghysdael, Achim Leutz, Hartmut Beug, and Björn Vennström. 1986. 'The c-erb-A protein is a high-affinity receptor for thyroid hormone', *nature*, 324: 635-40.

Sapp, Peter C, Betsy A Hosler, Diane McKenna-Yasek, Wendy Chin, Amity Gann, Hilary Genise, Julie Gorenstein, Michael Huang, Wen Sailer, and Meg Scheffler. 2003. 'Identification of two novel loci for dominantly inherited familial amyotrophic lateral sclerosis', *The American Journal of Human Genetics*, 73: 397-403.

Schaefer, Jeremy S, and John R Klein. 2011. 'Immunological regulation of metabolism—a novel quintessential role for the immune system in health and disease', *The FASEB Journal*, 25: 29-34.

Schiaffino, Stefano, and Carlo Reggiani. 2011. 'Fiber types in mammalian skeletal muscles', *Physiological reviews*, 91: 1447-531.

Schimmel, Martin, and Robert D Utiger. 1977. 'Thyroidal and peripheral production of thyroid hormones: review of recent findings and their clinical implications', *Annals of internal medicine*, 87: 760-68.

Schindelin, Johannes, Ignacio Arganda-Carreras, Erwin Frise, Verena Kaynig, Mark Longair, Tobias Pietzsch, Stephan Preibisch, Curtis Rueden, Stephan Saalfeld, and Benjamin Schmid. 2012. 'Fiji: an open-source platform for biological-image analysis', *Nature methods*, 9: 676-82.

Seko, Daiki, Shizuka Ogawa, Tao-Sheng Li, Akihiro Taimura, and Yusuke Ono. 2015. 'μ-Crystallin controls muscle function through thyroid hormone action', *The FASEB Journal*, 30: 1733-40.

Seko, Daiki, Shizuka Ogawa, Tao-Sheng Li, Akihiro Taimura, and Yusuke Ono. 2016. 'μ-Crystallin controls muscle function through thyroid hormone action', *The FASEB Journal*, 30: 1733-40.

Senese, Rosalba, Federica Cioffi, Pieter de Lange, Fernando Goglia, and Antonia Lanni. 2014. 'Thyroid: biological actions of 'nonclassical' thyroid hormones', *J Endocrinol*, 221: R1-12.

Serrano, Marta, Maria Moreno, Francisco José Ortega, Gemma Xifra, Wifredo Ricart, José María Moreno-Navarrete, and José Manuel Fernández-Real. 2014. 'Adipose Tissue μ -Crystallin Is a Thyroid Hormone-Binding Protein Associated With Systemic Insulin Sensitivity', *The Journal of Clinical Endocrinology & Metabolism*, 99: E2259-E68.

Shen, ZP, AA Brayman, L Chen, and CH Miao. 2008. 'Ultrasound with microbubbles enhances gene expression of plasmid DNA in the liver via intraportal delivery', *Gene therapy*, 15: 1147-55.

Sheng, Juan-Juan, and Jian-Ping Jin. 2016. 'TNNI1, TNNI2 and TNNI3: Evolution, regulation, and protein structure–function relationships', *Gene*, 576: 385-94.

Shirley, Jamie L, Ype P de Jong, Cox Terhorst, and Roland W Herzog. 2020. 'Immune responses to viral gene therapy vectors', *Molecular Therapy*, 28: 709-22.

Siler, TM, SSC Yen, W Vale, and R Guillemin. 1974. 'Inhibition by somatostatin on the release of TSH induced in man by thyrotropin-releasing factor', *The Journal of Clinical Endocrinology & Metabolism*, 38: 742-45.

Silva, J Enrique. 2005. 'Thyroid hormone and the energetic cost of keeping body temperature', *Bioscience Reports*, 25: 129-48.

Sivagnanasundaram, Sinthuja, Ben Crossett, Irina Dedova, Stuart Cordwell, and Izuru Matsumoto. 2007. 'Abnormal pathways in the genu of the corpus callosum in schizophrenia pathogenesis: a proteome study', *PROTEOMICS–Clinical Applications*, 1: 1291-305.

Smith, Constance M, Terry F Hayamizu, Jacqueline H Finger, Susan M Bello, Ingeborg J McCright, Jingxia Xu, Richard M Baldarelli, Jonathan S Beal, Jeffrey Campbell, and Lori E Corbani. 2019. 'The mouse gene expression database (GXD): 2019 update', *Nucleic acids research*, 47: D774-D79.

Snyder, Peter J, and Robert D Utiger. 1972. 'Response to thyrotropin releasing hormone (TRH) in normal man', *The Journal of Clinical Endocrinology & Metabolism*, 34: 380-85.

Sotelo-Rivera, Israim, Antonieta Cote-Vélez, Rosa-María Uribe, Jean-Louis Charli, and Patricia Joseph-Bravo. 2017. 'Glucocorticoids curtail stimuli-induced CREB phosphorylation in TRH neurons through interaction of the glucocorticoid receptor with the catalytic subunit of protein kinase A', *Endocrine*, 55: 861-71.

Spangenburg, Espen E, Stephen JP Pratt, Lindsay M Wohlers, and Richard M Lovering. 2011. 'Use of BODIPY (493/503) to visualize intramuscular lipid droplets in skeletal muscle', *Journal of Biomedicine and Biotechnology*, 2011.

Sterling, Kenneth, Gordon A Campbell, and Milton A Brenner. 1984. 'Purification of the mitochondrial triiodothyronine (T3) receptor from rat liver', *European Journal of Endocrinology*, 105: 391-97.

Strack, Rita L, Birka Hein, Dibyendu Bhattacharyya, Stefan W Hell, Robert J Keenan, and Benjamin S Glick. 2009. 'A rapidly maturing far-red derivative of DsRed-Express2 for whole-cell labeling', *Biochemistry*, 48: 8279-81.

Suzuki, Satoru, Nobuyoshi Suzuki, Jun-ichirou Mori, Aki Oshima, Shinichi Usami, and Kiyoshi Hashizume. 2007. ' μ -Crystallin as an intracellular 3, 5, 3'-triiodothyronine holder in vivo', *Molecular endocrinology*, 21: 885-94.

Tagami, Tetsuya, Hiroyuki Yamamoto, Kenji Moriyama, Kuniko Sawai, Takeshi Usui, Akira Shimatsu, and Mitsuhide Naruse. 2010. 'Identification of a novel human thyroid hormone receptor β isoform as a transcriptional modulator', *Biochemical and biophysical research communications*, 396: 983-88.

Tata, Jamshed R. 1958. 'A cellular thyroxine-binding protein fraction', *Biochimica et biophysica acta*, 28: 91-94.

Tawil, Rabi, Silvère M Van Der Maarel, and Stephen J Tapscott. 2014.

'Facioscapulohumeral dystrophy: the path to consensus on pathophysiology', *Skeletal muscle*, 4: 12.

Taylor, Peter N, Diana Albrecht, Anna Scholz, Gala Gutierrez-Buey, John H Lazarus, Colin M Dayan, and Onyebuchi E Okosieme. 2018. 'Global epidemiology of hyperthyroidism and hypothyroidism', *Nature Reviews Endocrinology*, 14: 301.

Taylor, Sean C, Katia Nadeau, Meysam Abbasi, Claude Lachance, Marie Nguyen, and Joshua Fenrich. 2019. 'The ultimate qPCR experiment: producing publication quality, reproducible data the first time', *Trends in biotechnology*, 37: 761-74.

Tennessen, Jacob A, Abigail W Bigham, Timothy D O'Connor, Wenqing Fu, Eimear E Kenny, Simon Gravel, Sean McGee, Ron Do, Xiaoming Liu, and Goo Jun. 2012. 'Evolution and functional impact of rare coding variation from deep sequencing of human exomes', *Science*, 337: 64-69.

Thul, Peter J, Lovisa Åkesson, Mikaela Wiking, Diana Mahdessian, Aikaterini Geladaki, Hammou Ait Blal, Tove Alm, Anna Asplund, Lars Björk, and Lisa M Breckels. 2017. 'A subcellular map of the human proteome', *Science*, 356: eaal3321.

Uhlén, Mathias, Linn Fagerberg, Björn M Hallström, Cecilia Lindskog, Per Oksvold, Adil Mardinoglu, Åsa Sivertsson, Caroline Kampf, Evelina Sjöstedt, and Anna Asplund. 2015. 'Tissue-based map of the human proteome', *Science*, 347: 1260419.

van Mullem, Alies A, Anja LM van Gucht, W Edward Visser, Marcel E Meima, Robin P Peeters, and Theo J Visser. 2016. 'Effects of thyroid hormone transporters MCT8 and MCT10 on nuclear activity of T3', *Molecular and cellular endocrinology*, 437: 252-60.

Vanderplanck, Céline, Eugénie Anseau, Sébastien Charron, Nadia Stricwant, Alexandra Tassin, Dalila Laoudj-Chenivesse, Steve D Wilton, Frédérique Coppée, and Alexandra Belayew. 2011. 'The FSHD atrophic myotube phenotype is caused by DUX4 expression', *PloS one*, 6: e26820.

Velasco, Lara FR, Marie Togashi, Paul G Walfish, Rutinéia P Pessanha, Fanny N Moura, Gustavo B Barra, Phuong Nguyen, Rachelle Rebong, Chaoshen Yuan, and Luiz A Simeoni. 2007. 'Thyroid hormone response element organization dictates the composition of active receptor', *Journal of Biological Chemistry*, 282: 12458-66.

Visser, W Edward, Edith CH Friesema, and Theo J Visser. 2011. 'Minireview: thyroid hormone transporters: the knowns and the unknowns', *Molecular endocrinology*, 25: 1-14.

Visser, W Edward, Wing S Wong, Alies AA Van Mullem, Edith CH Friesema, Joachim Geyer, and Theo J Visser. 2010. 'Study of the transport of thyroid hormone by transporters of the SLC10 family', *Molecular and cellular endocrinology*, 315: 138-45.

Vlangos, Christopher N, Amanda N Siuniak, Dan Robinson, Arul M Chinnaiyan, Robert H Lyons Jr, James D Cavalcoli, and Catherine E Keegan. 2013. 'Next-generation sequencing identifies the Danforth's short tail mouse mutation as a retrotransposon insertion affecting Ptf1a expression', *PLoS Genet*, 9: e1003205.

Walker, Deena M, Xianxiao Zhao, Aarthi Ramakrishnan, Hannah M Cates, Ashley M Cunningham, Catherine Jensen Pena, Rosemary C Bagot, Orna Issler, Yentl Van der Zee, and Andrew P Lipschultz. 2020. 'Adolescent Social Isolation Reprograms the Medial Amygdala: Transcriptome and Sex Differences in Reward', *bioRxiv*.

Watanabe, Yui, and Roy E Weiss. 2018. 'Thyroid hormone action.' in, *Encyclopedia of Endocrine Diseases* (Elsevier).

Weinberger, Cary, Catherine C Thompson, Estelita S Ong, Roger Lebo, Donald J Gruol, and Ronald M Evans. 1986. 'The c-erb-A gene encodes a thyroid hormone receptor', *nature*, 324: 641-46.

Williams, Graham R. 2000. 'Cloning and characterization of two novel thyroid hormone receptor β isoforms', *Molecular and cellular biology*, 20: 8329-42.

- Williams, Graham R, and JH Duncan Bassett. 2011. 'THEMATIC REVIEW Deiodinases: the balance of thyroid hormone Local control of thyroid hormone action: role of type 2 deiodinase', *Journal of endocrinology*, 209: 261-72.
- Wistow, Graeme, and Hyong Kim. 1991. 'Lens protein expression in mammals: taxon-specificity and the recruitment of crystallins', *Journal of molecular evolution*, 32: 262-69.
- Xie, Fuliang, Peng Xiao, Dongliang Chen, Lei Xu, and Baohong Zhang. 2012. 'miRDeepFinder: a miRNA analysis tool for deep sequencing of plant small RNAs', *Plant molecular biology*, 80: 75-84.
- Yarbrough, George G. 1979. 'On the neuropharmacology of thyrotropin releasing hormone (TRH)', *Progress in neurobiology*, 12: 291-312.
- Zaiontz, Charles. 2020. "Real Statistics Resource Pack software (Release 6.8)." In. www.real-statistics.com.
- Zetsche, Bernd, Jonathan S Gootenberg, Omar O Abudayyeh, Ian M Slaymaker, Kira S Makarova, Patrick Essletzbichler, Sara E Volz, Julia Joung, John Van Der Oost, and Aviv Regev. 2015. 'Cpf1 is a single RNA-guided endonuclease of a class 2 CRISPR-Cas system', *Cell*, 163: 759-71.

Zetsche, Bernd, Matthias Heidenreich, Prarthana Mohanraju, Iana Fedorova, Jeroen Kneppers, Ellen M DeGennaro, Nerges Winblad, Sourav R Choudhury, Omar O Abudayyeh, and Jonathan S Gootenberg. 2017. 'Multiplex gene editing by CRISPR–Cpf1 using a single crRNA array', *Nature biotechnology*, 35: 31-34.

Zimmermann, Ralf C, Lois E Krahn, George G Klee, Edward C Ditkoff, Steven J Ory, and Mark V Sauer. 2001. 'Prolonged inhibition of presynaptic catecholamine synthesis with α -methyl-para-tyrosine attenuates the circadian rhythm of human TSH secretion', *Journal of the Society for Gynecologic Investigation*, 8: 174-78.

Comprehensive Bibliography

Abdalla SM, and Bianco AC. Defending plasma T3 is a biological priority. *Clinical endocrinology* 81: 633-641, 2014.

Abe S, Katagiri T, Saito-Hisaminato A, Usami S-i, Inoue Y, Tsunoda T, and Nakamura Y. Identification of CRYM as a candidate responsible for nonsyndromic deafness, through cDNA microarray analysis of human cochlear and vestibular tissues. *The American Journal of Human Genetics* 72: 73-82, 2003.

Aguet F, Van De Ville D, and Unser M. Model-based 2.5-D deconvolution for extended depth of field in brightfield microscopy. *IEEE Transactions on Image Processing* 17: 1144-1153, 2008.

Ahmed JN, Diamand KE, Bellchambers HM, and Arkell RM. Systematized reporter assays reveal ZIC protein regulatory abilities are Subclass-specific and dependent upon transcription factor binding site context. *Scientific reports* 10: 1-14, 2020.

Apriletti JW, Ribeiro RC, Wagner RL, Feng W, Webb P, Kushner PJ, West BL, Nilsson S, Scanlan TS, and Fletterick RJ. Molecular and structural biology of thyroid hormone receptors. *Clinical and Experimental Pharmacology and Physiology* 25: S2-S11, 1998.

Arion D, Unger T, Lewis DA, Levitt P, and Mirnics K. Molecular evidence for increased expression of genes related to immune and chaperone function in the prefrontal cortex in schizophrenia. *Biological psychiatry* 62: 711-721, 2007.

Arlotta P, Molyneaux BJ, Chen J, Inoue J, Kominami R, and Macklis JD. Neuronal subtype-specific genes that control corticospinal motor neuron development in vivo. *Neuron* 45: 207-221, 2005.

Bancroft JD, and Gamble M. *Theory and practice of histological techniques*. Elsevier health sciences, 2008.

Bansal D, Miyake K, Vogel SS, Groh S, Chen C-C, Williamson R, McNeil PL, and Campbell KP. Defective membrane repair in dysferlin-deficient muscular dystrophy. *Nature* 423: 168-172, 2003.

Bashir R, Britton S, Strachan T, Keers S, Vafiadaki E, Lako M, Richard I, Marchand S, Bourg N, and Argov Z. A gene related to *Caenorhabditis elegans* spermatogenesis factor *fer-1* is mutated in limb-girdle muscular dystrophy type 2B. *Nature genetics* 20: 37-42, 1998.

Beasley CL, Pennington K, Behan A, Wait R, Dunn MJ, and Cotter D. Proteomic analysis of the anterior cingulate cortex in the major psychiatric disorders: evidence for disease-associated changes. *Proteomics* 6: 3414-3425, 2006.

- Beckett GJ, and Arthur JR. 3 The iodothyronine deiodinases and 5'-deiodination. *Baillière's clinical endocrinology and metabolism* 8: 285-304, 1994.
- Bello F, and Bakari A. Hypothyroidism in adults: A review and recent advances in management. *J Diabetes Endocrinol* 3: 57-69, 2012.
- Beslin A, Vié M-P, Blondeau J-P, and Francon J. Identification by photoaffinity labelling of a pyridine nucleotide-dependent tri-iodothyronine-binding protein in the cytosol of cultured astroglial cells. *Biochemical Journal* 305: 729-737, 1995.
- Béziat V, Li J, Lin J-X, Ma CS, Li P, Bousfiha A, Pellier I, Zoghi S, Baris S, and Keles S. A recessive form of hyper-IgE syndrome by disruption of ZNF341-dependent STAT3 transcription and activity. *Science immunology* 3: 2018.
- Bianco AC, and Kim BW. Deiodinases: implications of the local control of thyroid hormone action. *The Journal of clinical investigation* 116: 2571-2579, 2006.
- Bishopric NH, and Kedes L. Adrenergic regulation of the skeletal alpha-actin gene promoter during myocardial cell hypertrophy. *Proceedings of the National Academy of Sciences* 88: 2132-2136, 1991.
- Bittel DC, Chandra G, Tirunagri L, Deora AB, Medikayala S, Scheffer L, Defour A, and Jaiswal JK. Annexin A2 mediates dysferlin accumulation and muscle cell membrane repair. *Cells* 9: 1919, 2020.

Borel F, Hachi I, Palencia A, Gaillard MC, and Ferrer JL. Crystal structure of mouse mu-crystallin complexed with NADPH and the T3 thyroid hormone. *The FEBS journal* 281: 1598-1612, 2014.

Brent GA. Mechanisms of thyroid hormone action. *The Journal of clinical investigation* 122: 3035-3043, 2012.

Briguet A, Courdier-Fruh I, Foster M, Meier T, and Magyar JP. Histological parameters for the quantitative assessment of muscular dystrophy in the mdx-mouse. *Neuromuscular disorders* 14: 675-682, 2004.

Brochier C, Gaillard M-C, Diguët E, Caudy N, Dossat C, Ségurens B, Wincker P, Roze E, Caboche J, and Hantraye P. Quantitative gene expression profiling of mouse brain regions reveals differential transcripts conserved in human and affected in disease models. *Physiological genomics* 33: 170-179, 2008.

Brooke MH, and Kaiser KK. Three "myosin adenosine triphosphatase" systems: the nature of their pH lability and sulfhydryl dependence. *Journal of Histochemistry & Cytochemistry* 18: 670-672, 1970.

Burke CW, Suk JS, Kim AJ, Hsiang Y-HJ, Klibanov AL, Hanes J, and Price RJ. Markedly enhanced skeletal muscle transfection achieved by the ultrasound-targeted delivery of non-viral gene nanocarriers with microbubbles. *Journal of controlled release* 162: 414-421, 2012.

Burks TN, Andres-Mateos E, Marx R, Mejias R, Van Erp C, Simmers JL, Walston JD, Ward CW, and Cohn RD. Losartan restores skeletal muscle remodeling and protects against disuse atrophy in sarcopenia. *Science translational medicine* 3: 82ra37-82ra37, 2011.

Capecchi MR. High efficiency transformation by direct microinjection of DNA into cultured mammalian cells. *Cell* 22: 479-488, 1980.

Casas F, Busson M, Grandemange S, Seyer P, Carazo A, Pessemesse L, Wrutniak-Cabello C, and Cabello G. Characterization of a novel thyroid hormone receptor α variant involved in the regulation of myoblast differentiation. *Molecular endocrinology* 20: 749-763, 2006.

Casas F, Rochard P, Rodier A, Cassar-Malek I, Marchal-Victorion S, Wiesner RJ, Cabello G, and Wrutniak C. A variant form of the nuclear triiodothyronine receptor c-ErbA α 1 plays a direct role in regulation of mitochondrial RNA synthesis. *Molecular and cellular biology* 19: 7913-7924, 1999.

Chassande O, Fraichard A, Gauthier K, Flamant Fdr, Legrand C, Savatier P, Laudet V, and Samarut J. Identification of transcripts initiated from an internal promoter in the c-erbA α locus that encode inhibitors of retinoic acid receptor- α and triiodothyronine receptor activities. *Molecular Endocrinology* 11: 1278-1290, 1997.

Chen X, McClusky R, Chen J, Beaven SW, Tontonoz P, Arnold AP, and Reue K. The number of x chromosomes causes sex differences in adiposity in mice. *PLoS Genet* 8: e1002709, 2012.

Chong WK, Papadopoulou V, and Dayton PA. Imaging with ultrasound contrast agents: current status and future. *Abdominal Radiology* 43: 762-772, 2018.

Chopra IJ. A study of extrathyroidal conversion of thyroxine (T4) to 3, 3', 5-triiodothyronine (T3) in vitro. *Endocrinology* 101: 453-463, 1977.

Ciciliot S, Rossi AC, Dyar KA, Blaauw B, and Schiaffino S. Muscle type and fiber type specificity in muscle wasting. *The international journal of biochemistry & cell biology* 45: 2191-2199, 2013.

Clément K, Viguier N, Diehn M, Alizadeh A, Barbe P, Thalamas C, Storey JD, Brown PO, Barsh GS, and Langin D. In vivo regulation of human skeletal muscle gene expression by thyroid hormone. *Genome research* 12: 281-291, 2002.

Close R. Force: velocity properties of mouse muscles. *Nature* 206: 718-719, 1965.

Collie E, and Muscat GE. The human skeletal alpha-actin promoter is regulated by thyroid hormone: identification of a thyroid hormone response element. *Cell growth & differentiation: the molecular biology journal of the American Association for Cancer Research* 3: 31-42, 1992.

Daoud H, Valdmanis PN, Gros-Louis F, Belzil V, Spiegelman D, Henrion E, Diallo O, Desjarlais A, Gauthier J, and Camu W. Resequencing of 29 candidate genes in patients with familial and sporadic amyotrophic lateral sclerosis. *Archives of neurology* 68: 587-593, 2011.

Dème D, Fimiani E, Pommier J, and Nunez J. Free diiodotyrosine effects on protein iodination and thyroid hormone synthesis catalyzed by thyroid peroxidase. *European journal of biochemistry* 51: 329-336, 1975.

DiFranco M, Tran P, Quinonez M, and Vergara JL. Functional expression of transgenic α 1sDHPR channels in adult mammalian skeletal muscle fibres. *The Journal of physiology* 589: 1421-1442, 2011.

Dixit M, Anseau E, Tassin A, Winokur S, Shi R, Qian H, Sauvage S, Mattéotti C, van Acker AM, and Leo O. DUX4, a candidate gene of facioscapulohumeral muscular dystrophy, encodes a transcriptional activator of PITX1. *Proceedings of the National Academy of Sciences* 104: 18157-18162, 2007.

Dorfer V, Pichler P, Stranzl T, Stadlmann J, Taus T, Winkler S, and Mechtler K. MS Amanda, a universal identification algorithm optimized for high accuracy tandem mass spectra. *Journal of proteome research* 13: 3679-3684, 2014.

Drexler HC, Ruhs A, Konzer A, Mendler L, Bruckskotten M, Looso M, Günther S, Boettger T, Krüger M, and Braun T. On marathons and Sprints: an integrated

quantitative proteomics and transcriptomics analysis of differences between slow and fast muscle fibers. *Molecular & Cellular Proteomics* 11: M111. 010801, 2012.

Dubowitz V, Sewry CA, and Oldfors A. *Muscle biopsy: a practical approach: expert consult; online and print*. Elsevier Health Sciences, 2013.

Ducros G, and Trippenbach T. Respiratory effects of lactic acid injected into the jugular vein of newborn rabbits. *Pediatric research* 29: 548-552, 1991.

Ebashi S, Endo M, and Ohtsuki I. Control of muscle contraction. *Quarterly reviews of biophysics* 2: 351-384, 1969.

Eckey M, Moehren U, and Baniahmad A. Gene silencing by the thyroid hormone receptor. *Molecular and cellular endocrinology* 213: 13-22, 2003.

Encarnacion-Rivera L, Foltz S, Hartzell HC, and Choo H. Myosoft: An automated muscle histology analysis tool using machine learning algorithm utilizing FIJI/ImageJ software. *PloS one* 15: e0229041, 2020.

Eng JK, Fischer B, Grossmann J, and MacCoss MJ. A fast SEQUEST cross correlation algorithm. *Journal of proteome research* 7: 4598-4602, 2008.

Fan Z, Kumon RE, and Deng CX. Mechanisms of microbubble-facilitated sonoporation for drug and gene delivery. *Therapeutic delivery* 5: 467-486, 2014.

Fechheimer M, Boylan JF, Parker S, Sisken JE, Patel GL, and Zimmer SG.

Transfection of mammalian cells with plasmid DNA by scrape loading and sonication loading. *Proceedings of the National Academy of Sciences* 84: 8463-8467, 1987.

Fechheimer M, Denny C, Murphy R, and Taylor D. Measurement of cytoplasmic pH in *Dictyostelium discoideum* by using a new method for introducing macromolecules into living cells. *European journal of cell biology* 40: 242-247, 1986.

Fekete C, and Lechan RM. Negative feedback regulation of hypophysiotropic thyrotropin-releasing hormone (TRH) synthesizing neurons: role of neuronal afferents and type 2 deiodinase. *Frontiers in neuroendocrinology* 28: 97-114, 2007.

Fekete C, Kelly J, Mihály E, Sarkar S, Rand WM, Légrádi Gb, Emerson CH, and Lechan RM. Neuropeptide Y has a central inhibitory action on the hypothalamic-pituitary-thyroid axis. *Endocrinology* 142: 2606-2613, 2001.

Fekete C, Mihály E, Luo L-G, Kelly J, Clausen JT, Mao Q, Rand WM, Moss LG, Kuhar M, and Emerson CH. Association of cocaine-and amphetamine-regulated transcript-immunoreactive elements with thyrotropin-releasing hormone-synthesizing neurons in the hypothalamic paraventricular nucleus and its role in the regulation of the hypothalamic–pituitary–thyroid axis during fasting. *Journal of Neuroscience* 20: 9224-9234, 2000.

Fekete C, Sarkar S, Rand WM, Harney JW, Emerson CH, Bianco AC, and Lechan RM. Agouti-related protein (AGRP) has a central inhibitory action on the hypothalamic-

pituitary-thyroid (HPT) axis; comparisons between the effect of AGRP and neuropeptide Y on energy homeostasis and the HPT axis. *Endocrinology* 143: 3846-3853, 2002.

Figueroa-Romero C, Hur J, Lunn JS, Paez-Colasante X, Bender DE, Yung R, Sakowski SA, and Feldman EL. Expression of microRNAs in human post-mortem amyotrophic lateral sclerosis spinal cords provides insight into disease mechanisms. *Molecular and Cellular Neuroscience* 71: 34-45, 2016.

Fink KL, Strittmatter SM, and Cafferty WB. Comprehensive corticospinal labeling with mu-crystallin transgene reveals axon regeneration after spinal cord trauma in *ngr1*^{-/-} mice. *Journal of Neuroscience* 35: 15403-15418, 2015.

Fitts RH, Brimmer CJ, Troup JP, and Unsworth BR. Contractile and fatigue properties of thyrotoxic rat skeletal muscle. *Muscle & Nerve: Official Journal of the American Association of Electrodiagnostic Medicine* 7: 470-477, 1984.

Fonfara I, Richter H, Bratovič M, Le Rhun A, and Charpentier E. The CRISPR-associated DNA-cleaving enzyme Cpf1 also processes precursor CRISPR RNA. *Nature* 532: 517-521, 2016.

Fornes O, Castro-Mondragon JA, Khan A, Van der Lee R, Zhang X, Richmond PA, Modi BP, Correard S, Gheorghe M, and Baranašić D. JASPAR 2020: update of the open-access database of transcription factor binding profiles. *Nucleic acids research* 48: D87-D92, 2020.

Francelle L, Galvan L, Gaillard M-C, Guillermier M, Houitte D, Bonvento G, Petit F, Jan C, Dufour N, and Hantraye P. Loss of the thyroid hormone-binding protein Crym renders striatal neurons more vulnerable to mutant huntingtin in Huntington's disease. *Human molecular genetics* 24: 1563-1573, 2015.

Freake HC, and Oppenheimer JH. Thermogenesis and thyroid function. *Annual review of nutrition* 15: 263-291, 1995.

Frey-Jakobs S, Hartberger JM, Fliegau M, Bossen C, Wehmeyer ML, Neubauer JC, Bulashevskaya A, Proietti M, Fröbel P, and Nöltner C. ZNF341 controls STAT3 expression and thereby immunocompetence. *Science immunology* 3: 2018.

Friesema EC, Docter R, Moerings EP, Stieger B, Hagenbuch B, Meier PJ, Krenning EP, Hennemann G, and Visser TJ. Identification of thyroid hormone transporters. *Biochemical and biophysical research communications* 254: 497-501, 1999.

Friesema EC, Jansen J, Jachtenberg J-w, Visser WE, Kester MH, and Visser TJ. Effective cellular uptake and efflux of thyroid hormone by human monocarboxylate transporter 10. *Molecular endocrinology* 22: 1357-1369, 2008.

Fukada Y, Yasui K, Kitayama M, Doi K, Nakano T, Watanabe Y, and Nakashima K. Gene expression analysis of the murine model of amyotrophic lateral sclerosis: studies of the Leu126delTT mutation in SOD1. *Brain research* 1160: 1-10, 2007.

Gagne R, Green JR, Dong H, Wade MG, and Yauk CL. Identification of thyroid hormone receptor binding sites in developing mouse cerebellum. *BMC genomics* 14: 341, 2013.

Gallagher DT, Monbouquette H, Schröder I, Robinson H, Holden MJ, and Smith N. Structure of alanine dehydrogenase from *Archaeoglobus*: active site analysis and relation to bacterial cyclodeaminases and mammalian mu crystallin. *Journal of molecular biology* 342: 119-130, 2004.

Gardiner-Garden M, and Frommer M. CpG islands in vertebrate genomes. *Journal of molecular biology* 196: 261-282, 1987.

Giger JM, Bodell PW, Zeng M, Baldwin KM, and Haddad F. Rapid muscle atrophy response to unloading: pretranslational processes involving MHC and actin. *Journal of Applied Physiology* 107: 1204-1212, 2009.

Graupner G, Wills KN, Tzukerman M, Zhang X-k, and Pfahl M. Dual regulatory role for thyroid-hormone receptors allows control of retinoic-acid receptor activity. *Nature* 340: 653-656, 1989.

Gunning P, Ponte P, Blau H, and Kedes L. alpha-skeletal and alpha-cardiac actin genes are coexpressed in adult human skeletal muscle and heart. *Molecular and cellular biology* 3: 1985-1995, 1983.

Gustafson TA, Markham BE, and Morkin E. Effects of thyroid hormone on alpha-actin and myosin heavy chain gene expression in cardiac and skeletal muscles of the rat:

measurement of mRNA content using synthetic oligonucleotide probes. *Circulation research* 59: 194-201, 1986.

Hakak Y, Walker JR, Li C, Wong WH, Davis KL, Buxbaum JD, Haroutunian V, and Fienberg AA. Genome-wide expression analysis reveals dysregulation of myelination-related genes in chronic schizophrenia. *Proceedings of the National Academy of Sciences* 98: 4746-4751, 2001.

Hallen A, and Cooper AJ. Reciprocal control of thyroid binding and the pipecolate pathway in the brain. *Neurochemical research* 42: 217-243, 2017.

Hallen A, Cooper AJ, Jamie JF, and Karuso P. Insights into enzyme catalysis and thyroid hormone regulation of cerebral ketimine reductase/ μ -crystallin under physiological conditions. *Neurochemical research* 40: 1252-1266, 2015.

Hallen A, Cooper AJ, Jamie JF, Haynes PA, and Willows RD. Mammalian forebrain ketimine reductase identified as μ -crystallin; potential regulation by thyroid hormones. *Journal of neurochemistry* 118: 379-387, 2011.

Hallen A, Cooper AJ, Smith JR, Jamie JF, and Karuso P. Ketimine reductase/CRYM catalyzes reductive alkylamination of α -keto acids, confirming its function as an imine reductase. *Amino acids* 47: 2457-2461, 2015.

Harris M, Aschkenasi C, Elias CF, Chandrankunnel A, Nillni EA, Bjørnbæk C, Elmquist JK, Flier JS, and Hollenberg AN. Transcriptional regulation of the

thyrotropin-releasing hormone gene by leptin and melanocortin signaling. *The Journal of clinical investigation* 107: 111-120, 2001.

Hashizume K, Kobayashi M, and Miyamoto T. Active and inactive forms of 3, 5, 3'-triiodo-L-thyronine (T3)-binding protein in rat kidney cytosol: possible role of nicotinamide adenine dinucleotide phosphate in activation of T3 binding. *Endocrinology* 119: 710-719, 1986.

Hashizume K, Miyamoto T, Ichikawa K, Yamauchi K, Kobayashi M, Sakurai A, Ohtsuka H, Nishii Y, and Yamada T. Purification and characterization of NADPH-dependent cytosolic 3, 5, 3'-triiodo-L-thyronine binding protein in rat kidney. *Journal of Biological Chemistry* 264: 4857-4863, 1989.

Hashizume K, Miyamoto T, Ichikawa K, Yamauchi K, Sakurai A, Ohtsuka H, Kobayashi M, Nishii Y, and Yamada T. Evidence for the presence of two active forms of cytosolic 3, 5, 3'-triiodo-L-thyronine (T3)-binding protein (CTBP) in rat kidney. Specialized functions of two CTBPs in intracellular T3 translocation. *Journal of Biological Chemistry* 264: 4864-4871, 1989.

Hashizume K, Miyamoto T, Kobayashi M, Suzuki S, Ichikawa K, Yamauchi K, Ohtsuka H, and Takeda T. Cytosolic 3, 5, 3'-triiodo-L-thyronine (T3)-binding protein (CTBP) regulation of nuclear T3 binding: evidence for the presence of T3-CTBP complex-binding sites in nuclei. *Endocrinology* 124: 2851-2856, 1989.

Hashizume K, Miyamoto T, Yamauchi K, Ichikawa K, Kobayashi M, Ohtsuka H, Sakurai A, Suzuki S, and Yamada T. Counterregulation of nuclear 3, 5, 3'-triiodo-L-thyronine (T3) binding by oxidized and reduced-nicotinamide adenine dinucleotide phosphates in the presence of cytosolic T3-binding protein in vitro. *Endocrinology* 124: 1678-1683, 1989.

Hernot S, and Klibanov AL. Microbubbles in ultrasound-triggered drug and gene delivery. *Advanced drug delivery reviews* 60: 1153-1166, 2008.

Heuer H, Schäfer MKH, O'Donnell D, Walker P, and Bauer K. Expression of thyrotropin-releasing hormone receptor 2 (TRH-R2) in the central nervous system of rats. *Journal of Comparative Neurology* 428: 319-336, 2000.

Hinaux H, Blin M, Fumey J, Legendre L, Heuze A, Casane D, and Retaux S. Lens defects in *A styanax mexicanus* Cavefish: Evolution of crystallins and a role for alphaA-crystallin. *Developmental neurobiology* 75: 505-521, 2015.

Ho M, Post CM, Donahue LR, Lidov HG, Bronson RT, Goolsby H, Watkins SC, Cox GA, and Brown Jr RH. Disruption of muscle membrane and phenotype divergence in two novel mouse models of dysferlin deficiency. *Human molecular genetics* 13: 1999-2010, 2004.

Hodges A, Strand AD, Aragaki AK, Kuhn A, Sengstag T, Hughes G, Elliston LA, Hartog C, Goldstein DR, and Thu D. Regional and cellular gene expression changes in human Huntington's disease brain. *Human molecular genetics* 15: 965-977, 2006.

Hodin RA, Lazar MA, Wintman BI, Darling DS, Koenig RJ, Larsen PR, Moore DD, and Chin WW. Identification of a thyroid hormone receptor that is pituitary-specific. *Science* 244: 76-79, 1989.

Hollowell JG, Staehling NW, Flanders WD, Hannon WH, Gunter EW, Spencer CA, and Braverman LE. Serum TSH, T4, and thyroid antibodies in the United States population (1988 to 1994): National Health and Nutrition Examination Survey (NHANES III). *The Journal of Clinical Endocrinology & Metabolism* 87: 489-499, 2002.

Homma S, Chen JC, Rahimov F, Beermann ML, Hanger K, Bibat GM, Wagner KR, Kunkel LM, Emerson Jr CP, and Miller JB. A unique library of myogenic cells from facioscapulohumeral muscular dystrophy subjects and unaffected relatives: family, disease and cell function. *European Journal of Human Genetics* 20: 404-410, 2012.

Hommyo R, Suzuki SO, Abolhassani N, Hamasaki H, Shijo M, Maeda N, Honda H, Nakabeppu Y, and Iwaki T. Expression of CRYM in different rat organs during development and its decreased expression in degenerating pyramidal tracts in amyotrophic lateral sclerosis. *Neuropathology* 38: 247-259, 2018.

Illa I, Serrano-Munuera C, Gallardo E, Lasa A, Rojas-García R, Palmer J, Gallano P, Baiget M, Matsuda C, and Brown RH. Distal anterior compartment myopathy: a dysferlin mutation causing a new muscular dystrophy phenotype. *Annals of Neurology*:

Official Journal of the American Neurological Association and the Child Neurology Society 49: 130-134, 2001.

Imai H, Ohta K, Yoshida A, Suzuki S, Hashizume K, Usami S, and Kikuchi T. μ -crystallin, new candidate protein in endotoxin-induced uveitis. *Investigative ophthalmology & visual science* 51: 3554-3559, 2010.

Jansen J, Friesema EC, Milici C, and Visser TJ. Thyroid hormone transporters in health and disease. *Thyroid* 15: 757-768, 2005.

Jhanwar SC, Chaganti R, and Croce CM. Germ-line chromosomal localization of humanc-erb-A oncogene. *Somatic cell and molecular genetics* 11: 99-102, 1985.

Johansson C, Lunde PK, Göthe S, Lännergren J, and Westerblad H. Isometric force and endurance in skeletal muscle of mice devoid of all known thyroid hormone receptors. *The Journal of physiology* 547: 789-796, 2003.

Johnston SA, and Tang D-C. The use of microparticle injection to introduce genes into animal cells in vitro and in vivo. *Genetic engineering* 225-236, 1993.

Johnston-Wilson N, Sims C, Hofmann J, Anderson L, Shore A, Torrey E, and Yolken RH. Disease-specific alterations in frontal cortex brain proteins in schizophrenia, bipolar disorder, and major depressive disorder. *Molecular psychiatry* 5: 142-149, 2000.

Joshi SS, Sethi M, Striz M, Cole N, Denegre JM, Ryan J, Lhamon ME, Agarwal A, Murray S, and Braun RE. Noninvasive sleep monitoring in large-scale screening of knock-out mice reveals novel sleep-related genes. *bioRxiv* 517680, 2019.

Kalmar B, Blanco G, and Greensmith L. Determination of muscle fiber type in rodents. *Current protocols in mouse biology* 2: 231-243, 2012.

Kalyanaraman H, Schwappacher R, Joshua J, Zhuang S, Scott BT, Klos M, Casteel DE, Frangos JA, Dillmann W, and Boss GR. Nongenomic thyroid hormone signaling occurs through a plasma membrane-localized receptor. *Science signaling* 7: ra48-ra48, 2014.

Kammoun M, Cassar-Malek I, Meunier B, and Picard B. A simplified immunohistochemical classification of skeletal muscle fibres in mouse. *European journal of histochemistry: EJH* 58: 2014.

Keown WA, Campbell CR, and Kucherlapati RS. Methods for introducing DNA into mammalian cells. *Methods in enzymology* 185: 527-537, 1990.

Kerr JP, Ward CW, and Bloch RJ. Dysferlin at transverse tubules regulates Ca²⁺ homeostasis in skeletal muscle. *Frontiers in physiology* 5: 89, 2014.

Kerr JP, Ziman AP, Mueller AL, Muriel JM, Kleinhans-Welte E, Gumerson JD, Vogel SS, Ward CW, Roche JA, and Bloch RJ. Dysferlin stabilizes stress-induced Ca²⁺ signaling in the transverse tubule membrane. *Proceedings of the National Academy of Sciences* 110: 20831-20836, 2013.

Kim D, Chen R, Sheu M, Kim N, Kim S, Islam N, Wier EM, Wang G, Li A, and Park A. Noncoding dsRNA induces retinoic acid synthesis to stimulate hair follicle regeneration via TLR3. *Nature Communications* 10: 2811, 2019.

Kim RY, Gasser R, and Wistow GJ. mu-crystallin is a mammalian homologue of *Agrobacterium* ornithine cyclodeaminase and is expressed in human retina. *Proceedings of the National Academy of Sciences* 89: 9292-9296, 1992.

Kinney CJ, and Bloch RJ. μ -Crystallin: A Thyroid Hormone Binding Protein. *Endocrine Regulations* 2021.

Kinney CJ, O'Neill A, Noland K, Huang W, Muriel JM, Lukyanenko V, Kane MA, Ward CW, Collier AF, Roche JA, McLenithan JC, Reed PW, and Bloch RJ. μ -Crystallin in Mouse Skeletal Muscle Promotes a Shift from Glycolytic toward Oxidative Metabolism. *Current Research in Physiology* 2020.

Klooster R, Straasheijm K, Shah B, Sowden J, Frants R, Thornton C, Tawil R, and Van Der Maarel S. Comprehensive expression analysis of FSHD candidate genes at the mRNA and protein level. *European Journal of Human Genetics* 17: 1615, 2009.

Kobayashi M, Hashizume K, Suzuki S, Ichikawa K, and Takeda T. A Novel NADPH-Dependent Cytosolic 3, 5, 3'-Triiodo-LThyronine-Binding Protein (CTBP; 5. IS) in Rat Liver: A Comparison with 4.7 S NADPH-Dependent CTBP. *Endocrinology* 129: 1701-1708, 1991.

Kubota K, Uchimura H, Mitsuhashi T, Chiu SC, Kuzuya N, and Nagataki S. Effects of intrathyroidal metabolism of thyroxine on thyroid hormone secretion: increased degradation of thyroxine in mouse thyroids stimulated chronically with thyrotrophin. *European Journal of Endocrinology* 105: 57-65, 1984.

Laemmli UK. Cleavage of structural proteins during the assembly of the head of bacteriophage T4. *Nature* 227: 680-685, 1970.

Larsen PR, Silva JE, and Kaplan MM. Relationships between circulating and intracellular thyroid hormones: physiological and clinical implications. *Endocrine Reviews* 2: 87-102, 1981.

Lassche S, Stienen GJ, Irving TC, Van Der Maarel SM, Voermans NC, Padberg GW, Granzier H, van Engelen BG, and Ottenheijm CA. Sarcomeric dysfunction contributes to muscle weakness in facioscapulohumeral muscular dystrophy. *Neurology* 80: 733-737, 2013.

Latchman DS. Gene delivery and gene therapy with herpes simplex virus-based vectors. *Gene* 264: 1-9, 2001.

Légrádi Gb, Emerson CH, Ahima RS, Flier JS, and Lechan RM. Leptin prevents fasting-induced suppression of prothyrotropin-releasing hormone messenger ribonucleic acid in neurons of the hypothalamic paraventricular nucleus. *Endocrinology* 138: 2569-2576, 1997.

Lein ES, Hawrylycz MJ, Ao N, Ayres M, Bensinger A, Bernard A, Boe AF, Boguski MS, Brockway KS, and Byrnes EJ. Genome-wide atlas of gene expression in the adult mouse brain. *Nature* 445: 168-176, 2007.

Liu J, Aoki M, Illa I, Wu C, Fardeau M, Angelini C, Serrano C, Urtizberea JA, Hentati F, and Hamida MB. Dysferlin, a novel skeletal muscle gene, is mutated in Miyoshi myopathy and limb girdle muscular dystrophy. *Nature genetics* 20: 31-36, 1998.

Liu X, Wei S, Deng S, Li D, Liu K, Shan B, Shao Y, Wei W, Chen J, and Zhang L. Genome-wide identification and comparison of mRNA s, lnc RNA s and circ RNA s in porcine intramuscular, subcutaneous, retroperitoneal and mesenteric adipose tissues. *Animal genetics* 50: 228-241, 2019.

Liu Y-Y, Milanesi A, and Brent GA. Thyroid Hormones. In: *Hormonal Signaling in Biology and Medicine* Elsevier, 2020, p. 487-506.

Lonsdale J, Thomas J, Salvatore M, Phillips R, Lo E, Shad S, Hasz R, Walters G, Garcia F, and Young N. The genotype-tissue expression (GTEx) project. *Nature genetics* 45: 580-585, 2013.

Luff A. Dynamic properties of the inferior rectus, extensor digitorum longus, diaphragm and soleus muscles of the mouse. *The Journal of Physiology* 313: 161-171, 1981.

Lukyanenko V, Muriel JM, and Bloch RJ. Coupling of excitation to Ca²⁺ release is modulated by dysferlin. *The Journal of Physiology* 595: 5191-5207, 2017.

Lusk G. Animal calorimetry twenty-fourth paper. Analysis of the oxidation of mixtures of carbohydrate and fat. *Journal of Biological Chemistry* 59: 41-42, 1924.

Maksakova IA, and Mager DL. Transcriptional regulation of early transposon elements, an active family of mouse long terminal repeat retrotransposons. *Journal of virology* 79: 13865-13874, 2005.

Mansourian AR. A review on hyperthyroidism: thyrotoxicosis under surveillance. *Pakistan Journal of Biological Sciences* 13: 1066, 2010.

Martins-de-Souza D, Gattaz WF, Schmitt A, Maccarrone G, Hunyadi-Gulyás E, Eberlin MN, Souza GH, Marangoni S, Novello JC, and Turck CW. Proteomic analysis of dorsolateral prefrontal cortex indicates the involvement of cytoskeleton, oligodendrocyte, energy metabolism and new potential markers in schizophrenia. *Journal of psychiatric research* 43: 978-986, 2009.

Martins-de-Souza D, Gattaz WF, Schmitt A, Rewerts C, Maccarrone G, Dias-Neto E, and Turck CW. Prefrontal cortex shotgun proteome analysis reveals altered calcium homeostasis and immune system imbalance in schizophrenia. *European archives of psychiatry and clinical neuroscience* 259: 151-163, 2009.

Martins-de-Souza D, Maccarrone G, Wobrock T, Zerr I, Gormanns P, Reckow S, Falkai P, Schmitt A, and Turck CW. Proteome analysis of the thalamus and

cerebrospinal fluid reveals glycolysis dysfunction and potential biomarkers candidates for schizophrenia. *Journal of psychiatric research* 44: 1176-1189, 2010.

Mendoza A, and Hollenberg AN. New insights into thyroid hormone action. *Pharmacology & therapeutics* 173: 135-145, 2017.

Mengeling BJ, Pan F, and Privalsky ML. Novel mode of deoxyribonucleic acid recognition by thyroid hormone receptors: Thyroid hormone receptor β -isoforms can bind as trimers to natural response elements comprised of reiterated half-sites. *Molecular Endocrinology* 19: 35-51, 2005.

Middleton FA, Mirnics K, Pierri JN, Lewis DA, and Levitt P. Gene expression profiling reveals alterations of specific metabolic pathways in schizophrenia. *Journal of Neuroscience* 22: 2718-2729, 2002.

Miga KH, Eisenhart C, and Kent WJ. Utilizing mapping targets of sequences underrepresented in the reference assembly to reduce false positive alignments. *Nucleic acids research* 43: e133-e133, 2015.

Mihály E, Fekete C, Tatro JB, Liposits Z, Stopa EG, and Lechan RM. Hypophysiotropic thyrotropin-releasing hormone-synthesizing neurons in the human hypothalamus are innervated by neuropeptide Y, agouti-related protein, and α -melanocyte-stimulating hormone. *The Journal of Clinical Endocrinology & Metabolism* 85: 2596-2603, 2000.

- Miklos GLG, and Maleszka R. Microarray reality checks in the context of a complex disease. *Nature biotechnology* 22: 615-621, 2004.
- Miller DL, Pislaru SV, and Greenleaf JF. Sonoporation: mechanical DNA delivery by ultrasonic cavitation. *Somatic cell and molecular genetics* 27: 115-134, 2002.
- Mitchell A, Tom M, and Mortimer R. Thyroid hormone export from cells: contribution of P-glycoprotein. *Journal of endocrinology* 185: 93-98, 2005.
- Mori J-i, Suzuki S, Kobayashi M, Inagaki T, Komatsu A, Takeda T, Miyamoto T, Ichikawa K, and Hashizume K. Nicotinamide adenine dinucleotide phosphate-dependent cytosolic T3 binding protein as a regulator for T3-mediated transactivation. *Endocrinology* 143: 1538-1544, 2002.
- Morley JE. Extrahypothalamic thyrotropin releasing hormone (TRH)—its distribution and its functions. *Life sciences* 25: 1539-1550, 1979.
- Motulsky HJ, and Brown RE. Detecting outliers when fitting data with nonlinear regression—a new method based on robust nonlinear regression and the false discovery rate. *BMC bioinformatics* 7: 123, 2006.
- Mukai M, Replogle K, Drnevich J, Wang G, Wacker D, Band M, Clayton DF, and Wingfield JC. Seasonal differences of gene expression profiles in song sparrow (*Melospiza melodia*) hypothalamus in relation to territorial aggression. *PloS one* 4: 2009.

O'shea P, and Williams G. Insight into the physiological actions of thyroid hormone receptors from genetically modified mice. *The Journal of endocrinology* 175: 553, 2002.

Ohkubo Y, Sekido T, Nishio S-i, Sekido K, Kitahara J, Suzuki S, and Komatsu M. Loss of μ -crystallin causes PPAR γ activation and obesity in high-fat diet-fed mice. *Biochemical and biophysical research communications* 508: 914-920, 2019.

Ojha A, and Watve M. Blind fish: An eye opener. *Evolution, Medicine, and Public Health* 2018: 186-189, 2018.

Olojo RO, Ziman AP, Hernández-Ochoa EO, Allen PD, Schneider MF, and Ward CW. Mice null for calsequestrin 1 exhibit deficits in functional performance and sarcoplasmic reticulum calcium handling. *PLoS One* 6: e27036, 2011.

Oshima A, Suzuki S, Takumi Y, Hashizume K, Abe S, and Usami S. CRYM mutations cause deafness through thyroid hormone binding properties in the fibrocytes of the cochlea. *Journal of medical genetics* 43: e25-e25, 2006.

Pantos C, and Mourouzis I. Thyroid hormone receptor α 1 as a novel therapeutic target for tissue repair. *Annals of translational medicine* 6: 2018.

Pensato V, Magri S, Bella ED, Tannorella P, Bersano E, Sorarù G, Gatti M, Ticozzi N, Taroni F, and Lauria G. Sorting rare ALS genetic variants by targeted re-sequencing panel in Italian patients: OPTN, VCP, and SQSTM1 variants account for 3% of rare genetic forms. *Journal of clinical medicine* 9: 412, 2020.

Pette D, and Staron RS. Mammalian skeletal muscle fiber type transitions. In: *International Review of Cytology* Elsevier, 1997, p. 143-223.

Phan L, Jin Y, Zhang H, Qiang W, Shekhtman E, Shao D, Revoe D, Villamarin R, Ivanchenko E, and Kimura M. ALFA: Allele Frequency Aggregator. *National Center for Biotechnology Information, US National Library of Medicine Available online: www.ncbi.nlm.nih.gov/snp/docs/gsr/alfa/(accessed on 10 March 2020) 2020.*

Pihlajamäki J, Boes T, Kim E-Y, Dearie F, Kim BW, Schroeder J, Mun E, Nasser I, Park PJ, and Bianco AC. Thyroid hormone-related regulation of gene expression in human fatty liver. *The Journal of Clinical Endocrinology & Metabolism* 94: 3521-3529, 2009.

Pirahanchi Y, and Jialal I. Physiology, Thyroid Stimulating Hormone (TSH). In: *StatPearls*. Treasure Island (FL): StatPearls Publishing StatPearls Publishing LLC., 2019.

Raparti G, Jain S, Ramteke K, Murthy M, Ghanghas R, Ramanand S, and Ramanand J. Selective thyroid hormone receptor modulators. *Indian journal of endocrinology and metabolism* 17: 211, 2013.

Reed PW, Corse AM, Porter NC, Flanigan KM, and Bloch RJ. Abnormal expression of mu-crystallin in facioscapulohumeral muscular dystrophy. *Experimental neurology* 205: 583-586, 2007.

Roche JA, Ford-Speelman DL, Ru LW, Densmore AL, Roche R, Reed PW, and Bloch RJ. Physiological and histological changes in skeletal muscle following in vivo gene transfer by electroporation. *American Journal of Physiology-Cell Physiology* 301: C1239-C1250, 2011.

Rodríguez-Rodríguez A, Lazcano I, Sánchez-Jaramillo E, Uribe RM, Jaimes-Hoy L, Joseph-Bravo P, and Charli J-L. Tanycytes and the control of thyrotropin-releasing hormone flux into portal capillaries. *Frontiers in Endocrinology* 10: 401, 2019.

Saetre P, Lindberg J, Leonard JA, Olsson K, Pettersson U, Ellegren H, Bergström TF, Vila C, and Jazin E. From wild wolf to domestic dog: gene expression changes in the brain. *Molecular brain research* 126: 198-206, 2004.

Samocha KE, Robinson EB, Sanders SJ, Stevens C, Sabo A, McGrath LM, Kosmicki JA, Rehnström K, Mallick S, and Kirby A. A framework for the interpretation of de novo mutation in human disease. *Nature genetics* 46: 944-950, 2014.

Sánchez E, Uribe RM, Corkidi G, Zoeller RT, Cisneros M, Zacarias M, Morales-Chapa C, Charli J-L, and Joseph-Bravo P. Differential responses of thyrotropin-releasing hormone (TRH) neurons to cold exposure or suckling indicate functional heterogeneity of the TRH system in the paraventricular nucleus of the rat hypothalamus. *Neuroendocrinology* 74: 407-422, 2001.

Sandler B, Webb P, Apriletti JW, Huber BR, Togashi M, Lima STC, Juric S, Nilsson S, Wagner R, and Fletterick RJ. Thyroxine-thyroid hormone receptor interactions. *Journal of Biological Chemistry* 279: 55801-55808, 2004.

Sap J, Muñoz A, Damm K, Goldberg Y, Ghysdael J, Leutz A, Beug H, and Vennström B. The c-erb-A protein is a high-affinity receptor for thyroid hormone. *Nature* 324: 635-640, 1986.

Sapp PC, Hosler BA, McKenna-Yasek D, Chin W, Gann A, Genise H, Gorenstein J, Huang M, Sailer W, and Scheffler M. Identification of two novel loci for dominantly inherited familial amyotrophic lateral sclerosis. *The American Journal of Human Genetics* 73: 397-403, 2003.

Schaefer JS, and Klein JR. Immunological regulation of metabolism—a novel quintessential role for the immune system in health and disease. *The FASEB Journal* 25: 29-34, 2011.

Schiaffino S, and Reggiani C. Fiber types in mammalian skeletal muscles. *Physiological reviews* 91: 1447-1531, 2011.

Schimmel M, and Utiger RD. Thyroidal and peripheral production of thyroid hormones: review of recent findings and their clinical implications. *Annals of internal medicine* 87: 760-768, 1977.

Schindelin J, Arganda-Carreras I, Frise E, Kaynig V, Longair M, Pietzsch T, Preibisch S, Rueden C, Saalfeld S, and Schmid B. Fiji: an open-source platform for biological-image analysis. *Nature methods* 9: 676-682, 2012.

Seko D, Ogawa S, Li TS, Taimura A, and Ono Y. μ -Crystallin controls muscle function through thyroid hormone action. *The FASEB Journal* 30: 1733-1740, 2016.

Senese R, Cioffi F, de Lange P, Goglia F, and Lanni A. Thyroid: biological actions of ‘nonclassical’ thyroid hormones. *J Endocrinol* 221: R1-12, 2014.

Serrano M, Moreno M, Ortega FJ, Xifra G, Ricart W, Moreno-Navarrete JM, and Fernández-Real JM. Adipose Tissue μ -Crystallin Is a Thyroid Hormone-Binding Protein Associated With Systemic Insulin Sensitivity. *The Journal of Clinical Endocrinology & Metabolism* 99: E2259-E2268, 2014.

Shen Z, Brayman A, Chen L, and Miao C. Ultrasound with microbubbles enhances gene expression of plasmid DNA in the liver via intraportal delivery. *Gene therapy* 15: 1147-1155, 2008.

Sheng J-J, and Jin J-P. TNNI1, TNNI2 and TNNI3: Evolution, regulation, and protein structure–function relationships. *Gene* 576: 385-394, 2016.

Shirley JL, de Jong YP, Terhorst C, and Herzog RW. Immune responses to viral gene therapy vectors. *Molecular Therapy* 28: 709-722, 2020.

Siler T, Yen S, Vale W, and Guillemin R. Inhibition by somatostatin on the release of TSH induced in man by thyrotropin-releasing factor. *The Journal of Clinical Endocrinology & Metabolism* 38: 742-745, 1974.

Silva JE. Thyroid hormone and the energetic cost of keeping body temperature. *Bioscience Reports* 25: 129-148, 2005.

Sivagnanasundaram S, Crossett B, Dedova I, Cordwell S, and Matsumoto I. Abnormal pathways in the genu of the corpus callosum in schizophrenia pathogenesis: a proteome study. *PROTEOMICS–Clinical Applications* 1: 1291-1305, 2007.

Smith CM, Hayamizu TF, Finger JH, Bello SM, McCright IJ, Xu J, Baldarelli RM, Beal JS, Campbell J, and Corbani LE. The mouse gene expression database (GXD): 2019 update. *Nucleic acids research* 47: D774-D779, 2019.

Snyder PJ, and Utiger RD. Response to thyrotropin releasing hormone (TRH) in normal man. *The Journal of Clinical Endocrinology & Metabolism* 34: 380-385, 1972.

Sotelo-Rivera I, Cote-Vélez A, Uribe R-M, Charli J-L, and Joseph-Bravo P. Glucocorticoids curtail stimuli-induced CREB phosphorylation in TRH neurons through interaction of the glucocorticoid receptor with the catalytic subunit of protein kinase A. *Endocrine* 55: 861-871, 2017.

Spangenburg EE, Pratt SJ, Wohlers LM, and Lovering RM. Use of BODIPY (493/503) to visualize intramuscular lipid droplets in skeletal muscle. *Journal of Biomedicine and Biotechnology* 2011: 2011.

Sterling K, Campbell GA, and Brenner MA. Purification of the mitochondrial triiodothyronine (T3) receptor from rat liver. *European Journal of Endocrinology* 105: 391-397, 1984.

Strack RL, Hein B, Bhattacharyya D, Hell SW, Keenan RJ, and Glick BS. A rapidly maturing far-red derivative of DsRed-Express2 for whole-cell labeling. *Biochemistry* 48: 8279-8281, 2009.

Suzuki S, Suzuki N, Mori J-i, Oshima A, Usami S, and Hashizume K. μ -Crystallin as an intracellular 3, 5, 3'-triiodothyronine holder in vivo. *Molecular endocrinology* 21: 885-894, 2007.

Tagami T, Yamamoto H, Moriyama K, Sawai K, Usui T, Shimatsu A, and Naruse M. Identification of a novel human thyroid hormone receptor β isoform as a transcriptional modulator. *Biochemical and biophysical research communications* 396: 983-988, 2010.

Tata JR. A cellular thyroxine-binding protein fraction. *Biochimica et biophysica acta* 28: 91-94, 1958.

Tawil R, Van Der Maarel SM, and Tapscott SJ. Facioscapulohumeral dystrophy: the path to consensus on pathophysiology. *Skeletal muscle* 4: 12, 2014.

Taylor PN, Albrecht D, Scholz A, Gutierrez-Buey G, Lazarus JH, Dayan CM, and Okosieme OE. Global epidemiology of hyperthyroidism and hypothyroidism. *Nature Reviews Endocrinology* 14: 301, 2018.

Taylor SC, Nadeau K, Abbasi M, Lachance C, Nguyen M, and Fenrich J. The ultimate qPCR experiment: producing publication quality, reproducible data the first time. *Trends in biotechnology* 37: 761-774, 2019.

Tennessen JA, Bigham AW, O'Connor TD, Fu W, Kenny EE, Gravel S, McGee S, Do R, Liu X, and Jun G. Evolution and functional impact of rare coding variation from deep sequencing of human exomes. *science* 337: 64-69, 2012.

Thul PJ, Åkesson L, Wiking M, Mahdessian D, Geladaki A, Blal HA, Alm T, Asplund A, Björk L, and Breckels LM. A subcellular map of the human proteome. *Science* 356: eaal3321, 2017.

Uhlén M, Fagerberg L, Hallström BM, Lindskog C, Oksvold P, Mardinoglu A, Sivertsson Å, Kampf C, Sjöstedt E, and Asplund A. Tissue-based map of the human proteome. *Science* 347: 1260419, 2015.

van Mullem AA, van Gucht AL, Visser WE, Meima ME, Peeters RP, and Visser TJ. Effects of thyroid hormone transporters MCT8 and MCT10 on nuclear activity of T3. *Molecular and cellular endocrinology* 437: 252-260, 2016.

Vanderplanck C, Anseau E, Charron S, Stricwant N, Tassin A, Laoudj-Chenivesse D, Wilton SD, Coppée F, and Belayew A. The FSHD atrophic myotube phenotype is caused by DUX4 expression. *PloS one* 6: e26820, 2011.

Velasco LF, Togashi M, Walfish PG, Pessanha RP, Moura FN, Barra GB, Nguyen P, Rebono R, Yuan C, and Simeoni LA. Thyroid hormone response element organization dictates the composition of active receptor. *Journal of Biological Chemistry* 282: 12458-12466, 2007.

Visser WE, Friesema EC, and Visser TJ. Minireview: thyroid hormone transporters: the knowns and the unknowns. *Molecular endocrinology* 25: 1-14, 2011.

Visser WE, Wong WS, Van Mullem AA, Friesema EC, Geyer J, and Visser TJ. Study of the transport of thyroid hormone by transporters of the SLC10 family. *Molecular and cellular endocrinology* 315: 138-145, 2010.

Vlangos CN, Siuniak AN, Robinson D, Chinnaiyan AM, Lyons Jr RH, Cavalcoli JD, and Keegan CE. Next-generation sequencing identifies the Danforth's short tail mouse mutation as a retrotransposon insertion affecting Ptf1a expression. *PLoS Genet* 9: e1003205, 2013.

Walker DM, Zhao X, Ramakrishnan A, Cates HM, Cunningham AM, Pena CJ, Bagot RC, Issler O, Van der Zee Y, and Lipschultz AP. Adolescent Social Isolation Reprograms the Medial Amygdala: Transcriptome and Sex Differences in Reward. *bioRxiv* 2020.

- Wang M, Li Q, Deng A, Zhu X, and Yang J. Identification of a novel mutation in CRYM in a Chinese family with hearing loss using whole-exome sequencing. *Experimental and Therapeutic Medicine* 20: 1447-1454, 2020.
- Watanabe Y, and Weiss RE. Thyroid hormone action. In: *Encyclopedia of Endocrine Diseases* Elsevier, 2018, p. 452-462.
- Weinberger C, Thompson CC, Ong ES, Lebo R, Gruol DJ, and Evans RM. The c-erb-A gene encodes a thyroid hormone receptor. *Nature* 324: 641-646, 1986.
- Williams GR, and Bassett JD. THEMATIC REVIEW Deiodinases: the balance of thyroid hormone Local control of thyroid hormone action: role of type 2 deiodinase. *Journal of Endocrinology* 209: 261-272, 2011.
- Williams GR. Cloning and characterization of two novel thyroid hormone receptor β isoforms. *Molecular and cellular biology* 20: 8329-8342, 2000.
- Wistow G, and Kim H. Lens protein expression in mammals: taxon-specificity and the recruitment of crystallins. *Journal of molecular evolution* 32: 262-269, 1991.
- Xie F, Xiao P, Chen D, Xu L, and Zhang B. miRDeepFinder: a miRNA analysis tool for deep sequencing of plant small RNAs. *Plant molecular biology* 80: 75-84, 2012.
- Yarbrough GG. On the neuropharmacology of thyrotropin releasing hormone (TRH). *Progress in neurobiology* 12: 291-312, 1979.

Zaiontz C. Real Statistics Resource Pack software (Release 6.8). www.real-statistics.com: 2020.

Zetsche B, Gootenberg JS, Abudayyeh OO, Slaymaker IM, Makarova KS, Essletzbichler P, Volz SE, Joung J, Van Der Oost J, and Regev A. Cpf1 is a single RNA-guided endonuclease of a class 2 CRISPR-Cas system. *Cell* 163: 759-771, 2015.

Zetsche B, Heidenreich M, Mohanraju P, Fedorova I, Kneppers J, DeGennaro EM, Winblad N, Choudhury SR, Abudayyeh OO, and Gootenberg JS. Multiplex gene editing by CRISPR–Cpf1 using a single crRNA array. *Nature biotechnology* 35: 31-34, 2017.

Zimmermann RC, Krahn LE, Klee GG, Ditkoff EC, Ory SJ, and Sauer MV. Prolonged inhibition of presynaptic catecholamine synthesis with α -methyl-para-tyrosine attenuates the circadian rhythm of human TSH secretion. *Journal of the Society for Gynecologic Investigation* 8: 174-178, 2001.